YIELD AND QUALITY PREDICTION USING SATELLITE PASSIVE IMAGERY AND GROUND-BASED ACTIVE OPTICAL SENSORS IN SUGAR BEET, SPRING WHEAT, CORN, AND SUNFLOWER

A Thesis
Submitted to the Graduate Faculty
of the
North Dakota State University
of Agriculture and Applied Science

By

Honggang Bu

In Partial Fulfillment
for the Degree of
MASTER OF SCIENCE

Major Department:
Soil Science

April 2014

Fargo, North Dakota

North Dakota State University
Graduate School

Title

Yield and Quality Prediction Using Satellite Passive Imagery and Ground-Based Active Optical Sensors in Sugar Beet, Spring Wheat, Corn, and Sunflower

By

Honggang Bu

The Supervisory Committee certifies that this ***disquisition*** complies with North Dakota State University's regulations and meets the accepted standards for the degree of

MASTER OF SCIENCE

SUPERVISORY COMMITTEE:

David Franzen
Chair

Tom DeSutter

Amitava Chatterjee

Kendall Nygard

Approved:

May 9, 2014
Date

Frank Casey
Department Chair

ABSTRACT

Remote sensing is one possible approach for improving crop nitrogen use efficiency to save fertilizer costs, reduce environmental pollution, and improve crop yield and quality. Feasibility and potential of using remote sensing tools to predict crop yields and quality as well as to detect nitrogen requirements, application timing, rate, and places in season were investigated based on a two-year (2012-2013) and four-crop (corn, spring wheat, sugar beet, and sunflower) study. Two ground-based active optical sensors, GreenSeeker™ and Holland Scientific Crop Circle™, and the RapidEye™ satellite imagery were used to collect sensing data. Highly significant statistical relationships between INSEY (NDVI normalized by growing degree days) and crop yield and quality indices were found for all crops, indicating that remote sensing tools may be useful for managing in-season crop yield and quality prediction.

ACKNOWLEDGMENTS

I would like to extend my thanks and gratitude especially to Dr. David Franzen, my advisor, for his spiritual, financial, and academic support, guidance, patience, time, warm encouragement, and friendship with this project and throughout my graduate studies. He is one of the best people I ever met, whether as an advisor, or as a senior, or as a friend.

My heartfelt thanks would be given to my committee members, Dr. Tom DeSutter, Dr. Amitava Chatterjee, and Dr. Kendall Nygard, for their patience and guidance they have given me during this research and thesis editing.

Special thanks to Lakesh Sharma for his warm-hearted and patient assistance in my field work, off-field experiments, and data analysis.

I would also like to sincerely thank Eric Momsen for his patience and time spent in teaching me the basic operations of GRASS GIS software, thank Brad Schmidt and Eric Schultz for their professional help in field work.

In addition, I would like to thank the US National Science Foundation for funding this project.

Finally, I owe my deepest gratitude to all my family members, my parents, my wife, and my daughters, for their unconditional and unlimited love, support, and encouragement, without which I would not be where I am today.

TABLE OF CONTENTS

LIST OF TABLES

LIST OF FIGURES

LIST OF ABBREVIATIONS

ANOVA…….analysis of variance

CC……..…Crop Circle

CI……chlorophyll index

CV……..…coefficient of variation

EONR……economic optimum nitrogen rate

G…….green

GDD……..growing degree days

GNDVI……..…green normalized difference vegetation index

GS……..GreenSeeker

INSEY……....in season estimate of yield

LAI…….…leaf area index

N…….nitrogen

NDVI…….normalized difference vegetation index

NFOA…….…nitrogen fertilization optimization algorithm

NIR……....near infrared

NUE……...nitrogen use efficiency

RGNDVI……relative green normalized difference vegetation index

RI……..….response index

YP……..…yield potential

LIST OF APPENDIX TABLES

GENERAL INTRODUCTION

Due to their unbeatable strengths in data collecting and analysis, remote sensing technologies are being widely and successfully used in precision agriculture to help establish information and technology-based agricultural management system, and hence benefit the farmers and environment, and optimize relevant logistics as well. Precision agricultural management practices include variable rate fertilizing or herbicide spraying or planting or irrigation, site-specific harvesting, in-season crop yield and quality prediction, soil and land survey, etc. Precision nitrogen (N) management based on remote sensing technologies is one of the most representative examples as N was found to be one of the most critical nutrients for crop growth (Havlin et al., 2005). Improving nitrogen use efficiency (NUE) saves fertilizer cost, improves crops yield and quality, and reduces environmental pollutions caused by loss of N in the field (Havlin et al., 2005).

An in-season variable N fertilization algorithm for winter wheat and corn based on optical sensing data was proposed (Raun et al., 2002; Raun et al., 2005) and widely recognized. One of the fundamental components of this algorithm is the in-season yield prediction using the statistical relationship between remote sensing data and crop yield. Specifically, the independent variable was in season estimate of yield (INSEY), which was obtained by dividing normalized difference vegetation index (NDVI) by accumulated positive growing degree days (GDD). Using this algorithm, in-season site-specific crop N deficiency and requirement can be determined. Crop qualities were also related with in-season ground-based or space remote sensing data (Gehl

and Boring, 2011; Humburg et al., 2006). Besides helping make variable N fertilization, crop yield and quality prediction may also support possible crop production parameters estimation and optimize the logistics decision-makings.

Generally, there are three types of remote sensing systems (Mulla, 2013): space sensing (satellite imagery), aerial sensing (aerial photography), and ground-based sensing (proximal sensor readings). In this research, two ground-based active optical sensors, GreenSeeker™ (NTech Industries, Inc., Ukiah, CA, USA) and Holland Crop Circle™, (Holland Scientific Inc., Lincoln, Nebraska, USA), and a type of passive optical satellite imagery, the RapidEye™ Ortho Products (Level 3A) satellite imagery (http://blackbridge.com/rapideye/products/ortho.htm) were employed to collect sensing data. Four NDVI maps can be computed from each set of RapidEye satellite imagery, as illustrated in Figure 1. Average NDVI for each sub-plot can be further extracted according to the GPS coordinates of the corner points of each sub-plot. The studied four crops were sugar beet, spring wheat, corn, and sunflower. The overall objective of this research is to further validate the feasibility of using remote sensing data to make in-season predications of four crops yield and quality by investigating the statistical relationships between remote sensing data and crops yield or quality based on two-year data. Other objectives include comparison of the performance the three optical remote sensing systems, comparison of the performance of three regression models, and evaluation of the impact of including plant height into regression models.

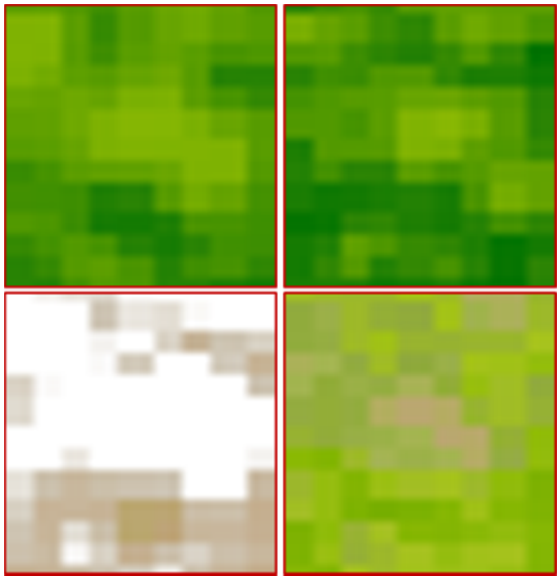

Figure 1. NDVI maps extracted from RapidEye satellite imagery (left top: red NDVI; right top: blue NDVI; left bottom: red edge NDVI; right bottom: green NDVI).

The rest of this thesis is organized as follows: chapter “LITERATURE REVIEW” makes a thorough review of relevant reported work, with focuses on crop yield and quality prediction using ground-based active optical sensing and passive optical satellite remote sensing; all the necessary experimental data including crops, site-years, plot design, remote sensing data, plant height data, and crop yield and quality data, and their collecting methods as well are presented in detail in chapter “MATERIALS AND METHODS”, where the adopted statistical data analysis methods and software are explained, too; chapter “RESULTS AND DISCUSSIONS FOR SUGAR BEET”, chapter “RESULTS AND DISCUSSIONS FOR SPRING WHEAT”, chapter “RESULTS AND DISCUSSIONS FOR CORN”, and chapter “RESULTS AND DISCUSSIONS FOR SUNFLOWER” discuss the statistical relationships between remote sensing data and the yield (quality) of the four studied crops, respectively; conclusions for the entire study and suggestions for future work are given in the last chapter.

LITERATURE REVIEW

Importance of Nitrogen and Nitrogen Use Efficiency

N is one of the most important nutrients for plant growth, yet it is also the one that is most commonly deficient in most non-legume cropping systems (Havlin et al., 2005). It ranks behind only C, H, and O in total quantity needed and is the mineral element most demanded by plants. Nitrogen is a major part of chlorophyll and the green color of plants and is responsible for lush, vigorous (Brady and Weil, 1999).

Although N is the most abundant element in our atmosphere, plants cannot use it until it is naturally transformed in the soil, or added as chemical fertilizer such as ammonium nitrate, urea, or anhydrous ammonia, before or during the crop growing season. Growth and yield, however, will be reduced if the sum of soil N availability and N rate applied is less than the total N required for optimal growth and development. Deficient N application cannot produce optimal yield and therefore is unfavorable to meeting the increasing demands of humans and animals; on the other hand, excessive N application will result in low NUE and environmental degradation (Hirel et al., 2007; Raun and Johnson, 1999; Sowers et al., 1994). The over-application of N increases N loss through several pathways: immobilization, volatilization, denitrification and leaching, that results in economic loss to growers, nitrate pollution of ground and surface waters (Havlin et al., 2005) and possible production of nitrous oxides.

There are a number of definitions for NUE (Liang and Mackenzie, 1994; Moll et al., 1982; Raun and Johnson, 1999; Semenov et al., 2007; Spargo et al., 2008). A simple yet

reasonable definition of NUE is the difference between N uptake in an treated plot divided by the total N application rate (Arnall et al., 2009). Raun and Johnson (1999) pointed out that NUE for cereal crop production is as low as 33% worldwide, and that an increase in NUE of 1% and 20% could save about $234 million and more than $4.7 billion, respectively, in N fertilizer costs per year. Currently, yield is not the only factor that affects farmers economically. Qualities such as wheat protein content, sugar beet recoverable sugar per unit area, sunflower oil content, greatly affect the price received for crop delivery. Inappropriate N fertilization has negative impacts on not only the crop yield but also crop quality. Franzen (2003) referred to numerous studies which indicated that excess N uptake decreases sugar beet sucrose levels and increases impurities that increase sugar beet processing costs. Improvement in NUE would be expected to improve crop yield and quality, maximizing farmer's economic return, and reducing environmental pollution.

Possible techniques for improving NUE include use of nitrification inhibitors, urease inhibitors, urea polymer or other coatings, use of a balanced fertilizer program, splitting of N fertilizer application timing, applying N at the time when it is least susceptible to loss, and accounting for temporally variable influences on crop N needs. Crop N requirement determination and improvement of NUE may also be aided through the use of remote sensing tools for N status determination, yield potential prediction and crop quality prediction.

Precision Agriculture and Remote Sensing

Precision agriculture, viewed as one of the top ten revolutions in agriculture during the past 50 years (Crookston, 2006), is perhaps the best solution to improving NUE through site-

specific and variable-rate N application. The basic foundation of precision agriculture is to replace the conventional management practices that apply uniform treatments to the whole field with much more flexible practices by dividing the farm into small management zones with each zone receiving different applications based on its individual needs (Mulla, 2013). Improved management usually improves crop productivity, farm economic return, and protects environmental quality. Representative precision agricultural practices include the management of fertilizer rate, herbicide type and rate, irrigation timing and rate, soil organic matter, yield, quality, and seed selection and rate. In-season N management and crop yield or quality prediction is just part of precision agriculture, which aims at improved field management by doing the right practice at the right time and right place in response to variations across years and landscape. Just as Bakhsh et al. (2000) pointed out, there was significant variability of crop yield and yield response to N fertilizer across years due to climate change. Also, extensive soil sampling, optical sensor measurements of plants, and geostatistical analyses indicated that statistically significant differences in nitrogen availability existed at a 1 m^2 spatial scale (Raun et al., 1998; Solie et al., 1999).

Soil testing and plant testing have been used as target monitoring methods in precision agriculture, but in recent decades remote sensing has become more popular and more widely used. Remote sensing is “the acquisition of information about an object without being in physical contact with it” (Elachi and Zyl, 2006). Remote sensors based on light absorption or reflection measures the electromagnetic radiation reflected or emitted from the target. Remote sensing has

many advantages over soil testing or plant testing: firstly, it provides a non-destructive way of sampling; secondly, larger amounts of data can be collected and analyzed efficiently; thirdly, remote sensing data have been proved reliable by a vast number of researches and applications in the past decades; fourthly, it is a cost-effective way of data collection and analysis.

Remote sensing systems can be classified into three categories: ground-based, aerial (aircraft), and space (satellite) (Mulla, 2013). Ground-based sensing is also called proximal remote sensing; its corresponding sensors can be either hand-held or tractor-mounted. Images from aerial and space sensing systems can cover larger areas in a shorter period but the quality of most of them is strongly affected by the cloud cover (Mulla, 2013).

In terms of energy source of emission and reflectance, remote sensing systems can be classified into two categories: passive sensing and active sensing (Lo and Yeung, 2007). Passive remote sensing systems rely on independent or external energy sources to sample emitted and reflected radiation from target surfaces. Usually, the sun is the most common energy source for passive sensors (Lo and Yeung, 2007). Active remote sensing systems have their own energy sources that send out electromagnetic radiation at specified wavelengths to the surfaces and receive the corresponding reflectance (Lo and Yeung, 2007). Some active remote sensing systems can be used both in the day and in the night, and are not influenced by cloud cover due to their pulsated light (Graham, 1999).

In terms of spectral bands quantity and width, remote sensing systems can be classified into three categories: hyperspectral, multispectral, mono-spectral. Typically, monospectral

remote sensing systems use the near infrared (NIR) band (Christy, 2008; Long et al., 2008). However, multispectral and hyperspectral sensing systems are more common and frequently used. Multispectral sensors usually only have several (in most cases less than 10) broadbands, each with greater than 40 nm width and are centered on NIR or on one of the visible light spectrum regions such as red, green, blue, or red edge (Mulla, 2013). Hyperspectral sensing usually has hundreds or even thousands of spectral bands that cover a wide range of spectrum and each band tends to be narrow (about 10 nm wide) (Mulla, 2013). Hyperspectral sensing can provide larger spectral range cover and higher spectral resolution of bands and therefore can provide more information than multispectral sensing. Figure 2 is an illustration of the electromagnetic spectrum, which shows the range of all possible frequencies of electromagnetic radiation.

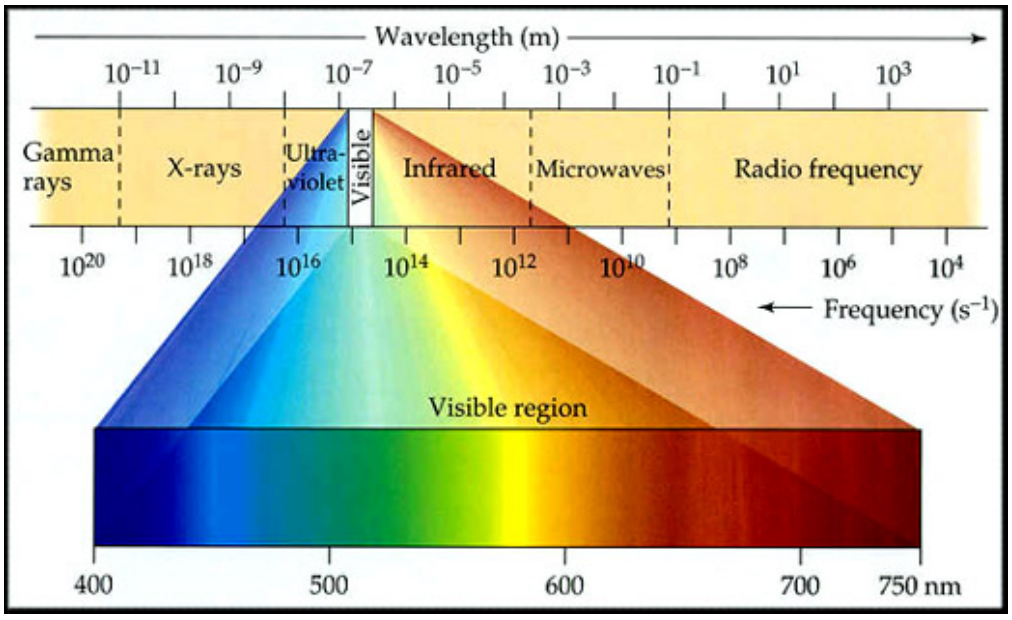

Figure 2. Electromagnetic spectrum (http://scioly.org/wiki/index.php/Remote_Sensing).

Remote sensing has been widely applied to various agricultural researches and practices including crop N status monitoring (Bausch and Khosla, 2010; Cabrera-Bosquet et al., 2011; Erdle et al., 2011; Li et al., 2010b; Raper et al., 2013; Solari et al., 2008; Tang et al., 2010), crop yield prediction (Bredemeier et al., 2013; Gehl and Boring, 2011; Harrell et al., 2011; Holzapfel et al., 2009; Inman et al., 2007; Lofton et al., 2012a; Lofton et al., 2012b; Mayfield and Trengove, 2009; Solari et al., 2008; Yang and Everitt, 2012), crop quality prediction (Gehl and Boring, 2011; Long et al., 2008; Mayfield and Trengove, 2009; Soderstrom et al., 2010), crop biomass estimation (Cabrera-Bosquet et al., 2011; Erdle et al., 2011; Flynn et al., 2008; Freeman et al., 2007; Li et al., 2010a; Montes et al., 2011), soil organic matter content estimation (Genu et al., 2013; Liu et al., 2013; Stamatiadis et al., 2013), irrigation (Akkuzu et al., 2013; Awan et al., 2013; Kharrou et al., 2013; Moller et al., 2007), soil water status (Li et al., 2013; Li et al., 2012; Moller et al., 2007; Neale et al., 2012; Obade et al., 2013).

The improvement of farm NUE is an important issue due to economic and environmental concerns. There is a solid rationale behind the relationship between crop N status and sensing data. For many crops there is a strong linear relationship between leaf N and chlorophyll concentration (Blackmer and Schepers, 1995; Evans, 1983; Olfs et al., 2005). Therefore, chlorophyll content of a plant, the greenness of the plant, can be a good indicator for leaf N concentration. Visible light, especially blue and red light, is absorbed by plant chlorophyll as an energy source during photosynthesis. NIR radiation (about 760 to 900 nm) is not used in photosynthesis; much of the radiation is reflected from the living green plants. NIR reflectance is

mainly controlled by the structure of the spongy mesophyll and has a positive correlation with crop condition and yield. Typically 2 to 10% of the visible light is reflected from the canopy of the green vegetation, and 35 to 60% for NIR light (Holland Scientific, 2011). In general, healthier plants absorb more visible light and reflect more NIR. Based on this relationship, useful vegetation indices can be created based on NIR and visible light reflectance to monitor crop N status. For hyper-spectral data, there are many options available to derive different vegetation indexes (VIs).

Introduction to Vegetation Indices

Vegetation Indices (VIs) are combinations of surface reflectance at two or more wavelengths designed to highlight a particular property of vegetation. Depending on the width of the spectral band, VIs can be classified into multispectral broadband VIs and hyper-spectral narrow band VIs (Mulla, 2013; Thenkabail et al., 2002). Multispectral broadband VIs are usually produced using one NIR band and one visible band. Many of the hyperspectral narrow-band indices have a similar form as that of the hyperspectral bands with the difference mainly being the width of the bands used. Depending on whether a N-rich referenced plot is used, VIs can be divided into two general categories, absolute spectral indices and relative spectral indices (Sripada et al., 2008).

The two most popular and typical broadband and absolute spectral VIs are NDVI (Rouse et al., 1973; Tucker, 1979) and Simple Ratio (SR) (Jordan, 1969). Normalized difference vegetation index (NDVI) is defined as

$$NDVI = (NIR - red) / (NIR + red) \quad (1)$$

and SR is defined as

$$SR = NIR / red \quad (2)$$

where NIR and red refer to near infrared and red spectral reflectance measurements, respectively. Generalized NDVI definition uses any visible spectral reflectance including red spectral reflectance:

$$\text{Generalized NDVI} = (NIR - red) / (NIR + red) \quad (3)$$

The mentioned NDVIs hereafter all refer to generalized NDVI. Usually greater NDVI or SR values indicate higher plant N content in the leaf. Two main drawbacks of NDVI are interference by soil background when canopy density is low and inability to detect changes in leaf chlorophyll content in canopies that have a high leaf area index value exceeding 2 or 3 (Thenkabail et al., 2000). A soil adjusted vegetation index (SAVI) is also widely used:

$$SAVI = (NIR-RED) / (NIR+ RED+ L) * (1+L) \quad (4)$$

where L = soil brightness factor (Shaver et al., 2011). Cao et al. (2013) found that the red edge band (710 nm) NDVI obtained from a Holland Crop Circle Sensor^{TM} in his experiment could

better predict rice N status than could red-based NDVI. In the estimation of leaf N and chlorophyll contents in corn using remote sensing, Schlemmer et al. (2013) indicated that indices extracted using NIR and red-edge spectral bands were one of the best choices of VIs tested.

Blackmer et al. (1994) indicated that the green (G) wavelength reflectance was particularly sensitive to leaf N content change. A simple ratio based on mid-infrared and green bands were found to be the single most effective ratio for the prediction of barley protein content (Soderstrom et al., 2010). Gitelson et al. (2005) tested two chlorophyll indices (CIs), each of which was equal to the SR minus 1, with one based on G spectral and NIR, and the other red edge and NIR, and found that both indices have a very strong linear relationship with chlorophyll content. Schepers et al. (1996) found that a strong relationship (r^2=0.97) existed between the G/NIR ratio and chlorophyll meter readings in a greenhouse maize experiment. Comparisons between NDVI and GNDVI indicated that GNDVI could produce a better correlation with grain yield than did NDVI (Blackmer et al., 1996; Shanahan et al., 2001). Here GNDVI refers to Green Normalized Vegetation Index and is defined as (Gitelson et al., 1996)

$$GNDVI = (NIR - G) / (NIR + G) \quad (5)$$

GNDVI extracted from Landsat imagery was found to be the consistently best vegetation index to linearly relate to beet sucrose concentration in terms of r^2 value as far as single image was involved (Humburg et al., 2006). Clay et al. (2006) compared GNDVI with NDVI and

demonstrated that each of the two indices have their own strength. NDVI was more sensitive to water stress and GNDVI was more sensitive to N stress.

Using raw NDVI data directly for plant N status or crop yield prediction usually is not a wise choice. For example, a study trying to use raw NDVI from the Holland Crop Circle Sensor to predict cotton leaf N status found that the relationship between sensor readings and leaf N content was inconsistent (Raper et al., 2013). Several studies have indicated that a reference area of non-limited N supply could normalize the differences between hybrids, soil, and other environmental conditions and therefore might strengthen relationships (Dellinger et al., 2008; Shanahan et al., 2001). In a study of estimating of corn N requirements, it was revealed that the economic optimum nitrogen rate (EONR) could be best predicted using Relative Green Difference Normalized Vegetation Index by ratio (RGNDVI) from the Holland Crop Circle Sensor at V6 stage ($r^2 = 0.79$) (Sripada et al., 2008):

$$RGNDVI = GNDVI_{plot} / GNDVI_{reference\ plot} \quad (6)$$

Another corn study showed that EONR was strongly related to RGNDVI when control and manure preplant treatments were used ($r^2 = 0.84$), but not so when ammonium nitrate was applied (Dellinger et al., 2008). Normalized Green NDVI, which is in essence similar to relative GNDVI, extracted from QuickBird™ satellite imagery was found to be a good predictor of in-season corn N status (Bausch and Khosla, 2010). A two-year corn study indicated that NDVI ratio ($NDVI_{plot}$ / $NDVI_{reference}$ plot) had a better relationship with grain yield ($r^2 = 0.65$) than did

INSEY with grain yield (r^2=0.58) (Inman et al., 2007). This NDVI-ratio is the inverse of the Reponse Index of NDVI (RI_{NDVI}) in developing an in-season N recommendation algorithm (Johnson and Raun, 2003; Raun et al., 2005).

A special relative VI is the In-Season Estimate of Yield (INSEY), which is NDVI divided by growing degree days (GDD) from planting date, and reflects the biomass produced per day of positive growth for a particular crop (Raun et al., 2001; Teal et al., 2006). In-season estimate of yield (INSEY) has been proven useful for yield and quality prediction in several crops (Gehl and Boring, 2011; Li et al., 2009; Ortiz-Monasterio and Raun, 2007; Raun et al., 2001; Raun et al., 2002; Raun et al., 2005; Singh et al., 2011; Teal et al., 2006). Normalizing NDVI with GDD does not necessarily improve yield potential prediction significantly, but its use makes it feasible to combine years and sites of spectral data in predictive regression model establishment (Teal et al., 2006). A detailed list of the hyper-spectral narrowband vegetation indices can be found in reference (Mulla, 2013).

Ground-Based Active Optical Sensing and N Fertilizer Requirements Determination

There are three types of typical and commercial ground-based active optical sensing systems that can be used to estimate plant N status in real-time and thus enable the in-season variable rate N fertilization on-the-go. These systems include GreenSeeker™ (NTech Industries, Inc., Ukiah, CA, USA), Holland Crop Circle™, or Crop Circle (Holland Scientific Inc., Lincoln, Nebraska, USA), and Yara N-sensor ALS™ (Yara International, Oslo, Norway). The first

generation of GreenSeeker had only NIR (770 nm) and red (660 nm) two optical channels. The latest second generation provides two more red edge bands at 710 nm and 735 nm. An affordable and easy-to-use handheld GreenSeeker crop sensor was also commercially released in 2013. The latest Crop Circle ACS-470 sensor is supplied with 6 narrowband interference filters to determine its spectral response. At one time only three of the filters are used because the sensor has only three optical measurement channels. The 6 filter wavelength includes 532 nm, 550 nm, 670 nm, 700 nm, 730 nm, and 760 nm. A latest advancement in active crop canopy sensing solutions is the RapidSCAN CS-45^{TM} system developed by Holland Scientific, Inc. and integrating a data logger, graphical display, GPS, crop sensor and power source into one small compact instrument. This handheld sensor provides three optical measurement bands: NIR (780 nm), red (670 nm), and red edge (730 nm). The first Yara N-Sensor was introduced in 1999 in Germany for use on cereals. Unlike the first Yara N-Sensor which was a passive optical sensor, the Yara N-Sensor ALS launched in 2006 is an active multispectral sensor that can measure crop reflectance characteristics at selected wavelength in the region from 450 nm to 900 nm (Samborski et al., 2009).

GreenSeeker

Raun et al. (2001) developed the INSEY index and an innovative technique based on an active canopy sensor for grain yield potential with zero-N fertilization (YP0) prediction of winter wheat (*Triticum aestivum*, L). A significant exponential relationship was found between estimated yield and measured yield when all 9-location and two-year data were included. The

estimated yield explained 83% of the variability of grain yield predicted from 6 out of 9 locations. Based on INSEY, Lukina et al. (2001) developed a winter wheat in-season N fertilization recommendation algorithm. In-season N needs were estimated by subtracting predicted early-season plant N uptake (at the time of sensing) from predicted total grain N uptake (predicted yield potential times grain N percent), and then divided by the expected NUE of 0.70.

In order to quantitatively characterize the crops' in-season likelihood to respond to additional N for each field, the concept of response index (RI) was introduced (Johnson and Raun, 2003). The actual crop grain response to applied N at harvest was defined as $RI_{Harvest}$ = (highest mean yield N treatment) / (mean yield of the check treatment) (Mullen et al., 2003). A response index based on NDVI was also introduced to predict in-season $RI_{Harvest}$, and a strong linear relationship was found between $RI_{Harvest}$ and RI_{NDVI} (Mullen et al., 2003).

An effective N fertilization optimization algorithm (NFOA) (Raun et al., 2002) for winter wheat was developed based on the predicted YP0 (Raun et al., 2001) and a field-specific NDVI-based Responsive Index RI_{NDVI}. Steps in the development of the algorithm include: 1) predict YP0 using the relationship equation between actual grain yield and INSEY (Raun et al. 2001); 2) predict RI at Harvest ($RI_{Harvest}$) using RI_{NDVI}, which is computed as mean NDVI readings of adequate N rate treatment divided by mean NDVI readings of pre-plant N rate. To accomplish this step, NDVI measurements were collected from from Feekes 4 to Feekes 6 growth stages. The $RI_{Harvest}$ was well correlated with RI_{NDVI} and was defined as the grain yield from N-adequate plots divided by the yield from the plots receiving the pre-plant N rate; 3) determine Yield

Potential (YP) using pre-plant N rates YPN and equation YPN = YP0 × RI_{NDVI}; 4) Predict percent N in the grain (PNG) with a linear relationship equation between PNG and YPN; 5) predict grain N uptake (GNUP) by multiplying YPN with PNG; 6) predict forage N uptake (FNUP) based an exponential relationship equation between FNUP and NDVI; and 7) determine in-season fertilizer N requirement (FNR) using equation FNR =(GNUP - FNUP)/expected NUE. The expected NUE used in this research was the theoretical maximum NUE of an in-season N application, 0.70 (Raun et al., 2002).

Based on the previous NFOA (Raun et al., 2002), an improved version of NFOA was proposed (Raun et al., 2005). In the previous NFOA algorithm, the sensing and fertilizing resolution was 1 m^2. The greatest difference in this improved algorithm was including the coefficient of variation (CV) from NDVI readings, which reflects the spatial variability within each 0.4 m^2 area, into the algorithm. The improved algorithm consists of three important components, INSEY, $RI_{Harvest}$ that can be predicted using RI_{NDVI}, and CV. This study also demonstrated that with only two years of field data, one might establish reliable crop yield potential prediction equations. Several NFOA-based different algorithms and a fixed N rate method were evaluated and compared in a corn study, where it was found that the algorithm of NFOA based on RI alone was the best one tested (Tubana et al., 2008b).

The parameter CV is of great significance for improving the accuracy of the NFOA especially when spatial variability is large. Use of the CV's of the plot NDVI reading was related to stand density in winter wheat. When the CVs of plot NDVI readings were less than 18%, it

was still possible for the winter wheat to recovery from N stress (Morris et al., 2006). When CVs were greater than 20%, the possibility of recovery with N application of winter wheat would be considered poor because the stand density would most probably be less than 100 plants m^{-2} (Arnall et al., 2006). Response Index (RI) can be adjusted based on the CV of NDVI readings (Raun et al., 2005). Arnall et al. (2013) made a further evaluation of the utilizing of CV in improving winter wheat $RI_{Harvest}$ prediction based on RI_{NDVI}. According to the results of CV's experiments conducted on resolutions of both small 1.48 m2 and large 17.0 m2 areas, no improved RI prediction was observed. To improve the RI prediction accuracy, Chung et al. (2010) established an equation for adjusting RI_{NDVI} based on the original RI_{NDVI} and the days where growing degree days are positive.

Instead of using a constant NUE of 0.70 employed in previous studies (Raun et al., 2001; Raun et al., 2002; Raun et al., 2005), dynamic NUE values were estimated using $RI_{Harvest}$ or RI_{NDVI} or both because NUE estimated from crop grain yield was not a constant and was dependent on time and N application rate (Arnall et al., 2009). When both were used to establish a linear regression model between NUE and RI, the r^2 was significantly higher than using one type of RI alone. Previous studies (Raun et al., 2001; Raun et al., 2002; Raun et al., 2005) combined grain yield potential and nitrogen response to determine the in-season optimal N fertilization rates, but did not consider the relationship between grain yield potential and nitrogen response. Since they both have impact on fertilizer N requirements, it is necessary to find out if they are independent of each other and hence help justify any in-season N rate recommendation

algorithm already developed. Grain yield potential and nitrogen response were found to be independent in a long-term winter wheat study (Raun et al., 2011).

Determining the optimal resolution for sensing and analyzing field variation is also important for achieving the best prediction from an in-season N management algorithm. The optimal spatial scale depends on the specific soil class and properties, the crop type, and landscape position. Focusing on small-scale spatial variation is not always helpful because it could be time-consuming, unprofitable, and produces cluttered data that is difficult to analyze and condense into meaningful forms (Biermacher et al., 2009; Boyer et al., 2011). A spatial scale that is too large cannot realize the potential benefits of site-specific nutrient management. Best sensing resolutions have been documented for both winter wheat (Tubana et al., 2008a) and corn (Chung et al., 2008). It is worthwhile to examine the economic effect resulting from the application of variable-rate N directed by optical sensor N recommendation algorithms. A recent study (Boyer et al., 2011) indicated that on average the fixed 90 kg ha^{-1} treatment was more profitable than variable N rate treatments suggested by an optimization algorithm (Raun et al., 2005). The proposed optimum yield predication and/or N fertilization algorithms (Raun et al., 2001; Raun et al., 2002; Raun et al., 2005) have been widely applied and confirmed (Inman et al., 2007; Li et al., 2009; Lofton et al., 2012b; Morris et al., 2006; Ortiz-Monasterio and Raun, 2007; Roberts et al., 2011; Singh et al., 2011; Teal et al., 2006; Tubana et al., 2008b; Tubana et al., 2011).

The N-rich reference strip, which still seems to be the most common adopted strategy due to its simplicity and utility, is also a key element in a variable N application optimization algorithm. The premise of its advantages, however, is that the correct and usually difficult choice of the place for N-rich strip establishment must be made with consideration of soil spatial variability. Statistically significant differences in N availability in the field have been observed (Cao et al., 2012; Raun et al., 1998; Solie et al., 1999). There are two possible ways to establish N-rich strips (Samborski et al., 2009). One is to enable the reference strips to traverse as many growing conditions and soil types as possible, the other is to establish more than one N-rich strips positioned on different soil types and use different adequate N rate. Bausch and Brodahl (2012) discussed several strategies for evaluating the quality of reference strips for in-season, field-scale, irrigated corn nitrogen sufficiency. Other types of reference strips other than N-rich strips include zero-N reference plot (Olivier et al., 2006), ramped calibration strips (Raun et al., 2008), and a virtual reference strip (Holland Scientific, 2013).

Instead of using INSEY, some researchers explored alternative ways of using GreenSeeker NDVI readings to make crop yield or quality prediction. To predict sugar beet quality and N status using GreenSeeker, Gehl and Boring (2011) classified GDD into several intervals and then set up the relationship between NDVI and quality or N status for each interval or group. Their research indicated that at the stages of midseason when GDD between 1200 and 1400, or when GDD between 1900 and 2300, or at the harvest stage, the NDVI readings had strong exponential relationships with recoverable sugar yield. They also found that harvest

NDVI had a strong relationship with canopy total N. The same sensor and similar method of grouping NDVI based on GDD was practiced in a rice grain yield potential estimation study that came to a conclusion that this method is superior to the using of INSEY (Harrell et al., 2011). Inman et al. (2007) related NDVI-ratio (the ratio of NDVI from any plot to NDVI from N-rich plot) to the corn grain yield and compared the results with that obtained using INSEY and found that the relationship between NDVI-ratio and the corn grain yield was stronger than that between INSEY and corn grain yield (r^2=0.65 vs. r^2=0.58).

Some other issues regarding GreenSeeker are summarized below. Walsh et al. (2013) conducted a trial which incorporated soil moisture into the GreenSeeker INSEY-based N recommendation algorithm; however no significant contribution of the soil moisture to the improvement of the algorithm was observed. Girma et al. (2006) also found soil moisture was not a good predictor for winter wheat yield prediction, but at the same time they found that the use of plant height improved prediction. A most tested commercial GreenSeeker system that can be used on-the-go for variable rate N application in the field is the GreenSeeker RT200 system, whose effectiveness has been tested and proven in soft red winter wheat N application studies (Thomason et al., 2011).

Crop Circle

In a study developing N fertilizer recommendations for corn using Crop Circle ACS-210, Dellinger et al. (2008) related the relative Green NDVI (RGNDVI) with the economic optimum

nitrogen rate (EONR). The RGNDVI was defined as the ratio of GNDVI from a test plot and that from the N-rich strip. Strong linear-plateau relationships were found between RGNDVI and EONR from either control plots or manure-preplant applied plots or from the combination of those plots ($p<0.0001$, $r^2=0.84$). On the contrary, poor statistical relationship between GNDVI and EONR was found based on the data from ammonium nitrate fertilizer-applied plots.

To find the best vegetation index for estimating EONR based on active Crop Circle, a number of indices were evaluated and the RGNDVI was found to be superior at corn growth stage V6 (Sripada et al., 2008). The established relationship equation between EONR and RGNDVI was a linear-floor model with a coefficient of determination of 0.79. The authors also investigated the N:corn price ratio and EONR so that EONR estimated using Crop Circle could be further adjusted according to the current N:corn price ratio to improve its usefulness to corn growers. Scharf and Lory (2009) also developed and calibrated a similar N sidedress recommendation algorithm for corn at stage V6-V7. Oliveria et al. (2013) further calibrated the EONR prediction algorithm (Scharf and Lory, 2009) and determined the best growth stage for sensor-based side-dressing as well as the sensor height, model, and wavelengths that best predict N need.

Quadratic-plateau regression models reflecting the relationship between Crop Circle ACS-210 sensor indices and differential from economic optimum nitrogen rate were established for corn to assess corn N stress at the V10 to V12 growth stages (Barker and Sawyer, 2010). Among a variety of vegetation indices, this study suggested three indices that best suited for

Crop Circle: RGNDVI, relative simple ratio index (RSRI), relative modified simple ratio index (RMSRI), and relative green difference vegetation index (RGDVI).

The above in-season N recommendation algorithms based on the Crop Circle are direct application and are also related to economic optimization, and therefore have the potential for benefits to corn growers. However, indirect solutions have also been developed. In a corn study, NDVI590 index (based on visible 590 nm and NIR 880 nm bands) from Crop Circle were used to estimate N status and grain yield (Solari et al., 2008). The comparison with the results obtained from the chlorophyll meter index CI590 showed that NDVI590 from Crop Circle was inferior in directing variable N applications. To make use of the advantages of both active optical sensor and passive chlorophyll meter, Solari et al. (2010) developed a Crop Circle algorithm for irrigated corn N recommendations based on 1) a previously-developed SPAD chlorophyll meter algorithm where a quadratic relationship was established between N application rate and the sufficiency index (SI) of the chlorophyll meter, and 2) a significant linear relationship found between SIs of chlorophyll meter and Crop Circle (Varvel et al., 2007).

Yara-N Sensor

Only a few published studies have been conducted using Yara N-sensor. Using simple ratio based VI from the Yara N-sensor, the biomass of winter wheat was estimated and the corresponding N redistribution strategies were then developed (Berntsen et al., 2006). A Yara N-Sensor based real-time variable N requirement computation algorithm, which was based on

relationships between chlorophyll content and crop N status, was determined for winter wheat and triticale (Zillmann et al., 2006). Partial least squares regression models based on Yara N-Sensor sensor readings and weather data such as air temperature and daily precipitation were constructed to predict protein content in malting barley (Soderstrom et al., 2010). The authors compared the models that utilized all possible combinations of wavelengths in simple ratios as input and those that only used some selected wavelengths. The middle infrared spectral band was very important in ensuring model performance. Mayfield and Trengove (2009) compared the outputs from the Yara N-Sensor with the measurements of wheat biomass, N uptake, and N content and found a high correlation between sensor data and all measurements except N content. Portz et al. (2012) derived a VI, which was 100 times the difference between reflectance from the bands of R760 and R730, from Yara N-Sensor^{TM} ALS to correlate to sugarcane N uptake and biomass, and found significant exponential relationships between sensor VI and N uptake or biomass.

Ground-based Active Optical Sensor Comparisons

Raper et al. (2013) compared three optical sensors, GreenSeeker, Crop Circle, and Yara N Sensor, in cotton leaf N status estimation using NDVI directly and found no significant performance difference among these sensors. Performance of Greenseeker and Crop Circle in N variability determination in corn was compared and both sensors were found to perform well, with no significant performance differences between them (Shaver et al., 2011). Similar conclusions were found in a sugarcane study (Amaral et al., 2013). In a cotton study where

GreenSeeker, Crop Circle, and CropScan were compared, the r^2 values of the relationships between each sensor readings and the EONR were found to be very close (Oliveira et al., 2013). Another study compared the performance of four spectral sensors including one passive radiometer and three active optical sensors in discriminating biomass parameters and N status in wheat cultivars (Erdle et al., 2011). The three active optical sensors were an active flash sensor (AFS), Crop Circle, and GreenSeeker. Because the first generation of GreenSeeker could only rely on NDVI-based indices and NDVI is strongly subject to the potential saturation effect, the other three sensors using indices based on NIR and red edge were found to be more reliable. The saturation effect occurs when leaves converge and overgrow the canopy. At that point, NDVI readings typically plateau between 0.9 and 0.9999, leaving little numerical room to record differences in crop status. Tremblay et al. (2009) compared the performance of GreenSeeker and Yara N-sensor in assessing the status of N in spring wheat and concluded that the NDVI values of the two sensors correlated well only at the early growth stage and that GreenSeeker only performed well where the NDVI values were greater than 0.5.

Since reported comparisons are currently very rare and unsystematic, and each sensor's company is still improving existing or developing new types of sensors, it's difficult to make a definite conclusion about which ground-based active-optical sensor is superior. Yara N-sensor seems to be the least to be used and it seems that until now GreenSeeker is more widely used because of the relatively mature algorithms for improving NUE. There is also abundant

information about the use of the GreenSeeker on the NUE website, http://nue.okstate.edu/, administered by Oklahoma State University.

Passive Optical Satellite Remote Sensing

Since the launch of Landsat 1 in 1972 (Mulla, 2013), satellite imagery has been more widely used in agriculture including crop N management and yield prediction. Bhatti et al. (1991) conducted a trial using Landsat imagery to estimate soil organic matter content and then used it as well as other ground-based measurements as auxiliary data to estimate wheat yield potential. Landsat 1 has four bands, green, red, and two infrared bands, with a resolution of 56 m × 79 m. On February 11, 2013, NASA launched Landsat 8 that provides moderate-resolution imagery from 15 meters to 100 meters and operates in the visible, near-infrared, short wave NIR, and thermal infrared spectrums (NASA, 2013). Other representative satellite imaging systems include: SPOT, MODIS, QuickBird, RapidEye, GeoEye, WorldView, NOAA-AVHRR, and etc., technical details of these systems can be easily found in corresponding website. Generally speaking, the newly launched satellite remote sensing systems provide higher spatial resolution, a greater variety of spectral bands, and higher revisit frequency. Satellite imagery in the visible and NIR bands are useful only when it is in the day and no cloud covering. Only the radar satellite remote sensing that is in essence an active sensing is not influenced by the weather condition.

Vegetation indices, especially NDVI, derived from satellite imagery have been reported to have high correlation with crop grain yield or N status. Shou et al. (2007) showed that the individual red, green, and blue spectral band reflectance values from QuickBird satellite imagery were highly correlated with winter wheat total N concentration and aboveground biomass. Mkhabela et al. (2005) found a strong linear relationship between cumulative NDVI derived from NOAA's (National Oceanographic and Atmospheric Agency) AVHRR (Advanced Very High Resolution Radiometer) satellite imagery and corn grain yield in the four agro-ecological regions of Swaziland. A strong correlation was found between vegetation condition index (VCI) derived from AVHRR remote sensing data and the winter wheat yield (Salazar et al., 2007). Later, the regression-based winter wheat yield prediction model was constructed using the principal components of a series of VCI. In a potato yield prediction study, three VIs including NDVI, LAI, and fraction of photosynthetically active radiation (fPAR) derived from coarse spatial resolution MODIS imagery were found to be highly correlated with potato yield (Bala and Islam, 2009). In exploring the potential of Sentinel-2 and Sentinel-3 satellite data in estimating total crop and grass chlorophyll and N content, the red-edge chlorophyll index ($CI_{red-edge}$), the green chlorophyll index (CI_{green}), and the MERIS terrestrial chlorophyll index (MTCI) were found to be most useful (Clevers and Gitelson, 2013).

The most convenient yet still effective way of predicting crop yield or N status using remote sensing data perhaps is to construct the empirical regression relationships between crop yield or N status and the vegetation indices from sensing data. To improve the prediction

accuracy, more often than not, other ancillary measurements other than the spectral indices were also incorporated into the regression model. A new vegetation index, general yield unified reference index, generated from AVHRR remote sensing data was found to be highly correlated with both field level yield and county level yield (Ferencz et al., 2004) and the developed yield prediction regression model was further evaluated using wheat and corn data in Hungary (Bognar et al., 2011). Bausch and Khosla (2010) extracted NGNDVI from QuickBird satellite multi-spectral data to estimate the nitrogen status of irrigated corn and proved the feasibility of using QuickBird satellite multi-spectral imagery for in-season N management at the V12 and later growth stage. In a sugar beet quality prediction using Landsat-5 and Landsat-7 imagery, Green NDVI was found to be the consistently best vegetation index to linearly relate beet sucrose concentration (Humburg et al., 2006). To estimate winter wheat yield with MODIS 250 m resolution imagery, Ren et al. (2008) established a multivariate linear regressive relationship between the spatial accumulation of NDVI and the winter wheat yield at the county level of Shandong Province, China, and concluded that the proposed model can be useful for regional crop yield prediction 40 days ahead the harvest time. Becker-Reshef et al. (2010) constructed a generalized regression-based model that took the seasonal maximum NDVI from MODIS as the main input parameter to predict winter wheat yields in Kansas and Ukraine. Power regression functions using the selected best 10-day average NDVI from MODIS data as independent variable were established to forecast the yields of four crops: barley, canola, field peas, and spring wheat (Mkhabela et al., 2011). Validation experiment results showed that the proposed

models can accurately predict yield one to two months before harvest. Soderstrom et al. (2010) constructed partial least squares models based on multispectral satellite remote sensing data (SPOT 5 and IRS-P6LISS-III) to make regional prediction of protein content in malting barley at the late growth stage. The models that used only remote sensing data were not as good as those that relied on both sensing data and weather data including air temperature and daily precipitation. Yang et al. (2009) evaluated the multispectral SPOT-5 satellite imagery in grain sorghum yield estimation. Based on the original 10-m resolution, images with pixel sizes of 20 and 30 m were also generated for comparison study. Vegetation indices, and the principal components as well, based on visible bands and mid-infrared band were derived from all three resolutions to relate to crop yield using stepwise multivariate linear regression. Results revealed that the coarser the resolution is, the more variation in yield can be explained by the sensing data. Prasad et al. (2006) predicted the corn yield of the state of Iowa using a piecewise linear regression model involving four independent variables: NDVI from AVHRR satellite imagery, soil moisture, surface temperature, and rainfall. A similar study conducted in Sudan for sorghum yield prediction based on remote sensing adopted the same four parameters mentioned above (Shamseddin and Adeeb, 2012). Schut et al. (2009) used a moisture stress index and the NDVI derived from either AVHRR or MODIS satellite imagery as the independent variables to construct partial least squares multivariate regression models for wheat yield prediction and concluded that these PLS models were better than their currently in-use yield forecasting system DAFWA.

Many approaches using satellite remote sensing were based on complicated crop growth models that utilize mathematical simulations, which are in contrast to the relatively simple empirical regression models adopted when using ground-based optical sensing. There are several limitations of the empirical regression models. Simple regression based approaches are applicable only for a given region and the same range of weather conditions where they were developed (Doraiswamy et al., 2005). Also, the accuracy of the empirical relationships between VI and yield is affected by the size of the data set used (Padilla et al., 2012). Regression models that rely only on the measurement of vegetation photosynthetic characteristics cannot capture the influence of events that reduce yield but do not reduce green biomass during vegetative growth (Becker-Reshef et al., 2010).

Crop growth model based yield predictions usually rely on leaf area index (LAI), or green leaf area index, or green area index (GAI) derived from satellite imagery. According to Fernandes et al. (2003), LAI is half the all-sided living foliage per unit ground surface area projected on the horizontal datum. Leaf area index is a key variable in many agricultural models and quantitatively measure the foliage density. It was reported that green LAI was closely related to wheat yield (Kouadio et al., 2012). Based on a 10-year winter wheat monitoring study, green LAI derived from MODIS satellite imagery was consistent with ground measurements at both regional scale and field level (Duveiller et al., 2012). Baez-Gonzalez et al. (2005) conducted a large-area corn yield prediction using Landsat-7 ETM+ data and LAI based yield prediction model. This model consists of two parts: LAI prediction using NDVI data from satellite imagery

and yield prediction using the predicted LAI. All of these predictions were based on some regression models. A regional corn and soybean crop yield simulation model was modified based on MODIS satellite imagery and climate-based physiological models that required daily average temperature, solar radiation and rainfall data (Doraiswamy et al., 2004; Doraiswamy et al., 2005). The LAI was first derived from the MODIS 250 m resolution NIR and VIS reflectance data and other parameters, and then LAI was used to help resolve the crop yield model parameters. Padilla et al. (2012) evaluated the GRAMI model (Maas, 1993a, b) developed to simulate the growth and yield of grain crops in estimating durum and bread wheat yield. The relationship between NDVI from Landsat-5 imagery and LAI was derived and used for LAI estimation. The estimated LAI was then used for the within-season calibration of GRAMI model. High spatial and temporal resolution Formosat-2 remote sensing NDVI data were used to estimate green LAI, which was further used to calibrate six parameters of the SAFY maize and sunflower biomass prediction models (Claverie et al., 2012). To predict corn, soybean, and spring wheat yield, green LAI was estimated using a modified transformed vegetation index derived from multispectral Landsat TM and SPOT data before it was further used by a functional crop model, STICS, to estimate crop yield (Jego et al., 2012). In a regional-level wheat yield prediction exercise, metrics derived from the shape of decreasing curves of green LAI temporal profiled were further used to construct a regression-based wheat yield prediction model (Kouadio et al., 2012). The green LAI in this study was estimated from MODIS satellite data. Another green LAI based corn grain yield prediction model was constructed using both MODIS data and

crop phenology information, and the model was verified and demonstrated to be useful for state level corn yield estimation (Sakamoto et al., 2013). Moriondo et al. (2007) used the AVHRR NDVI images and a crop phenology simulation model, CROPSYST, to predict regional-level wheat yield. Fraction of absorbed photosynthetically active radiation (FAPAR) was firstly estimated based on a linear relationship between FAPAR and NDVI, and FAPAR was then used to compute the above-ground biomass, and finally a harvest index obtained from the integration of the simulation sub-model and NDVI data transformed the biomass to yield.

In a comparison of different optical sensing systems, including the RapidEye^{TM} satellite remote sensing satellite, to predict site-specific N fertilization rate, it was found that satellite imagery would not be suitable for determining N-rates unless the red edge inflection point (REIP) were first calculated (Wagner and Hank, 2013). Other useful techniques in crop yield estimation or monitoring using satellite imagery include artificial neural network model development using NDVI and other measurements as input (Jiang et al., 2004), multiple-frame approach utilizing the advantages of two or more sampling data frames with one being complete but expensive to sample and other frames inexpensive to sample but incomplete (Das and Singh, 2013), and multi-temporal image fusion of satellite imagery with different spatial resolutions and from different sensors (Amoros-Lopez et al., 2013). Regression based models and crop growth based models are widely used, with either having their own advantages and disadvantages. There are currently few studies published that make direct and practical comparison of the two types of yield prediction models.

Summary

Numerous studies have confirmed the benefits of using optical sensing for N fertilizer management. Based on a mid-season N recommendation strategy supported by active optical sensing technology, the NUE of winter wheat has been improved more than 15% (Raun et al. 2002). Compared with a NUE of 33% based on 90 kg N ha-1 fertilization rate, a higher NUE of 41% was achieved based on optimum N rates obtained from an active optical sensor-based algorithm for winter wheat (Tubana et al. 2008a). In winter wheat, the NUE of using active optical sensing was 61.3% compared to a very low NUE of 13.1% resulted by common farmer practices (Li et al. 2009). Corn NUE has also been improved from 56% using a fixed N rate to 65% using NFOA-based N rates (Tubana et al. 2008b). Optical sensing based N management not only can improve NUE, but also can result in more homogeneous quality and less harvesting time and cost. For example, protein levels with greater consistency averaging 0.2-0.5% above target in cereal crops and an 80% reduction in lodging rates compared with crops where nitrogen was applied under conventional practices were observed (Yara-International, 2013). All these promising results indicate the potential of extension of optical remote sensing based algorithms in crop N management.

To continue to improve crop NUE is still a great challenge. When a crop is grown in different locations and years, NUE can be quite different even for the same genotype (Baligar et al., 2001). Therefore, including ancillary data such as plant (e.g., plant height, leaf temperature, etc.), soil (e.g., soil texture, soil bulk density, soil pH, etc.), and weather data (e.g., air

temperature, daily precipitation, etc.) in the N recommendation systems might be useful in increasing in-season N recommendation accuracy. In addition, remote sensing reflectance data quality and accordingly N status or crop yield or quality prediction can be greatly affected by a number of factors (Barker and Sawyer, 2013; Kim et al., 2012; Samborski et al., 2009).

N deficiency is not the only factor that influences crop yield and quality, other nutrients can also have significant impact on them, as can environmental and pest management factors. Therefore the causes for variability in crop yield or quality must be adequately understood to ensure the use of remote sensing based variable rate N application only when N is the main growth-limiting factor. To develop reliable and versatile in-season variable rate N recommendation algorithms, it is no easy a thing to optimally select the most appropriate optical remote sensing system, canopy reflectance vegetation indices, ancillary measurements, and prediction model combination. More profitability analyses of remote sensing-based methods used for in-season variable rate N application need to be conducted to encourage the adoption of improved site-specific nutrient strategies by farmers.

MATERIALS AND METHODS

Crops and Study Site-Years

Experiments were conducted in 2012 and 2013 on four crops; sugar beet (*Beta vulgaris*, L), spring wheat (*Triticum aestivum*, L.), corn (*Zea mays*, L.) and sunflower (*Helianthus annuus*, L.). Detailed site and crop production information is provided in Table 1.

Nitrogen Fertilization and Plot Design

The studies were organized using a randomized complete block design (RCBD) with four replications and six N rate treatments as ammonium nitrate (34-0-0) granules applied within about a week of seeding. The N treatments for corn, spring wheat, and sunflower were 0, 45, 90, 135, 180, and 225 kg ha^{-1}, and the treatments for sugar beet were 0, 34, 67, 101, 135, and 168 kg ha^{-1}. For all site years, each experimental unit was 9.1 m by 9.1 m. Row width and the GPS coordinates are listed in Table 1. Soil samples from the 0-15 cm and 15-60 cm depths were collected at each site in each year before fertilizer application to determine residual soil nitrate, plant available P, K and other relevant soil chemical properties. The tables in the appendix list the soil test results for each site-year.

Ground-Based Active Optical Sensors and Canopy Reflectance Data Collection

Two handheld ground-based active optical sensors were used to collect crop canopy optical reflectance data, as shown in Figure 3 and Figure 4. The Holland Crop Circle ACS-470 Sensor™ (Holland Scientific Inc., Lincoln, Nebraska, USA) was used in both years. This sensor has 6 narrowband interference filters but only three optical measurement channels, so each time

only three of the filters are used. The 6 filter wavelengths were 532 nm, 550 nm, 670 nm, 700 nm, 730 nm, and 760 nm. The 670 nm (red), 730 nm (red edge), and 760 nm (NIR) were used to calculate NDVI (using red and NIR band) and red edge NDVI (using red edge and NIR band). In 2012, the first generation of GreenSeeker^{TM} (NTech Industries, Inc., Ukiah, CA, USA), which provides 660 nm (red) and 770 nm (red edge) two channels, was used and NDVI was calculated. The latest second generation of GreenSeeker has two more red edge channels including 710 nm and 735 nm, and it was used in the 2013 growing season. Optical reflectance was measured using the sensors positioned about 50 cm above the crop canopy, with the operator and walking along a representative middle row within the defined area of each experimental unit/plot. Sensing date, growth stage, and other information such as planting date and harvesting date can be found in Table 2. In 2012, sensing for sugar beet was also conducted immediately before each harvest and the sensing date information is listed in Table 3.

Based on the NDVI data, In Season Estimate of Yield (INSEY) was calculated using the formula below:

$$INSEY = NDVI / GDD \quad (7)$$

where GDD refers to the accumulated positive growing degree days from planting date to sensing date and was obtained from the website of North Dakota Agricultural Weather Network (http://ndawn.ndsu.nodak.edu/).

Table 1. Background information for crops and soils in the experiments.

Year	Crop	Cultivar	Site	NW corner GPS coordinate	Previous crop	soil types and slope	row width	Seeding rate
							--- cm ---	-- seeds ha^{-1} --
2012	spring wheat	Kelby	Gardner, ND	47°10'19.425"N 96°55'12.471"W	soybean	Fargo-Enloe complex, 0 to 2 % slopes	20	3,850,000
2012	spring wheat	Argent	Valley City, ND	46°52'58.656"N 97°54'52.072"W	sunflower	Barnes-Svea loams, 3 to 6 % slopes	20	2,970,000
2013	spring wheat	Kelby	Gardner, ND	47°10'12.322"N 96°54'03.359"W	soybean	Fargo-Enloe complex, 0 to 2 % slopes	20	2,470,000
2013	spring wheat	Argent	Valley City, ND	46°52'41.906"N 97°54'46.331"W	sunflower	Barnes-Svea loams, 3 to 6 % slopes	20	2,570,000
2012	corn	DeKalb 42-72	Durbin, ND	46°50'59.021"N 97°09'29.045"W	corn	Fargo-Hegne silty clays, 0 to 1 % slopes	56	84,000
2012	corn	NK 17P	Valley City, ND	46°53'04.814"N 97°54'55.421"W	spring wheat	Swenoda-Barnes complex, 3 to 6 % slopes	76	70,400
2013	corn	DKC43-10 or Proseed 1193 VT3	Arthur, ND	47°02'04.176"N 97°07'48.268"W	soybean	Fargo silty clay loam, 0 to 1 % slopes	56	86,500
2013	corn	NK 17P	Valley City, ND	46°53'26.218"N 97°55'05.695"W	spring wheat	Swenoda-Barnes complex, 3 to 6 % slopes	76	65,700

(continues)

Table 1. Background information for crops and soils in the experiments (continued).

Year	Crop	Cultivar	Site	NW corner GPS coordinate	Previous crop	soil types and slope	row width	Seeding rate
							--- cm ---	-- seeds ha^{-1} --
2012	sugar beet	VanDerHave 36813RR	Crookston, MN	47°47'58.426"N 96°35'55.436"W	spring wheat	Bearden-Colvin complex, 0 to 1% slopes	56	141,000
2012	sugar beet	Crystal 095	Amenia, ND	46°58'34.623"N 97°15'04.762"W	spring wheat	Fargo silty clay, 0 to 1 % slopes	56	167,000
2013	sugar beet	Crystal 875	Casselton, ND	46°51'43.782"N 97°18'47.800"W	spring wheat	Fargo silty clay, saline, 0 to 1 % slopes	56	150,000
2013	sugar beet	Seedex Xavier	Thompson, ND	47°45'00.656"N 97°05'23.046"W	spring wheat	Bearden silty clay loam, 0 to 1 % slopes	56	148,000
2012	sunflower	CHS RH 1121 confection	Cummings, ND	47°31'45.677"N 97°06'52.330"W	corn	Glyndon silt loam, saline, 0 to 1 % slopes	76	44,500
2012	sunflower	CropPlan 555 NSCLDR	Valley City, ND	46°52'35.815"N 97°56'27.728"W	spring wheat	Fordville loam, 0 to 2 % slopes	76	64,000
2013	sunflower	CHS RH 1121 confection	Cummings, ND	47°32'31.989"N 97°01'41.687"W	corn	Divide loam, 0 to 2 % slopes	55	44,500
2013	sunflower	Syngenta 3495 oilseed	Valley City, ND	46°52'45.234"N 97°54'15.948"W	corn	Barnes-Buse loams, 3 to 6 % slopes	76	66,700

Table 2. Sensor reading information for spring wheat, sugar beet, corn and sunflower trials, 2012 and 2013.

Site-year	Crop	Planting date	First sensing date	First sensing growth stage	Second sensing date	Second sensing growth stage	Harvest date (s)
Gardner 2012	spring wheat	Apr. 7	May 23	V4	Jun. 6	Flag leaf	Jul. 26
Valley City 2012	spring wheat	Mar. 31	May 23	V4	Jun. 6	V5	Jul. 26
Gardner 2013	spring wheat	May 6	Jun. 17	V4	Jun. 25	V5	Aug. 12
Valley City 2013	spring wheat	May 7	Jun. 17	V4	Jul. 25	V5	Aug. 13
Durbin 2012	corn	May 3	Jun. 15	V6	Jun. 29	V12	Sep. 22
Valley City 2012	corn	May 3	Jun. 15	V6	Jun. 29	V12	Sep. 22
Arthur 2013	corn	May 10	Jun. 20	V6	Jul. 23	V14	Sep. 24
Valley City 2013	corn	May 15	Jun. 25	V6	Jul. 17	V12	Oct. 8

(continues)

Table 2. Sensor reading information for spring wheat, sugar beet, corn and sunflower trials, 2012 and 2013 (continued).

Site-year	Crop	Planting date	First sensing date	First sensing growth stage	Second sensing date	Second sensing growth stage	Harvest date (s)
Crookston 2012	sugar beet	Apr. 25	Jun. 4	V6	Jun. 21	V14	Aug. 15 (1st); Aug 29 (2nd); Sep. 15 (3rd)
Amenia 2012	sugar beet	Apr. 12	May 24	V6	Jun. 13	V14	Aug. 15 (1st); Aug 28 (2nd)
Casselton 2013	sugar beet	May 13	Jun. 20	V8	Jul. 10	V12 to 14	Aug. 27 (1st) ; Sep. 16 (2nd);Sep. 30 (3rd)
Thompson 2013	sugar beet	May 14	Jun. 20	V8	Jul. 10	V12	Aug. 27 (1st) ; Sep. 17 (2nd) ; Oct. 1 (3rd)
Cummings 2012	Sunflower (confectionery)	May 7	Jun. 19	V8	Jul. 3	V14	Sep. 24
Valley City 2012	Sunflower (oilseed)	May 16	Jun. 19	V6	Jul. 10	V12	Sep. 28
Cummings 2013	Sunflower (confectionery)	May 29	Jul. 2	V8	Jul. 18	V16	Oct. 17
Valley City 2013	Sunflower (oilseed)	Jun. 3	Jul. 3	V8	Jul. 22	V18	Oct. 8

Figure 3. Holland Crop Circle™ handheld system (http://hollandscientific.com/crop-circle-handheld-system/).

Figure 4. GreenSeeker™ handheld system (http://www.molisol.com/sitio/mapeo-de-indice-verde.php?sub=-1).

Table 3. 2012 sugar beet harvest sensing dates.

site-year	first harvest sensing	second harvest sensing	third harvest sensing
Crookston 2012	Aug. 15	Aug. 29	Sep. 15
Amenia 2012	Aug. 15	Aug. 28	Not conducted

Satellite Imagery

RapidEye™ Ortho Products (Level 3A) satellite imagery (http://blackbridge.com/rapideye/products/ortho.htm) was also used in our research as an alternative to the ground-based optical sensing data. Figure 5 illustrates this satellite imaging system. This level of imagery has already been subjected to radiometric, sensor and geometric corrections before being released. The imagery has a 5-meter spatial resolution and includes 5 broad spectral bands: Blue (440-510 nm), Green (520-590 nm), Red (630-685 nm), Red Edge (690-730 nm), and NIR (760-850 nm). Four different NDVI indices including red NDVI, blue NDVI, red edge NDVI, and green NDVI can be extracted from an imagery using different combinations of visible spectral band and NIR band. NDVI extraction from RapidEye satellite imagery was conducted using GRASS GIS 6.4.2 (GRASS Development Team, 2012), an open source and free GIS software, and MATLAB 8.0 (The Mathworks, Inc., 2012). The dates of the satellite imagery are provided in Table 4.

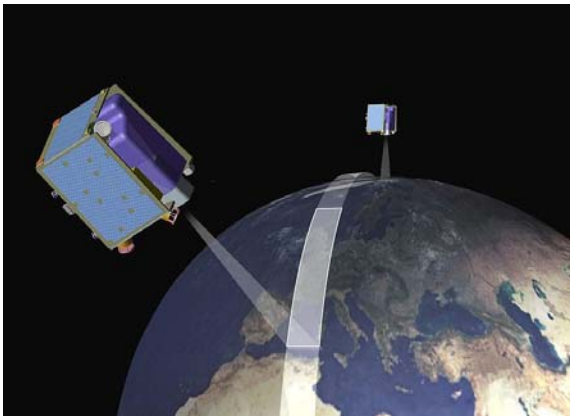

Figure 5. RapidEye™ satellite imagery system (RapidEye AG, Germany) (http://en.wikipedia.org/wiki/File:RapidEye_Satellites_Artist_Impression.jpg).

Table 4. Satellite imagery dates for spring wheat, corn, sugar beet and sunflower 2012 and 2013.

site-year	crop	imagery date
Gardner 2012	spring wheat	Jul. 03
Valley City 2012	spring wheat	not applicable
Gardner 2013	spring wheat	Jun. 24
Valley City 2013	spring wheat	Jun. 15
Durbin 2012	corn	Aug. 16
Valley City 2012	corn	Aug. 16
Arthur2013	corn	Jun. 24
Valley City 2013	corn	Jul. 21
Crookston 2012	sugar beet	Jul. 01; Aug. 16
Amenia 2012	sugar beet	Jul. 11; Aug. 16
Casselton 2013	sugar beet	Jun. 24
Thompson 2013	sugar beet	Aug. 13
Cummings 2012	Sunflower (confection)	Jul. 01; Aug. 16
Valley City 2012	Sunflower (oilseed)	Aug.10
Cummings 2013	Sunflower (confection)	Jun. 24
Valley City 2013	Sunflower (oilseed)	Jun. 24

Plant Height Data Measurement

Plant height in this thesis means the height from ground to the upmost mature leaf of the plant. In 2012, the plant height was measured using a tape by hand. In 2013, both a tape and an ultrasonic distance sensor (Senix Model; ToughSonic TSPC-30S1-232, Senix Corporation, Hinesburg, VT) mounted on a self-made special bicycle were used to measure the plant height. By default, plant height in our regression models refers to plant height measured by tape. For

2013 plant height data, the “tapeHeight” means plant height measured by tape and the “sensorHeight” stands for plant height measured by height sensor.

Crop Yield and Quality Data

The harvest dates of each site-year crop are listed in Table 2. Only the middle 1.22 m width of area in each spring wheat subplot was harvested. Only the middle row or the row close to middle of each subplot of Corn and sunflower was harvested by hand. In 2012, Amenia sugar beet were harvested two times and Crookston sugar beet 3 times, with each harvest consisting of 3.05 meters of row of each subplot. In 2012, the sugar beet canopy sample was also harvested for canopy total N analysis. In 2013, both Casselton and Thompson sugar beet were harvested thrice and no canopy samples collection was made.

Both the wheat and corn dry grain yield was determined using a weighing scale and a test machine, where the grain moisture and test weight were also measured. Spring wheat grain protein content was determined using an Infra Tec1226 grain analyzer made by Dresden, Germany (Franzen et al., 2008) and was adjusted based on 12.0 percent U.S. standard moisture basis (Wheat Marketing Center, 2008). Sunflower yield was measured using a weighing scale. Confectionery sunflower seeds were also subject to screening test, meat to shell ratio test, and maximum length and maximum width test at the USDA sunflower testing center. Through screening test, the total weight percentage of sunflower seeds that cannot pass the 0.87, 0.79, and 0.71 cm sieves, respectively, can be obtained, of which the most important one is the first one

(0.87 cm content). A nuclear magnetic resonance oil test (NMR test) was applied to NuSun oilseed sunflower seeds at the USDA sunflower testing center, Fargo, ND, to obtain the oil percent adjusted to 10% moisture. Besides determining 2012 sugar beet canopy total Kjeldahl nitrogen content, both years' beet root yield in metric ton per ha, recoverable beet sugar yield in kg per ha, and other indices such as beet stands per ha, concentration of ammonium N, concentration of K and P, etc. were analyzed at the East Grand Forks American Crystal Sugar Tare Laboratory.

Statistical Data Analysis Methods and Software

SAS 9.3 (SAS Institute, Inc., 2013) was used to perform analysis of variance (ANOVA) to determine the effect of N application rate on crops yield and quality. Yield and quality means were grouped based on LSD.

Two data preprocessing methods were compared in this study. One is directly using the individual sub-plot yield and averaged sensing data of each sub-plot to do regression analysis; the other is averaging the individual sub-plot yield and sensing data over each N fertilization treatment across all site-year plots involved in a model before doing any regression analysis. The better model in terms of coefficient of determination (r^2 value) and model significance was chosen according to the regression results from these two methods.

Three regression models, linear ($y = ax + b$), exponential ($y = ae^{bx}$), and quadratic polynomial ($y=ax^2+bx+c$), were compared in this study. The latter two can be viewed as general

linear models. All of these models were constructed and tested using the PROC REG of SAS 9.3 (SAS Institute, Inc., 2013). In analyzing any one of the three types of models, if the model p-value is greater than 0.05 or the p-value for the key coefficient is greater than 0.05, the model is regarded as insignificant or invalid. Key coefficients were the “a” in linear model, “b” in exponential model, and “a” in quadratic polynomial model. And “GS” and “CC” refers to GreenSeeker and Crop Circle, respectively.

For corn, ground-based sensing INSEY and satellite imagery INSEY were related to yield. For other crops, satellite imagery INSEY was related to both yield and quality, but the ground-based first sensing and second sensing (see Table 2 for details) INSEYs (including INSEY × plant height) were related to yield and quality, respectively. Besides, the sugar beet harvest sensing data, namely, ground-based sensing data collected on the same days of harvesting, were related to the corresponding harvest yield and quality. In 2012, two sugar beet quality indices, recoverable sugar yield and top total N were subjected to regression analysis; in 2013, only the recoverable sugar yield was considered. Except sugar beet root yield, yield for other crops refers to dry grain or dry seed yield, of which corn yield and sunflower yield were further adjusted using the corresponding plant stand information based on the following formula:

$$\text{Adjusted yield} = \text{yield} / \text{stand coefficient} \quad (8)$$

where, stand coefficient = plant stand of individual plot / average of plant stand over all plots.

Except sunflower, ground-based or satellite-based sensing data for the two sites of each of the other crops in each individual year were pooled for analysis. Sunflower data were firstly analyzed for each individual site-year, and then analyzed for two-year pooled data of each different type of sunflower seed (oilseed or confectionery). Comprehensive studies using all site-year data were also conducted.

RESULTS AND DISCUSSIONS FOR SUGAR BEET

Analysis of the Influence of N Fertilization Rate on Yield and Quality

ANOVA analysis results for the four site-year sugar beet yield and quality data are given in Table 5 through Table 14. In each of these tables, means with the same letter in the same column are not significantly different at the 0.05 significance level based on LSD t-test. Sugar beet yield means the beet root yield per hectare, and the most important quality index is the recoverable sugar yield per hectare. In 2012, the sugar beet top total N estimated from the top samples is an important quality index (Franzen, 2003) too. Gehl and Boring (2011) found that N rate had significant linear relationship with sugar beet root yield, but based on our two-year and four-site study, it seems that no clear trend of the influence of the N fertilization rate on the root yield or recoverable sugar yield per hectare could be found, which most probably due to high nitrate residuals (see Appendix Table A1-A4) or other extreme unfavorable conditions. However, it was found from Table 5 to Table 7 that N fertilization rate had a positive impact on the recoverable top total N per hectare. Most of the N absorbed by the sugar beet plant is accumulated in the top and the root needs only about 30% of the absorbed N (Gehl and Boring, 2011). So more extra N may go and accumulate to the top.

Table 5. Amenia 2012 first (August 15) harvest sugar beet ANOVA analysis.

N rate (kg ha^{-1})	Root yield (Mg ha^{-1})	Recoverable sugar yield (kg ha^{-1})	Recoverable sugar yield (kg (Mg beets)$^{-1}$)	Net sugar (%)	Sugar loss to molasses (%)	Amino-N (ppm)	Beet stands (thousand ha^{-1})	Top total N (kg ha^{-1})
0	39.61a†	7175.5a	181.5a	18.15a	1.37c	485.5c	126a	25.12c
34	42.21a	7474.8a	178.9a	17.89a	1.41bc	516.3bc	139a	37.65bc
67	41.75a	7581.3a	181.7a	18.17a	1.49bc	579.8bc	129a	49.03ab
101	47.00a	8007.3a	171.9a	17.19a	1.56b	615.8b	131a	53.78ab
135	47.87a	8315.5a	174.2a	17.42a	1.53bc	620.3b	132a	47.54abc
168	44.28a	7768.2a	175.7a	17.57a	1.79a	782.8a	144a	63.72a

† Means with the same letter in the same column are not significantly different at the 0.05 significance level based on LSD t-test.

Table 6. Amenia 2012 second (August 28) harvest sugar beet ANOVA analysis.

N rate (kg ha^{-1})	Root yield (Mg ha^{-1})	Recoverable sugar yield (kg ha^{-1})	Recoverable sugar yield (kg (Mg beets)$^{-1}$)	Net sugar (%)	Sugar loss to molasses (%)	Amino-N (ppm)	Beet stand (thousand ha^{-1})	Top total N (kg ha^{-1})
0	43.68b†	8,832a	202.7a	20.27a	1.40c	564 d	132a	31.10b
34	47.54ab	9,411a	199.5a	19.95a	1.58bc	674 cd	131a	53.39ab
67	48.20ab	9,556a	198.3a	19.83a	1.73b	797 bc	139a	75.41a
101	55.26a	9,988a	183.6a	18.36a	1.83ab	858.3ab	139a	64.87a
135	48.14ab	9,376a	196.1a	19.61a	1.78b	826.8ab	126a	69.87a
168	45.61ab	8,898a	195.2a	19.52a	2.03a	997.5a	125a	72.61a

† Means with the same letter in the same column are not significantly different at the 0.05 significance level based on LSD t-test.

Table 7. Crookston 2012 first (August 15) harvest sugar beet ANOVA analysis.

N rate (kg ha^{-1})	Root yield (Mg ha^{-1})	Recoverable sugar yield (kg ha^{-1})	Recoverable sugar yield (kg (Mg beets)$^{-1}$)	Net sugar (%)	Sugar loss to molasses (%)	Amino-N (ppm)	Beet stands (thousand ha^{-1})	Top total N (kg ha^{-1})
0	58.06a†	8,815a	151.8ab	15.18ab	1.32bc	443.3c	120a	76.9c
34	58.19a	9,124a	156.9a	15.69a	1.31c	434.5c	113a	70.4c
67	61.05a	9,256a	151.6ab	15.16ab	1.37bc	490.3bc	120a	93.9bc
101	61.12a	9,040a	147.8b	14.78b	1.42bc	518.0b	120a	107.4b
135	60.79a	8,866a	145.9bc	14.59bc	1.44b	517.3b	115a	140.0a
168	61.99a	8,697a	140.6c	14.06c	1.57a	587.5a	115a	144.2a

† Means with the same letter in the same column are not significantly different at the 0.05 significance level based on LSD t-test.

Table 8. Crookston 2012 second (August 29) harvest sugar beet ANOVA analysis.

N rate (kg ha^{-1})	Root yield (Mg ha^{-1})	Recoverable sugar yield (kg ha^{-1})	Recoverable sugar yield (kg (Mg beets)$^{-1}$)	Net sugar (%)	Sugar loss to molasses (%)	Amino-N (ppm)	Beet stands (thousand ha^{-1})	Top total N (kg ha^{-1})
0	67.24a†	11,930a	177.4a	17.74a	1.54a	579.8a	113ab	130.0a
34	69.91a	12,450a	178.1a	17.80a	1.51a	546.3a	120ab	120.7a
67	69.31a	12,580a	181.8a	18.18a	1.45a	514.3a	112ab	112.0a
101	64.25a	11,710a	182.7a	18.27a	1.45a	541.5a	106b	119.3a
135	66.98a	11,920a	178.1a	17.81a	1.40a	488.0a	128a	114.5a
168	65.91a	11,740a	179.1a	17.91a	1.51a	547.5a	104b	126.8a

† Means with the same letter in the same column are not significantly different at the 0.05 significance level based on LSD t-test.

Table 9. Casselton 2013 first (August 27) harvest sugar beet ANOVA analysis.

N rate (kg ha^{-1})	Root yield (Mg ha^{-1})	Recoverable sugar yield (kg ha^{-1})	Recoverable sugar yield (kg (Mg beets)$^{-1}$)	Net sugar (%)	Sugar loss to molasses (%)	Amino-N (ppm)	Beet stands (thousand ha^{-1})
0	31.96b†	5,796a	181.7a	18.17a	1.58c	505.3c	128a
34	32.56ab	5,872a	180.6ab	18.06ab	1.59c	524.5c	135a
67	32.69ab	5,996a	183.3a	18.33a	1.72bc	587.0bc	123a
101	33.96ab	6,142a	181.6a	18.16a	1.95ab	712.8ab	135a
135	33.76ab	5,934a	176.0ab	17.60ab	1.93ab	704.3ab	125a
168	36.42a	6,254a	172.3b	17.23b	2.10a	771.0a	135a

† Means with the same letter in the same column are not significantly different at the 0.05 significance level based on LSD t-test.

Table 10. Casselton 2013 second (September 16) harvest sugar beet ANOVA analysis.

N rate (kg ha^{-1})	Root yield (Mg ha^{-1})	Recoverable sugar yield (kg ha^{-1})	Recoverable sugar yield (kg (Mg beets)$^{-1}$)	Net sugar (%)	Sugar loss to molasses (%)	Amino-N (ppm)	Beet stands (thousand ha^{-1})
0	43.14a†	7,330a	169.8ab	16.98ab	1.17bc	348.3bc	131a
34	43.48a	7,500a	171.2a	17.12a	1.08c	314.0c	141a
67	45.54a	7,740a	170.0ab	17.00ab	1.36ab	461.5abc	125a
101	45.21a	7,590a	168.2ab	16.82ab	1.39ab	491.5ab	139a
135	49.40a	8,100a	164.0ab	16.40ab	1.45a	529.3a	131a
168	51.20a	8,250a	160.7b	16.07b	1.58a	609.3a	138a

† Means with the same letter in the same column are not significantly different at the 0.05 significance level based on LSD t-test.

Table 11. Casselton 2013 third (September 30) harvest sugar beet ANOVA analysis.

N rate (kg ha^{-1})	Root yield (Mg ha^{-1})	Recoverable sugar yield (kg ha^{-1})	Recoverable sugar yield (kg (Mg beets)$^{-1}$)	Net sugar (%)	Sugar loss to molasses (%)	Amino-N (ppm)	Beet stands (thousand ha^{-1})
0	47.27ab†	8,126ab	171.9ab	17.19ab	1.31cd	388.8cd	134a
34	42.54b	7,406b	173.1a	17.31a	1.14d	297.3d	132a
67	54.79ab	9,511ab	172.9a	17.29a	1.34c	399.5cd	113a
101	50.60ab	8,328ab	164.8abc	16.48abc	1.45bc	468.5bc	120a
135	60.45a	9,873a	163.4bc	16.34bc	1.52ab	510.8ab	141a
168	54.86ab	8,660ab	157.4c	15.74c	1.64a	607.0a	122a

† Means with the same letter in the same column are not significantly different at the 0.05 significance level based on LSD t-test.

Table 12. Thompson 2013 first (August 27) harvest sugar beet ANOVA analysis.

N rate (kg ha^{-1})	Root yield (Mg ha^{-1})	Recoverable sugar yield (kg ha^{-1})	Recoverable sugar yield (kg (Mg beets)$^{-1}$)	Net sugar (%)	Sugar loss to molasses (%)	Amino-N (ppm)	Beet stands (thousand ha^{-1})
0	42.34b†	6,693a	158.3ab	15.83ab	1.20ab	318.5ab	113a
34	54.59a	8,251a	151.0bcd	15.10bcd	1.23ab	342.8ab	109a
67	50.20ab	7,988a	159.1a	15.91a	1.12b	273.3b	100a
101	48.67ab	7,233a	148.3cd	14.83cd	1.32ab	362.5ab	109a
135	48.27ab	7,443a	155.3abc	15.53abc	1.35ab	375.0ab	103a
168	46.94ab	6,959a	147.3d	14.73d	1.42a	419.8a	101a

† Means with the same letter in the same column are not significantly different at the 0.05 significance level based on LSD t-test.

Table 13. Thompson 2013 second (September 17) harvest sugar beet ANOVA analysis.

N rate (kg ha^{-1})	Root yield (Mg ha^{-1})	Recoverable sugar yield (kg ha^{-1})	Recoverable sugar yield (kg (Mg beets)$^{-1}$)	Net sugar (%)	Sugar loss to molasses (%)	Amino-N (ppm)	Beet stands (thousand ha^{-1})
0	56.86c†	8,419b	148.4a	14.84a	0.81b	184.0b	100a
34	57.66bc	8,187b	141.6ab	14.16ab	0.82b	182.8b	100a
67	75.50a	11,170a	148.0a	14.80a	0.92ab	231.3ab	112a
101	63.98abc	9,369ab	146.6a	14.66a	0.95ab	247.0ab	97a
135	66.05abc	8,939b	133.1b	13.31b	1.07a	293.3a	88 a
168	70.31ab	9,303ab	133.4b	13.34b	1.11a	303.3a	91a

† Means with the same letter in the same column are not significantly different at the 0.05 significance level based on LSD t-test.

Table 14. Thompson 2013 third (October 1) harvest sugar beet ANOVA analysis.

N rate (kg ha^{-1})	Root yield (Mg ha^{-1})	Recoverable sugar yield (kg ha^{-1})	Recoverable sugar yield (kg (Mg beets)$^{-1}$)	Net sugar (%)	Sugar loss to molasses (%)	Amino-N (ppm)	Beet stands (thousand ha^{-1})
0	69.64a†	11,160a	160.2a	16.02a	0.86b	194.5b	109a
34	64.32a	9,737a	150.3a	15.03a	0.90ab	213.0b	113a
67	77.10a	12,170a	158.3a	15.83a	0.90ab	216.5b	107a
101	73.90a	11,780a	160.2a	16.02a	0.91ab	230.0ab	103ab
135	72.57a	11,490a	157.4a	15.74a	0.94ab	246.8ab	104a
168	66.71a	10,310a	154.6a	15.46a	1.02a	292.3a	84b

† Means with the same letter in the same column are not significantly different at the 0.05 significance level based on LSD t-test.

Relationships between Root Yield and Ground-Based Sensor Readings, 2012

First Harvest Root Yield Prediction

The INSEY data for each sensing period for both 2012 sites were pooled and related to the first harvest sugar beet root yield. A summary of the first (V6-8) and second (V12-14) GS sensing regression analysis results are listed in Table 15. Similarly, the r^2 values of the regression models based on CC first (V6-8) or second (V12-14) sensing data are given in Table 16. These models were based on the single plot regression method. Exponential models were found to be the best ones for relating CC first harvest sensing INSEY with the first harvest root yield, and the regression results are summarized in Table 17. No regression models were established between GS first harvest sensing INSEY and the first harvest root yield because no GS sensing was taken in 2012 at Amenia due to technical problems with the GS instrument.

Similar conclusions can be drawn from Table 15 and Table 16 in that 1) second sensing data without plant height information has closer relationships with the first harvest root yield, 2) only the plant height measured at the first time helped improve the model performance, 3)

exponential models and the linear models performed similarly and both of them were more consistent than the quadratic polynomial models. The reason for the poor performance of the second plant height is most probably due to the extremely dry weather in 2012, which hindered the plant from normal development. Take Amenia site in 2012 for example, sugar beet was planted in April and sensed the second time in June. According to NDAWN rainfall data (http://ndawn.ndsu.nodak.edu/get-table.html?station=23&variable=mdr&year=2014&ttype=monthly&quick_pick=&begin_date=2011-01&count=36), the total rainfall of April – June in 2012 was only half and one third of that in 2011 and 2013, respectively. The very high r^2 values in Table 17 indicate that the INSEY and the harvest beet yield in the same day are highly correlated with each other, and that INSEY is an excellent predictor of the sugar beet root yield the date of harvest.

Table 15. r^2 values of the relationships between 2012 GS INSEY and first harvest root yield.

Model†	GS V6-8 red INSEY	GS V6-8 red INSEY × plant height	GS V12-14 red INSEY	GS V12-14 red INSEY × plant height
Exponential	0.434	0.615	0.645	0.302
Linear	0.468	0.649	0.670	0.316

† Model is significant at 0.05 significance level.

Table 16. r^2 values of the relationships between 2012 CC INSEY and first harvest root yield.

Model†	CC V6-8 red INSEY	CC V6-8 red INSEY × plant height	CC V6-8 red edge INSEY	CC V6-8 red edge INSEY × plant height	CC V12-14 red INSEY	CC V12-14 red INSEY × plant height	CC V12-14 red edge INSEY	CC V12-14 red edge INSEY × plant height
Exponential	0.546	0.718	0.622	0.727	0.695	0.369	0.703	0.267
Linear	0.558	0.732	0.630	0.738	0.717	0.383	0.721	0.276

† Model is significant at 0.05 significance level.

Table 17. r^2 values of the relationships between 2012 CC first harvest INSEY and first harvest root yield

Model†	CC first harvest red edge INSEY	CC first harvest red edge INSEY × plant height	CC first harvest red INSEY	CC first harvest red INSEY × plant height
Exponential	0.913	0.857	0.944	0.872
Linear	0.909	0.854	0.939	0.870

† Model is significant at 0.05 significance level.

Second Harvest Root Yield Prediction

The INSEY data for each sensing period for both 2012 sites were pooled and related to the second harvest sugar beet root yield. Very similar regression results and same conclusions were obtained in this section as those obtained in last section. The r^2 values of the exponential and linear regression models were listed in Table 18 to Table 20. All the models listed in these tables are highly significant each with a p-value less than 0.0001. Since in most cases the quadratic models were not significant or consistent, they were not summarized here.

Table 18. r^2 values of the relationships between 2012 GS INSEY and second harvest root yield.

Model†	GS V6-8 red INSEY	GS V6-8 red INSEY × plant height	GS V12-14 red INSEY	GS V12-14 red INSEY × plant height
Exponential	0.387	0.559	0.647	0.373
Linear	0.397	0.579	0.649	0.366

† Model is significant at 0.05 significance level.

Table 19. r^2 values of the relationships between 2012 CC INSEY and second harvest root yield.

Model†	CC V6-8 red INSEY	CC V6-8 red INSEY × plant height	CC V6-8 red edge INSEY	CC V6-8 red edge INSEY × plant height	CC V12-14 red INSEY	CC V12-14 red INSEY × plant height	CC V12-14 red edge INSEY	CC V12-14 red edge INSEY × plant height
Exponential	0.411	0.595	0.452	0.596	0.677	0.424	0.667	0.321
Linear	0.415	0.609	0.454	0.609	0.676	0.417	0.661	0.312

† Model is significant at 0.05 significance level.

Table 20. r^2 values of the relationships between 2012 GS and CC second harvest INSEY and second harvest root yield.

Model†	GS second harvest red INSEY	GS second harvest red INSEY × plant height	CC second harvest red edge INSEY	CC second harvest red edge INSEY × plant height	CC second harvest red INSEY	CC second harvest red INSEY × plant height
Exponential	0.794	0.673	0.785	0.625	0.801	0.676
Linear	0.789	0.666	0.782	0.620	0.798	0.671

† Model is significant at 0.05 significance level.

Relationships between Root Yield and Ground-Based Sensor Readings, 2013

First Harvest Beet Root Yield Prediction

Pooled analysis of the two 2013 site INSEY and first sugar beet harvest root yield showed that the regressions were not significant. However, there were some significant models between some data sets, listed in Table 21. Including plant height into the models improved the r^2 values. The plant heights in Table 21 refer to the heights measured by tape. Table 21 also indicates that in 2013, relationships of sensor readings with first harvest root yield were poor. Reasons such as sensing samples or harvest samples were not representative could result in these poor results.

Table 21. r^2 values of the relationships between 2013 ground-based sensing INSEY and first harvest root yield.

Model†	GS V12-14 red INSEY × plant height	GS V12-14 red edge INSEY	GS V12-14 red edge INSEY × plant height	CC V12-14 red INSEY	CC V12-14 red INSEY × plant height
Exponential	0.250	0.215	0.313	0.110	0.270
Linear	0.256	0.221	0.321	0.105	0.272

† Model is significant at 0.05 significance level.

Second and Third Harvest Beet Root Yield Prediction

Only a few models were significant in second and third sugar beet root yield prediction, each with low r^2 values. As in the first harvest, including sugar beet canopy height improved prediction models between sensor reading and sugar beet root yield.

Relationships between Root Yield and Ground-Based Sensor Readings, 2012 and 2013

First Harvest Root Yield Prediction

With the pooled two-year and four-site data, three highly significant quadratic polynomial models with very high r^2 values (close to 1) were found between first sensing INSEY and first harvest root yield, as illustrated in Figure 6 to Figure 8. This thesis only investigated linear, exponential, and quadratic polynomial model. It seems from Figure 6 to Figure 8 that linear-plateau model might be a more reasonable choice. It was also possible that at very high INSEY position where N rate was usually very or extremely high, the balance of the nutrients in the soil was broken, resulting in slightly reduced yield. Highly significant exponential and linear models with similar performance were shown to be the best models for predicting sugar beet root yield using the second sensing INSEY, as demonstrated in Table 22. All the r^2 values in Table 22 are very high and similar. Including the plant height information into the models didn't improve the models' performance. GreenSeeker and Crop Circle performed similarly. The significant exponential or linear models for sugar beet root yield prediction were in consistent with the models found for wheat and corn (Raun et al., 2002; Inman et al., 2007).

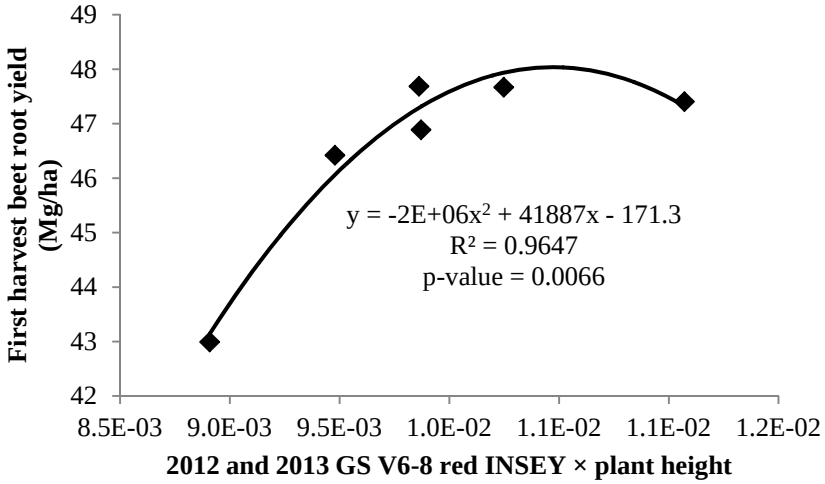

Figure 6. Relationship between two year GS V6-8 red INSEY × plant height and the first harvest beet root yield.

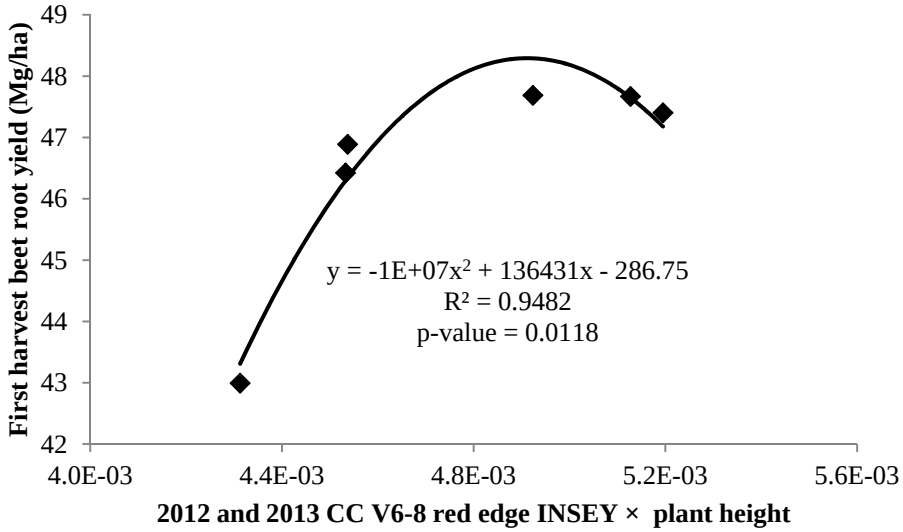

Figure 7. Relationship between two year CC V6-8 red edge INSEY × plant height and the first harvest beet root yield.

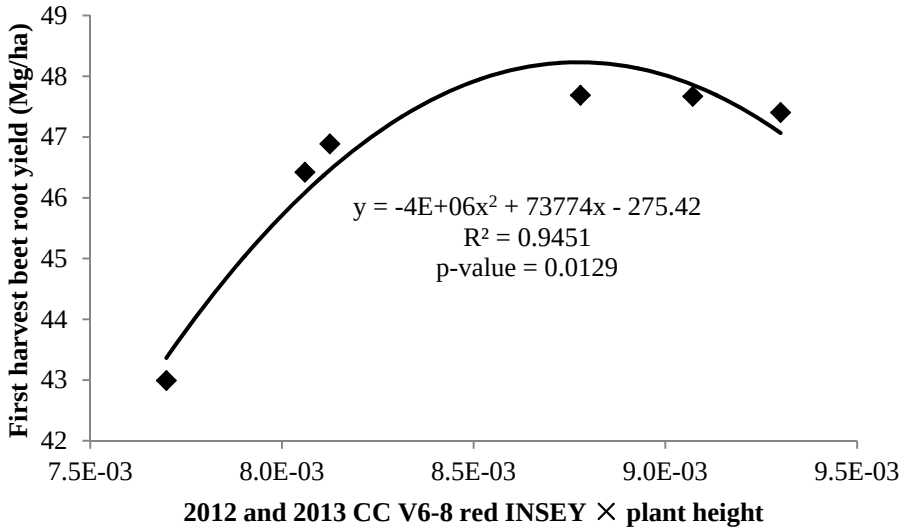

Figure 8. Relationship between two-year CC V6-8 red INSEY × plant height and the first harvest beet root yield.

Table 22. r^2 values of the relationships between 2012 and 2013 ground-based V12-14 sensing INSEY and first harvest sugar beet root yield.

Model†	GS V12-14 red INSEY	GS V12-14 red INSEY × plant height	CC V12-14 red edge INSEY	CC V12-14 red edge INSEY × plant height	CC V12-14 red INSEY	CC V12-14 red INSEY × plant height
Exponential	0.760	0.739	0.778	0.756	0.800	0.767
Linear	0.770	0.737	0.781	0.755	0.803	0.766

† Model is significant at 0.05 significance level.

Second Harvest Root Yield Prediction

Highly significant exponential and linear models with high r^2 values were also found in pooled data from 2012 and 2013, relating GS and CC second readings with sugar beet second harvest root yield (Table 23). The first sensing did not significantly relate to second sugar beet yields. At the second sensing, including plant height improved model performance in second harvest yield prediction. Figure 9 through Figure 11 illustrate the exponential models that include

plant height. These results again confirmed the superiority of using exponential model and linear model for sugar beet root yield predicion.

Table 23. r^2 values of the relationships between 2012 and 2013 ground-based sensing INSEY and second sugar beet harvest root yield.

Model†	GS V12-14 red INSEY	GS V12-14 red INSEY × plant height	CC V12-14 red edge INSEY	CC V12-14 red edge INSEY × plant height	CC V12-14 red INSEY	CC V12-14 red INSEY × plant height
Exponential	0.867	0.917	0.726	0.878	0.736	0.881
Linear	0.856	0.908	0.713	0.868	0.723	0.870

† Model is significant at 0.05 significance level.

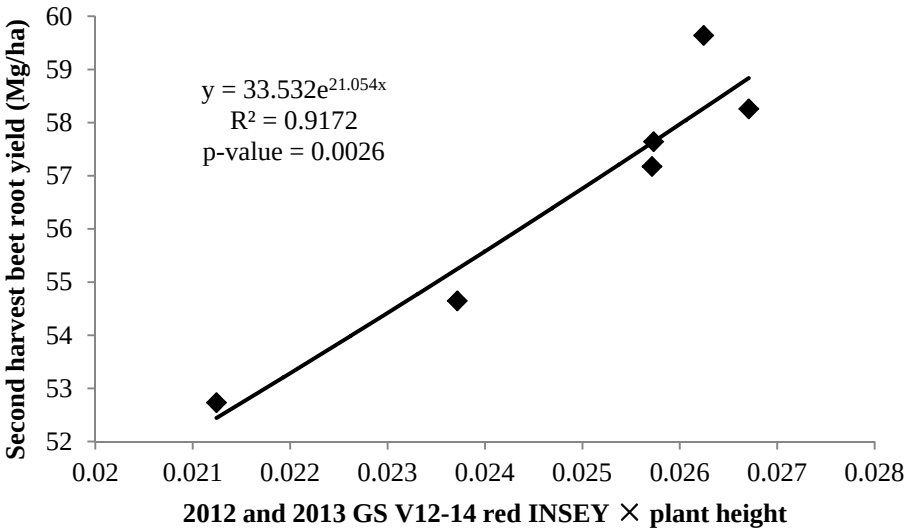

Figure 9. Relationship between two-year GS V12-14 red INSEY × plant height and the second harvest beet root yield.

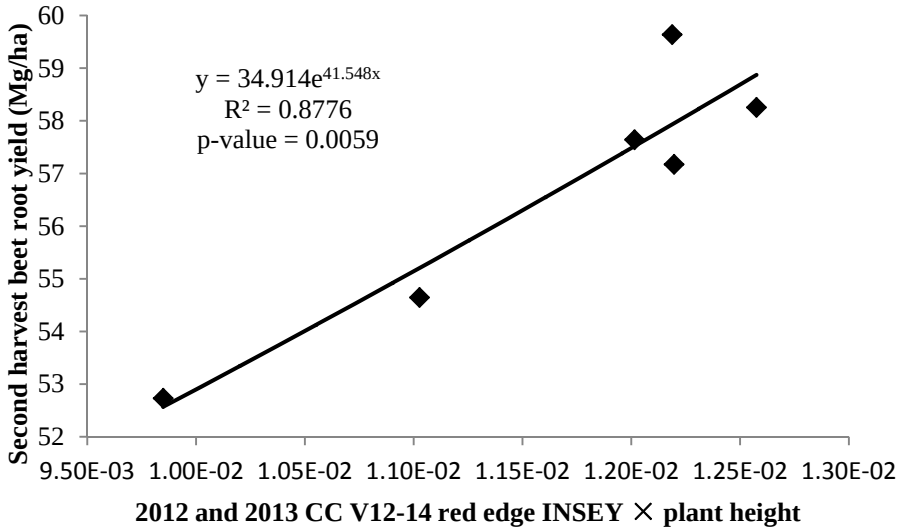

Figure 10. Relationship between two-year CC V12-14 red edge INSEY × plant height and the second harvest beet root yield.

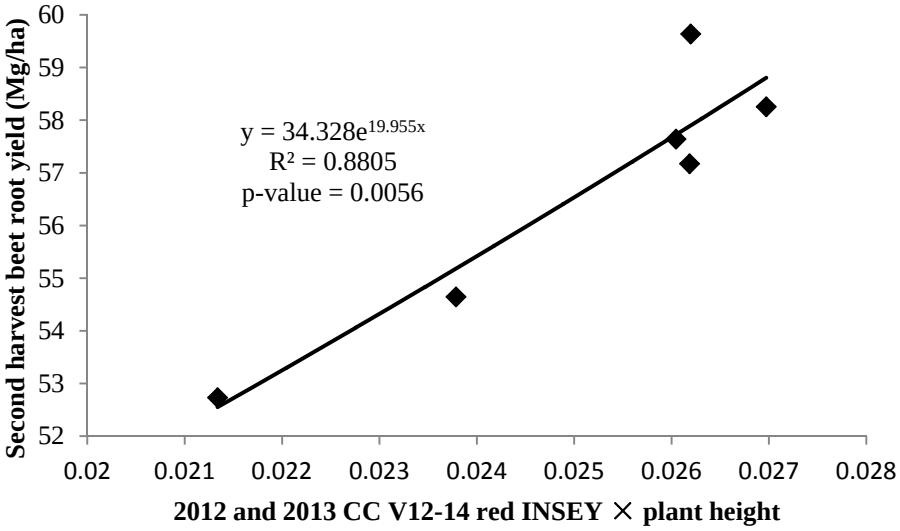

Figure 11. Relationship between two year CC V12-14 red INSEY × plant height and the second harvest beet root yield.

Relationships between Top Total N and Ground-Based Sensor Readings, 2012

First Harvest Top Total N Prediction

The first and second harvest sugar beet top total N was related to the pooled two-site INSEY day in 2012. Table 24 and Table 25 summarize the r^2 values of using GreenSeeker INSEY and Crop Circle INSEY, respectively, as the predictors of the first harvest sugar beet top total N. The two sensors and the two regression models performed similarly. Existing research also reported that exponential model was very suitable for sugar beet top total N prediction using GreenSeeker NDVI (Gehl and Boring, 2011). Combining the height information with the first sensing INSEY greatly improved the model performance, but not when using the second sensing INSEY and plant height. This was probably due to extremely dry weather in 2012 which hindered the normal growth of the plant height. Figure 12 and Figure 13 illustrate the best models using GreenSeeker and Crop Circle, respectively.

Table 24. r^2 values of the relationships between 2012 GS INSEY and first harvest top total N.

Model†	GS V6-8 red INSEY	GS V6-8 red INSEY × plant height	GS V12-14 red INSEY	GS V12-14 red INSEY × plant height
Exponential	0.264	0.532	0.563	0.358
Linear	0.253	0.597	0.569	0.322

† Model is significant at 0.05 significance level.

The relationships between 2012 CC sensing data obtained on the same day of the first harvest and the first harvest sugar beet top total N were also analyzed, and the r^2 values were listed in Table 26. All models in this table are highly significant with very high r^2 values, indicating that INSEY is an excellent predictor of the sugar beet top total N. Including plant

height into the models improved model performance. Figure 14 illustrates the best model listed in Table 26.

Table 25. r^2 values of the relationships between 2012 CC INSEY and first harvest top total N.

Model†	CC V6-8 red INSEY	CC V6-8 red INSEY × plant height	CC V6-8 red edge INSEY	CC V6-8 red edge INSEY × plant height	CC V12-14 red INSEY	CC V12-14 red INSEY × plant height	CC V12-14 red edge INSEY	CC V12-14 red edge INSEY × plant height
Exponential	0.345	0.633	0.393	0.654	0.591	0.405	0.583	0.314
Linear	0.289	0.671	0.338	0.707	0.582	0.363	0.557	0.264

† Model is significant at 0.05 significance level.

Table 26. r^2 values of the relationships between 2012 CC first harvest INSEY and first harvest top total N.

Model†	CC first Harvest red edge INSEY	CC first Harvest red edge INSEY × plant height	CC first Harvest red INSEY	CC first Harvest red INSEY × plant height
Exponential	0.966	0.977	0.903	0.960
Linear	0.932	0.972	0.856	0.952

† Model is significant at 0.05 significance level.

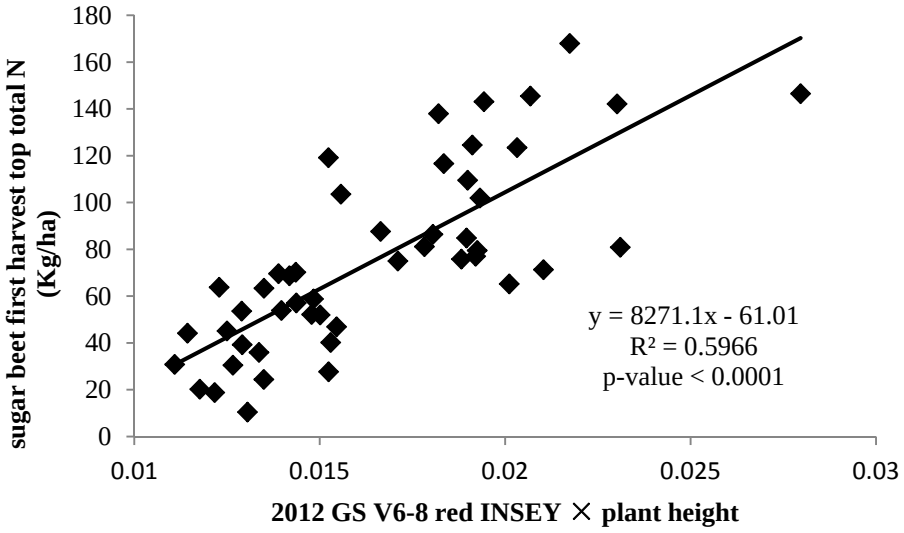

Figure 12. Relationship between 2012 GS V6-8 red INSEY × plant height and first harvest top total N.

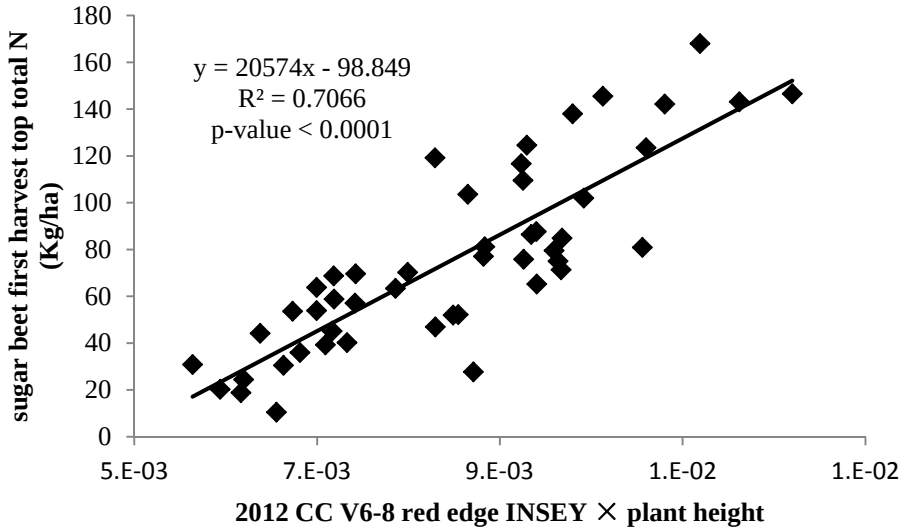

Figure 13. Relationship between 2012 CC V6-8 red edge INSEY × plant height and first harvest top total N.

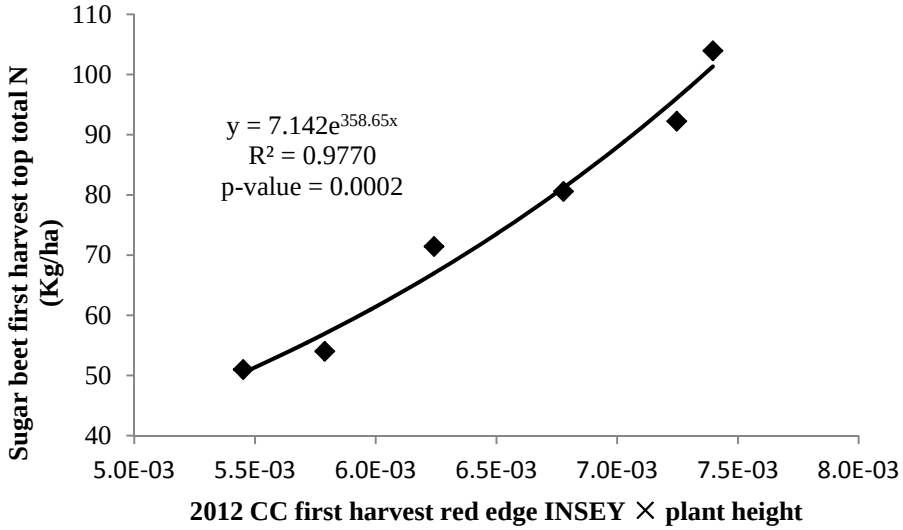

Figure 14. Relationship between 2012 CC first harvest red edge INSEY × plant height and first harvest top total N.

Second Harvest Top Total N Prediction

The first sensing INSEY, the second sensing INSEY, and the second harvest sensing INSEY, respectively, were related to the second harvest sugar beet top total N. For the first

sensing regression, the best regression analysis method is using all the individual plot data without averaging processing; for the second sensing and second harvest sensing data regression, the best regression analysis method is found to be the one averaging all individual plot data over each N application rate treatment.

Table 27 summarizes the r^2 values of the relationships between 2012 ground-based first sensing INSEY and the second harvest top total N of 2012 sugar beet. Using the regression method that averages all individual plot data over each N application rate treatment, no significant regression models were found using the second sensing INSEY or second harvest INSEY directly, but highly significant regression models with very high r^2 values using the INSEY × plant height information were revealed, as demonstrated in Table 28. Both Table 27 and Table 28 indicate that plant height information plays a positive role in improving the regression models performance in terms of both model significance and r^2 value. It seems that, compared to the first sensing regression, the second sensing and second harvest sensing are better sugar beet top total N predictors in this case. The exponential model is slightly better than the linear model. The models found here were consistent with those found in the first harvest top total N prediction. Figure 15 and Figure 16 illustrate the exponential relationships between CC second red INSEY × plant height or CC second harvest red INSEY × plant height and the second harvest top total N.

Table 27. r^2 values of the relationships between V6-8 sensing INSEY and the second harvest top total N of 2012 sugar beet.

Model†	GS V6-8 red INSEY	GS V6-8 red INSEY × plant height	CC V6-8 red INSEY	CC V6-8 red INSEY × plant height	CC V6-8 red edge INSEY	CC V6-8 red edge INSEY × plant height
Exponential	0.174	0.399	0.218	0.463	0.246	0.482
Linear	0.157	0.399	0.176	0.439	0.204	0.466

† Model is significant at 0.05 significance level.

Table 28. r^2 values of the relationships between V12-14 sensing INSEY ×plant height or second harvest sensing INSEY × plant height and the second harvest top total N of 2012 sugar beet.

Model†	GS V12-14 red INSEY × plant height	CC V12-14 red INSEY × plant height	CC V12-14 red edge INSEY × plant height	GS second harvest red INSEY × plant height	CC second harvest red INSEY × plant height	CC second harvest red edge INSEY × plant height
Exponential	0.760	0.820	0.814	0.867	0.894	0.868
Linear	0.739	0.800	0.794	0.864	0.890	0.868

† Model is significant at 0.05 significance level.

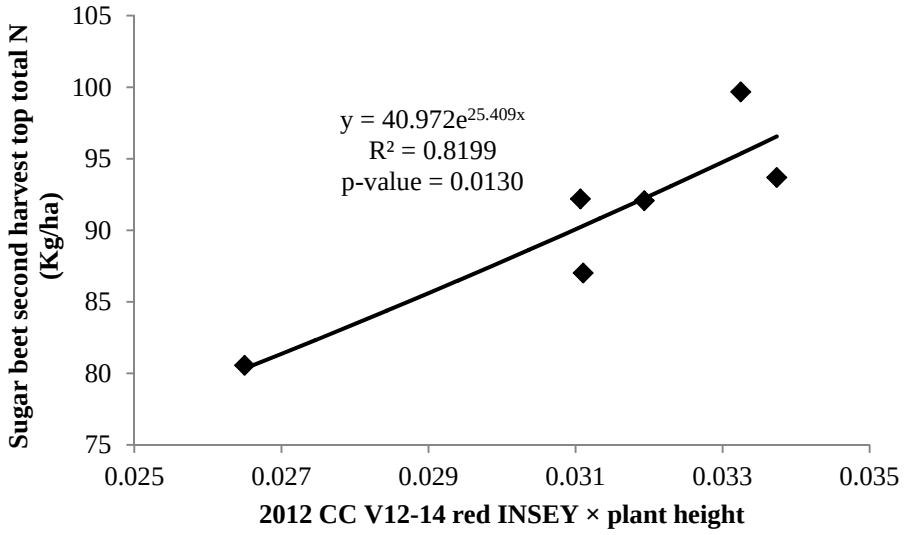

Figure 15. Relationship between 2012 CC V12-14 red INSEY × plant height and second harvest top total N.

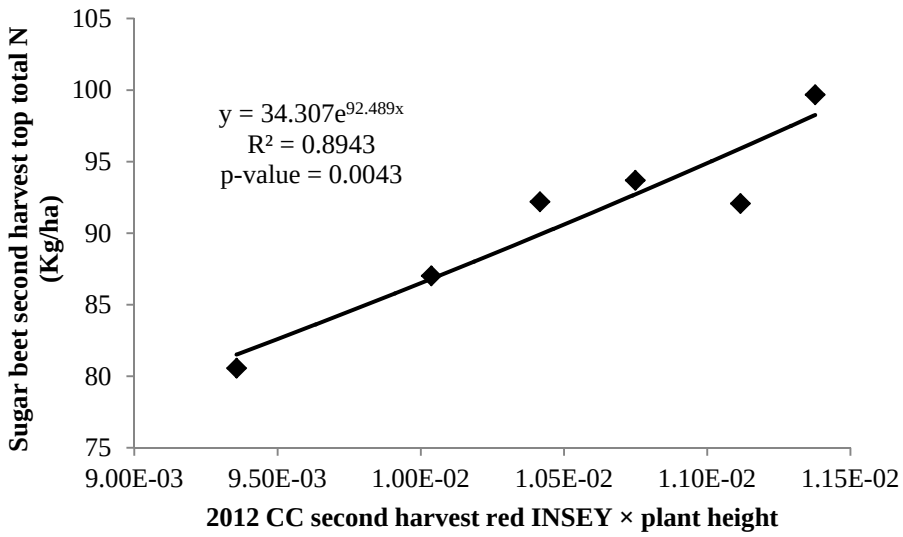

Figure 16. Relationship between 2012 CC second harvest red INSEY × plant height and second harvest top total N.

Relationships between Recoverable Sugar Yield and Ground-Based Sensor Readings, 2012

First Harvest Recoverable Sugar Yield Prediction

Each of the first sensing INSEY, second sensing INSEY, and the first harvest sensing INSEY was used to relate to the first harvest recoverable sugar yield of 2012. Table 29, Table 30, and Table 31 summarize the r^2 values of the significant regression models. Exponential model was found consistent and useful, which was in accordance with the research done by Gehl and Boring (2011). The difference was that they use NDVI instead of INSEY as the independent variable. Except slightly improving the performance of the first sensing INSEY-involved regression models, the plant height information decreases the performance of the rest models. The significant models without considering the plant height are good enough for recoverable sugar yield prediction with reasonably high r^2 values.

Table 29. r^2 values of the relationships between V6-8 sensing INSEY and the first harvest recoverable sugar of 2012 sugar beet.

Model†	GS V6-8 red INSEY	GS V6-8 red INSEY × plant height	CC V6-8 red INSEY	CC V6-8 red INSEY × plant height	CC V6-8 red edge INSEY	CC V6-8 red edge INSEY × plant height
Exponential	0.332	0.419	0.425	0.490	0.489	0.495
Linear	0.350	0.422	0.432	0.482	0.492	0.483

† Model is significant at 0.05 significance level.

Table 30. r^2 values of the relationships between V12-14 sensing INSEY and the first harvest recoverable sugar of 2012 sugar beet.

Model†	GS V12-14 red INSEY	GS V12-14 red INSEY × plant height	CC V12-14 red INSEY	CC V12-14 red INSEY × plant height	CC V12-14 red edge INSEY	CC V12-14 red edge INSEY × plant height
Exponential	0.414	0.177	0.459	0.225	0.481	0.165
Linear	0.417	0.173	0.462	0.220	0.482	0.160

† Model is significant at 0.05 significance level.

Table 31. r^2 values of the relationships between first harvest sensing INSEY and the first harvest recoverable sugar of 2012 sugar beet.

Model†	CC first harvest red INSEY	CC first harvest red INSEY × plant height	CC first harvest red edge INSEY	CC first harvest red edge INSEY × plant height
Polynomial 2	0.646	0.602	0.661	0.605

† Model is significant at 0.05 significance level.

Second Harvest Recoverable Sugar Yield Prediction

The first sensing INSEY, second sensing INSEY, and the second harvest sensing INSEY was related to the first harvest recoverable sugar yield of 2012. Table 32, Table 33, and Table 34 summarize the r^2 values of the significant regression models. Results here again indicated that exponential or simple linear models were the best choice. Plant height information improved the first sensing regression models performance, but decreased the second sensing and the second harvest sensing regression models performance. This showed that the role of plant height was not consistent taking into consideration of the relevant results presented earlier. As expected, the

harvest INSEY was the best predictor of harvest yield. The CC red INSEY slightly outperformed other INSEYs (Table 33 and Table 34). Figure 17 and Figure 18 illustrate the best two models from Table 33 and Table 34, respectively.

Table 32. r^2 values of the relationships between V6-8 sensing INSEY and the second harvest recoverable sugar of 2012 sugar beet.

Model†	GS V6-8 red INSEY	GS V6-8 red INSEY × plant height	CC V6-8 red INSEY	CC V6-8 red INSEY × plant height	CC V6-8 red edge INSEY	CC V6-8 red edge INSEY × plant height
Exponential	0.391	0.551	0.392	0.573	0.420	0.568
Linear	0.394	0.562	0.397	0.586	0.425	0.580

† Model is significant at 0.05 significance level.

Table 33. r^2 values of the relationships between V12-14 sensing INSEY and the second harvest recoverable sugar of 2012 sugar beet.

Model†	GS V12-14 red INSEY	GS V12-14 red INSEY × plant height	CC V12-14 red INSEY	CC V12-14 red INSEY × plant height	CC V12-14 red edge INSEY	CC V12-14 red edge INSEY × plant height
Exponential	0.682	0.404	0.685	0.442	0.657	0.330
Linear	0.679	0.392	0.684	0.431	0.651	0.317

† Model is significant at 0.05 significance level.

Table 34. r^2 values of the relationships between second harvest sensing INSEY and the second harvest recoverable sugar of 2012 sugar beet.

Model†	GS second harvest red INSEY	GS second harvest red INSEY × plant height	CC second harvest red INSEY	CC second harvest red INSEY × plant height	CC second harvest red edge INSEY	CC second harvest red edge INSEY × plant height
Exponential	0.745	0.619	0.754	0.624	0.707	0.555
Linear	0.739	0.607	0.750	0.614	0.703	0.544

† Model is significant at 0.05 significance level.

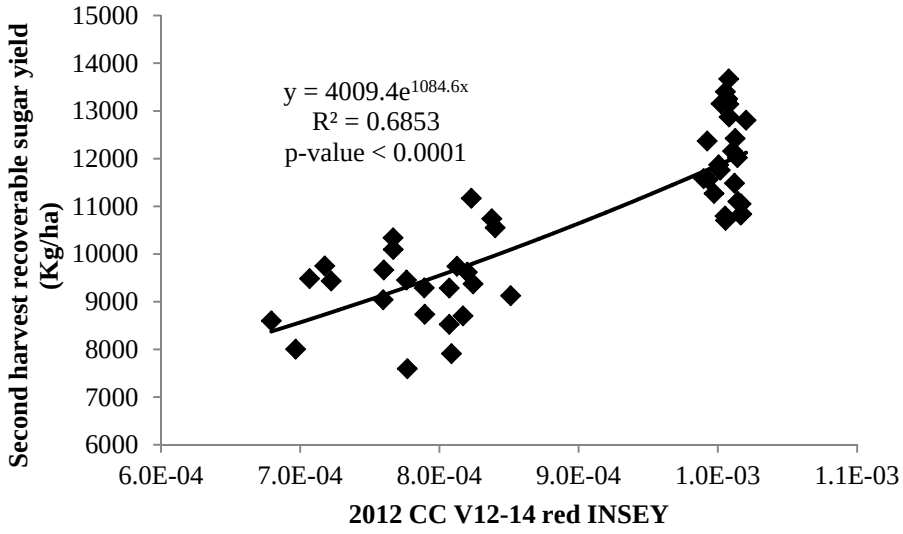

Figure 17. Relationship between 2012 CC V12-14 red INSEY and second harvest recoverable sugar yield.

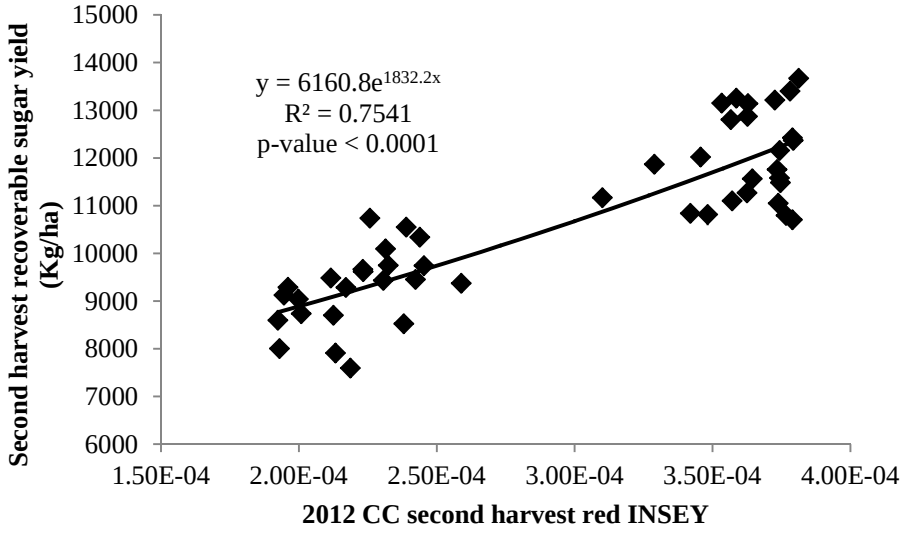

Figure 18. Relationship between 2012 CC second harvest red INSEY and second harvest recoverable sugar yield.

Relationships between Sugar Beet Recoverable Sugar Yield and Ground-Based Sensor Readings, 2013

Most of the regression models for 2013 recoverable sugar yield prediction were either insignificant or with very low r^2 values between sensor INSEY and recoverable sugar yield. However, there were a few regression models for the second harvest recoverable sugar yield prediction that were highly significant with high r^2 values, as shown in Table 35 and Figure 19. From Figure 19 it can be seen that very high INSEY (corresponding to high N rate or over application of N) resulted in reduced sugar yield, which was highly possible as reported by Franzen (2003) and Gehl and Boring (2011) especially when there was high nitrate residual level together with high N fertilizer application rate.

Table 35. r^2 values of the relationships between 2013 ground-based sensing INSEY and the second harvest recoverable sugar.

Model†	GS second red INSEY	GS second red edge INSEY	CC first red edge INSEY × tape measured height	CC first red INSEY × tape measured height	CC second red INSEY × tape measured height
Exponential	0.665	0.661	NS	NS	NS
Polynomial 2	NS	NS	0.949	0.925	0.865

† NS means model is not significant at 0.05 significance level; otherwise model is significant at 0.05 significance level.

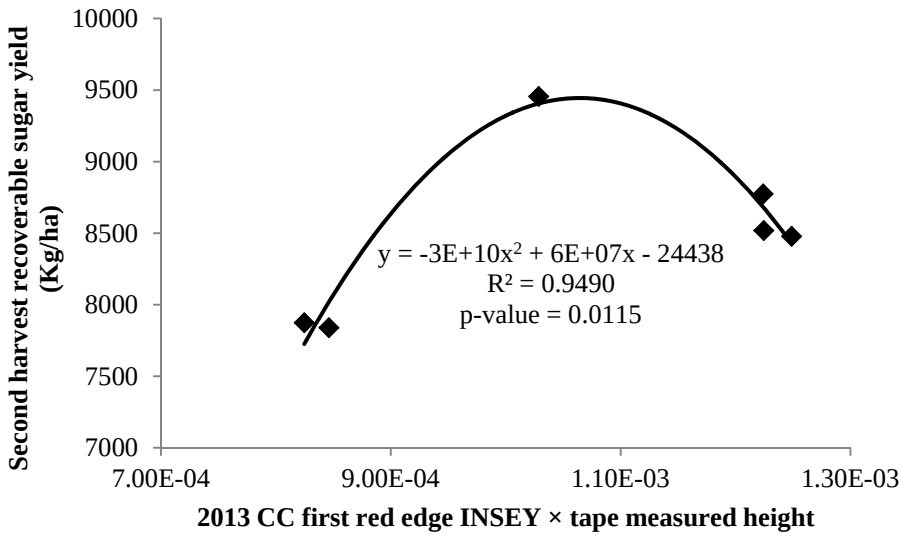

Figure 19. Relationship between 2013 CC first red edge INSEY × tape measured plant height and the second harvest recoverable sugar yield.

Relationships between Recoverable Sugar Yield and Ground-Based Sensor Readings, 2012 and 2013

First Harvest Recoverable Sugar Yield Prediction

Two and four-site data were pooled for regression analysis. A summary of the r^2 values of the significant relationships between first ground-based sensing INSEY and the first harvest recoverable sugar yield is shown in Table 36, where all models use the plant height information. This implies that the first plant height information has greatly improved the models performance (from insignificance to significant). For the second sensing INSEY, a quadratic polynomial model was found to be the best choice and the results were summarized in Table 37. Table 37 also demonstrates the positive role of the plant height information plays in improving model performance. The best quadratic polynomial model is illustrated in Figure 20. Exponential and linear models were found to better when using early season INSEY as predictor, while quadratic

polynomial model was shown to be better when V12-14 growth stage INSEY was used. As discussed earlier, all these three models for sugar yield prediction were possible based on only two-year data. The model type can be different when using INSEY data from different growth stage.

Table 36. r^2 values between 2012 and 2013 two-year ground-based V6-8 sensing INSEY and the first harvest recoverable sugar.

Model†	GS V6-8 red INSEY × plant height	CC V6-8 red INSEY × plant height	CC V6-8 red edge INSEY × plant height
Exponential	0.422	0.414	0.428
Linear	0.438	0.428	0.440

† Model is significant at 0.05 significance level.

Table 37. r^2 values of the relationships between 2012 and 2013 two-year ground-based V12-14 sensing INSEY and the first harvest recoverable sugar.

Model†	GS V12-14 red INSEY × plant height	CC V12-14 red INSEY × plant height	CC V12-14 red edge INSEY	CC V12-14 red edge INSEY × plant height
Polynomial 2	0.907	0.963	0.943	0.961

† Model is significant at 0.05 significance level.

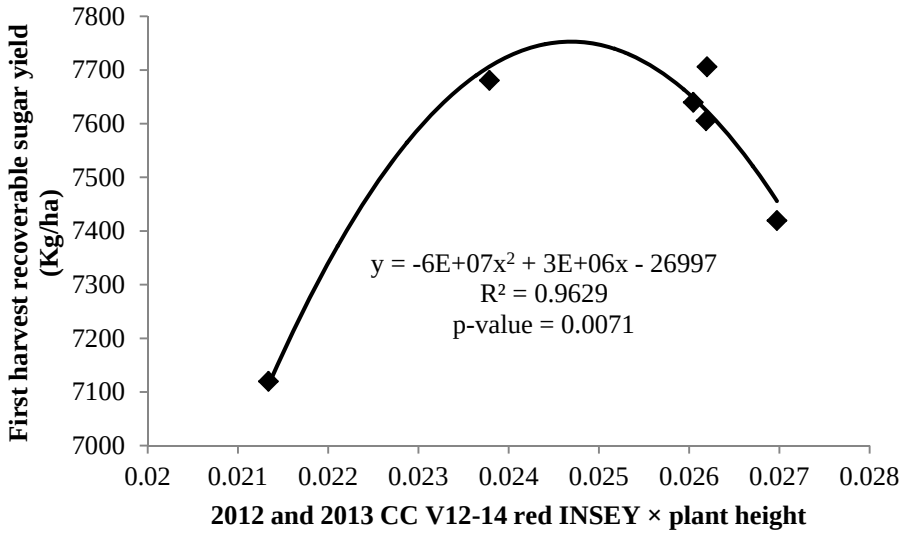

Figure 20. Relationship between 2012 and 2013 two-year CC V12-14 red INSEY × plant height and the first harvest recoverable sugar yield.

Second Harvest Recoverable Sugar Yield Prediction

There were significant relationships between the GS and CC red and red edge INSEY and the second harvest recoverable sugar yield (Table 38). The first and second measured plant height data generally improved model performance. From Table 38 we can also find that mid-season INSEY can better predict sugar yield than can early-season INSEY. Figure 21 illustrates the linear relationship between CC V12-14 red INSEY and the second harvest recoverable sugar yield.

Relationships between Root Yield and Satellite Imagery INSEY, 2012

The satellite imagery INSEY from Amenia July 11 and Crookston July 1 of 2012 were pooled and then related to each of the harvest sugar beet root yield. The same method applied to the satellite imagery INSEY from Amenia August 16 and Crookston August 16 in 2012. The r^2 values of the significant regression models are summarized in Table 39 and Table 40. From these two tables we can see that, generally speaking, both the July and August INSEYs have closer relationships with the first harvest root yield than with the second harvest root yield. Another observation is that August INSEYs are better related to each root yield than are July INSEYs in most cases. These two findings are due to the same fact that sensing at a closer date to the harvest leads to a stronger relationship between INSEY and root yield. For this year's study, red edge INSEY from satellite imagery seemed to be the best predictors of root yield in terms of r^2 values. Red edge NDVI was also reported to have better ability in plant leaf N prediction (Cao et

al., 2013; Schlemmer et al., 2013). Figure 22 and Figure 23 illustrate one July INSEY model and one August INSEY model, respectively.

Table 38. r^2 values of the relationships between 2012 and 2013 two-year INSEY and the second harvest recoverable sugar yield.

Model†	GS V6-8 red INSEY × plant height	CC V6-8 red edge INSEY	CC V6-8 red edge INSEY × plant height	GS V12-14 red INSEY	GS V12-14 red INSEY × plant height	CC V12-14 red edge INSEY	CC V12-14 red INSEY
Exponential	0.435	0.162	0.421	0.531	0.497	0.457	0.536
Linear	0.463	0.174	0.444	0.578	0.519	0.492	0.591

† NS means model is not significant at 0.05 significance level; otherwise model is significant at 0.05 significance level.

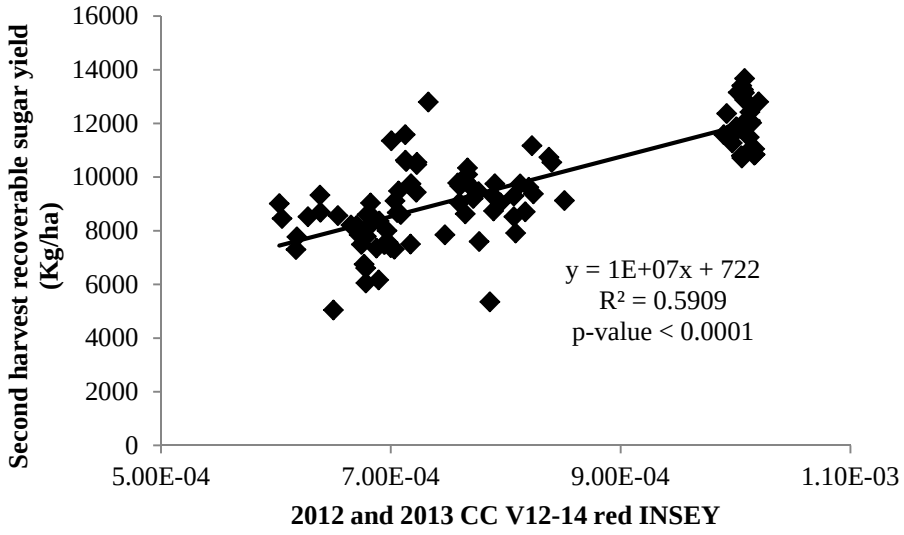

Figure 21. Relationship between 2012 and 2013 two-year CC V12-14 red INSEY and the second harvest recoverable sugar yield.

Table 39. r^2 values of the relationships between July 2012 satellite imagery INSEY and sugar beet root yield.

Model†	first harvest root yield			second harvest root yield
	red INSEY	red edge INSEY	green INSEY	red INSEY
Exponential	0.749	0.855	0.714	0.588
Linear	0.767	0.855	0.722	0.588

† NS means model is not significant at 0.05 significance level; otherwise model is significant at 0.05 significance level.

Table 40. r^2 values of the relationships between August 2012 satellite imagery INSEY and sugar beet root yield.

Model†	first harvest root yield				second harvest root yield		
	red INSEY	red edge INSEY	blue INSEY	green INSEY	red INSEY	red edge INSEY	blue INSEY
Exponential	0.861	0.901	0.885	0.864	0.691	0.470	0.668
Linear	0.864	0.904	0.892	0.864	0.689	0.469	0.671

† Model is significant at 0.05 significance level.

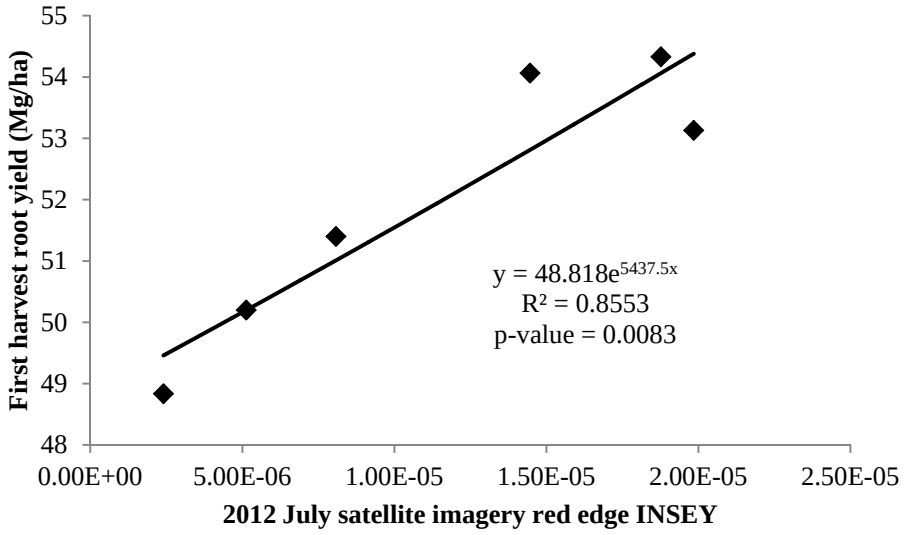

Figure 22. Relationship between 2012 July satellite imagery red edge INSEY and the first harvest sugar beet root yield.

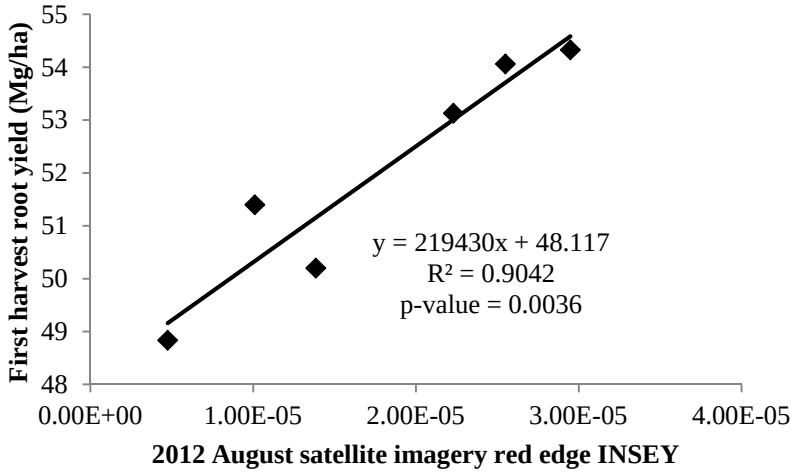

Figure 23. Relationship between 2012 August satellite imagery red edge INSEY and the first harvest sugar beet root yield.

Relationships between Root Yield and Satellite Imagery INSEY, 2013

In 2013, only the Casselton June 24 imagery and the Thompson August 13 imagery provided by the RapidEye satellite imagery company can be used for comparing imagery with sugar beet yield and quality. The quality of Casselton June 24 imagery was slightly affected by cloud haze. INSEY data obtained from these two imageries were pooled and related to each harvest sugar beet root yield. Table 41 summarized the r^2 values of all significant regression models. Even though the two imagery sets were taken with a relatively large time interval between them, the relationships with yield were significant. The normalizing effect of the growing degree days within INSEY made this possible. It is possible that with imagery taken at closer dates, improved relationships might be obtained. Figure 24 illustrates the exponential relationship between red edge INSEY and the first harvest sugar beet root yield.

Table 41. r^2 values of the relationships between 2013 satellite imagery INSEY and sugar beet root yield.

Harvest order	Model†	Red INSEY	Red edge INSEY	Blue INSEY	Green INSEY
first harvest	Exponential	0.463	0.632	0.613	0.625
	Linear	0.411	0.595	0.576	0.579
second harvest	Exponential	0.476	0.606	0.587	0.581
	Linear	0.425	0.559	0.539	0.534
third harvest	Exponential	0.545	0.542	0.576	0.575
	Linear	0.538	0.575	0.598	0.604

† Model is significant at 0.05 significance level.

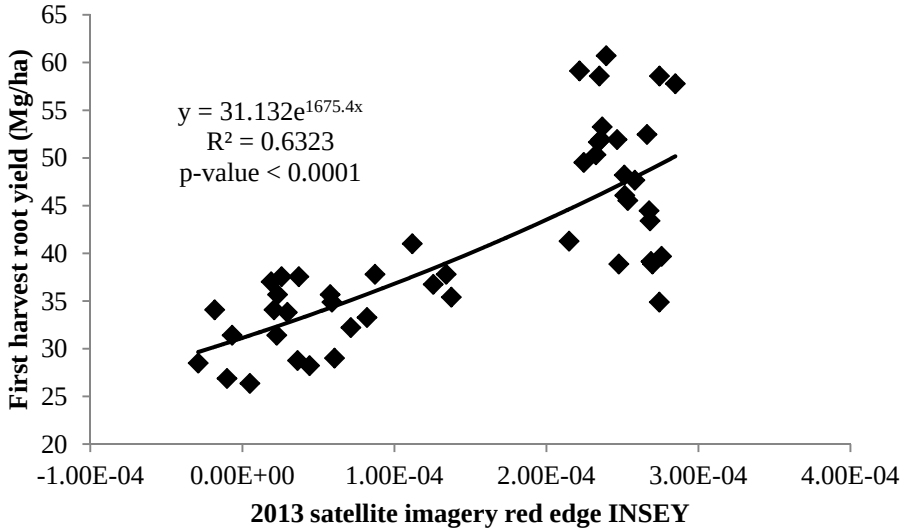

Figure 24. Relationship between 2013 satellite imagery red edge INSEY and the first harvest sugar beet root yield.

Relationships between Root Yield and Satellite Imagery INSEY, 2012 and 2013

Two-year and four-site INSEYs calculated from satellite imagery were pooled and related to each harvest sugar beet root yield, and the r^2 values of the significant regression models were summarized in Table 42. Due to the poor quality of the 2013 satellite imagery, the pooled data was not related as well to sugar beet root yield compared to ground-based sensors. Two-year data indicated that red INSEY and blue INSEY were more consistent. Taking into

consideration of the results for each individual year as well as combined two-year study, red INSEY became the most consistent and effective. In fact, red spectral band is an indispensable band for almost all optical sensors, either ground-based or space-based. Figure 25 illustrates the exponential relationship between red INSEY and the first harvest sugar beet root yield. Figure 26 illustrates the quadratic polynomial relationship between green INSEY and the first harvest sugar beet root yield.

Table 42. r^2 values of the significant relationships between 2012 and 2013 two-year satellite imagery INSEY and sugar beet root yield.

Model†	first harvest root yield			second harvest root yield	
	red INSEY	blue INSEY	green INSEY	red INSEY	blue INSEY
Exponential	0.588	0.506	NS	0.440	0.290
Linear	0.549	0.443	0.664	0.407	0.268

† NS means model is not significant at 0.05 significance level; otherwise model is significant at 0.05 significance level.

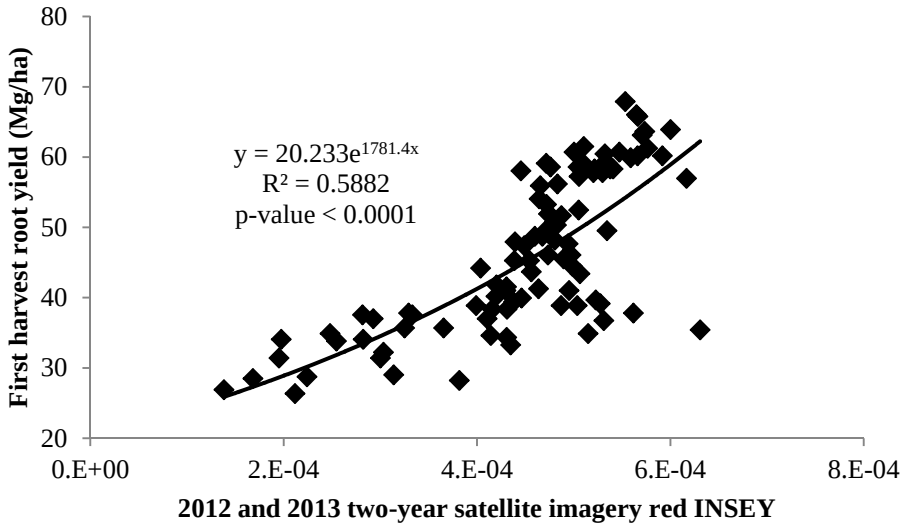

Figure 25. Relationship between 2012 and 2013 two-year satellite imagery red INSEY and the first harvest root yield.

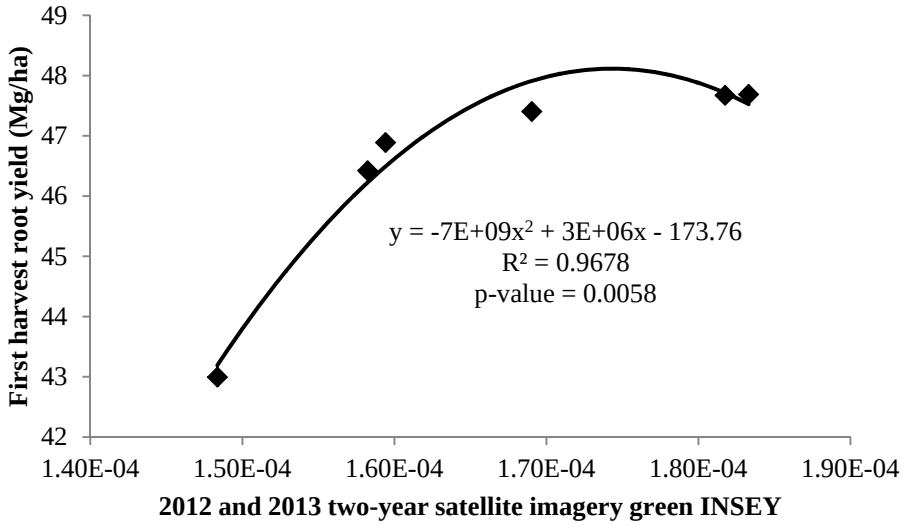

Figure 26. Relationship between 2012 and 2013 two-year satellite imagery green INSEY and the first harvest root yield.

Relationships between Top Total N and Satellite Imagery INSEY, 2012

The satellite imagery INSEY from Amenia July 11 and Crookston July 1 of 2012 were pooled and then related to each of the harvest sugar beet top total N. The satellite imagery INSEYs from Amenia August 16 and Crookston August 16 in 2012 were also pooled for regression analysis. Table 43 and Table 44 summarize the r^2 values of the significant regression models between July or August 2012 satellite imagery INSEY and each harvest sugar beet top total N. Data in these two tables show that both the July INSEY and august INSEY have closer relationships with the first harvest top total N than with the second harvest top total N. This was because the first harvest and second harvest were conducted in the middle of August and end of August, respectively. Both the July and the August INSEYs sensing date were closer to the first harvest date. The July red edge INSEY has a particularly high correlation with the first harvest top total N, as illustrated in Figure 27.

Table 43. r^2 values of the relationships between July 2012 satellite imagery INSEY and sugar beet top total N.

Model†	first harvest top total N		second harvest top total N	
	red INSEY	red edge INSEY	red INSEY	red edge INSEY
Exponential	0.536	0.954	0.420	0.682
Linear	0.529	0.957	0.420	0.683

† Model is significant at 0.05 significance level.

Table 44. r^2 values of the relationships between August 2012 satellite imagery INSEY and sugar beet top total N.

Model†	First harvest top total N				Second harvest top total N		
	red INSEY	red edge INSEY	blue INSEY	green INSEY	red INSEY	red edge INSEY	blue INSEY
Exponential	0.627	0.598	0.710	0.727	0.509	0.441	0.486
Linear	0.611	0.590	0.695	0.706	0.518	0.433	0.531

† Model is significant at 0.05 significance level.

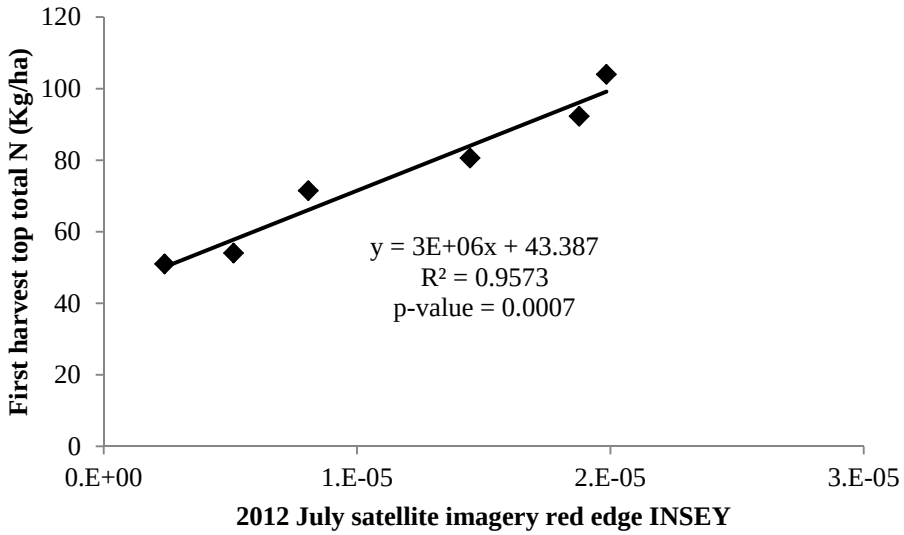

Figure 27. Relationship between 2012 July satellite imagery red edge INSEY and the first harvest sugar beet top total N.

Relationships between Recoverable Sugar Yield and Satellite Imagery INSEY, 2012

Table 45 and Table 46 summarize the r^2 values of the significant regression models between pooled July or August 2012 satellite imagery INSEY and each harvest sugar beet recoverable sugar yield. Humburg et al. (2006) found that Green NDVI was the most consistent VI to predict sugar beet sucrose concentration, but this was not the case in our study. It seems from these two tables that red INSEY is the most reliable INSEY for the study of year 2012 as in all cases there were at least two significant models with high r^2 values.

Table 45. r^2 values of the relationships between July 2012 satellite imagery INSEY and sugar beet recoverable sugar yield.

Model†	first harvest recoverable sugar		second harvest recoverable sugar
	red INSEY	green INSEY	red INSEY
Exponential	0.549	0.739	0.544
Linear	0.549	0.745	0.543

† Model is significant at 0.05 significance level.

Table 46. r^2 values of the relationships between August 2012 satellite imagery INSEY and sugar beet recoverable sugar yield.

Model†	first harvest recoverable sugar			second harvest recoverable sugar		
	red INSEY	red edge INSEY	blue INSEY	red INSEY	red edge INSEY	blue INSEY
Exponential	0.570	0.487	0.500	0.642	0.387	0.638
Linear	0.567	0.471	0.495	0.643	0.390	0.641

† Model is significant at 0.05 significance level.

Relationships between Recoverable Sugar Yield and Satellite Imagery INSEY, 2013

INSEYs calculated from the Casselton June 24 imagery and the Thompson August 13 imagery were pooled and related to each harvest recoverable sugar yield, and the r^2 values of the significant regression models are summarized in Table 47. Each of the satellite imagery INSEYs was better with the third harvest recoverable sugar yield, compared to the first and second

harvests. In this year, red INSEY was still good, but Green INSEY was the best among the compared four INSEYs, which was in accordance with the work of Humburg et al. (2006).

Table 47. r^2 values of the relationships between 2013 satellite imagery INSEY and sugar beet recoverable sugar yield.

Harvest order	model†	red INSEY	red edge INSEY	blue INSEY	green INSEY
first harvest	Exponential	0.274	0.359	0.346	0.370
	Linear	0.262	0.362	0.349	0.366
second harvest	Exponential	0.299	0.283	0.280	0.290
	Linear	0.293	0.290	0.284	0.294
third harvest	Exponential	0.463	0.415	0.446	0.458
	Linear	0.449	0.434	0.452	0.476
	Polynomial 2	0.501	0.495	0.508	0.524

† Model is significant at 0.05 significance level.

Relationships between Recoverable Sugar Yield and Satellite Imagery INSEY, 2012 and 2013

Two-year and four-site INSEYs calculated from satellite imageries were pooled and related to each harvest sugar beet recoverable sugar yield, and the r^2 values of the significant regression models were summarized in Table 48. Due to the poor quality of the 2013 satellite imagery, the overall pooled satellite imagery data was not as highly related to recoverable sugar yield compared to ground-sensor data. In general, Red INSEY outperformed other INSEYs in terms of consistency. Figure 28 illustrates the exponential relationship between red INSEY and the second harvest recoverable sugar yield. The widely validated exponential model (Raun et al., 2005) for crop yield prediction seemed also very effective for sugar beet recoverable sugar yield prediction.

Table 48. r^2 values of the relationships between 2012 and 2013 two-year satellite imagery INSEY and sugar beet recoverable sugar yield.

Model†	First harvest sugar yield		Second harvest sugar yield	
	red INSEY	blue INSEY	red INSEY	blue INSEY
Exponential	0.436	0.444	0.449	0.351
Linear	0.427	0.421	0.434	0.322

† Model is significant at 0.05 significance level.

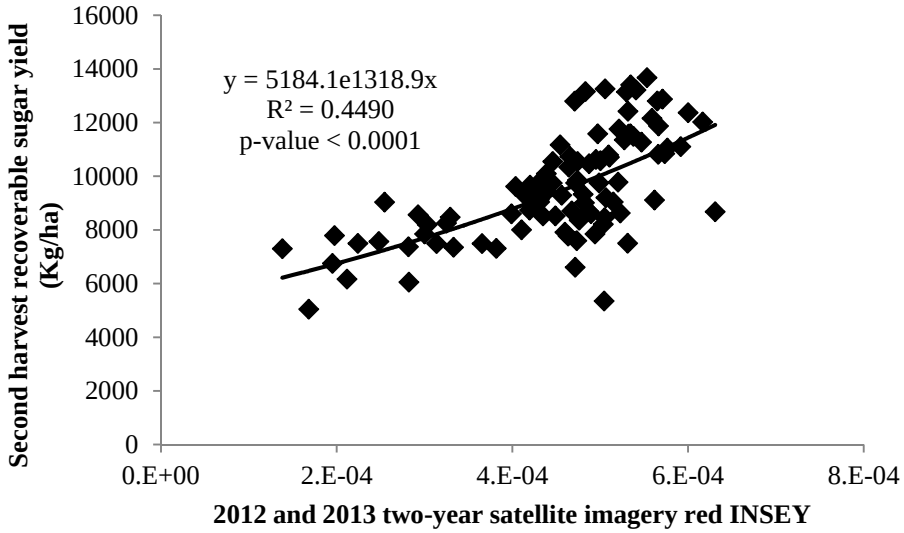

Figure 28. Relationship between 2012 and 2013 two-year satellite imagery red INSEY and the second harvest recoverable sugar yield.

Conclusions

INSEY extracted from optical sensing data are very good indicators of sugar beet root yield, recoverable sugar yield, and canopy top total N. Using optical sensing NDVI data to make in-season sugar beet yield or quality forecasting is feasible and therefore may benefit individual farmers and larger entities such as the fertilizer suppliers from whom they purchase nitrogen products. Exponential or linear model is sound for sugar beet root yield prediction, just as reported exponential model for corn and wheat (Raun et al., 2002; Raun et al. 2005); but the

most suitable model for recoverable sugar yield prediction using INSEY still needs more site-year data to select and validate. Our study on top total N prediction using harvest INSEY further support the argument that sugar beet top biomass and color (reflected by NDVI value) at harvest time is a good predictor of N availability for subsequent year (Franzen, 2003; Gehl and Boring, 2011).These experiments are not robust enough to indicate which NDVI source, GreenSeeker, Crop Circle, or RapidEye satellite imagery, is significantly better than the others. However, the active-optical ground-based sensors and passive satellite sensing each have their own strengths and weakness. Active-optical ground-based sensing can be conducted almost any time (Graham, 1999), which means that it would be particularly useful for real-time field input activities; however, their ability to collect large areas of imagery quickly for logistical purposes is poor. Passive satellite sensing is greatly influenced by weather conditions especially cloud or haze cover, or darkness, but with them large amounts of data can be collected in very short time. Satellites would be very effective in logistical data collection to aid in predicting in-season N fertilizer needs and screening fields for possible supplemental N. Plant height was not consistent in improving model performance, primarily due to dry conditions in 2012 and late summer 2013. Different soil type and weather conditions may have impacts on the quality and the predictability of our pooled data. To obtain more reliable prediction models, more site-years of experimentation and data analysis will be necessary.

RESULTS AND DISCUSSIONS FOR SPRING WHEAT

ANOVA Analysis of Yield and Quality Data

ANOVA analysis of the results for the four site-year spring wheat yield and quality data are provided in Table 49. Generally, N fertilizer rate had a significant and positive influence on both dry grain yield and protein content of spring wheat. This result was concordant with those of the study by Abedi et al. (2011) and by Brown et al. (2005). Since the available N or residual N in the soil for different plot of different or same site-year may be quite different, it would be unreliable to use N fertilizer rate to predict crop yield or quality directly. So statistical relationships will not be constructed and analyzed for these data.

Table 49. Spring wheat yield and protein content ANOVA analysis.

N rate (kg ha^{-1})	2012 Gardner		2012 Valley City		2013 Gardner		2013 Valley City	
	yield (Mg ha^{-1})	protein (%)	yield (Mg ha^{-1})	protein (%)	yield (Mg ha^{-1})	protein (%)	yield (Mg ha^{-1})	protein (%)
0	2.135 c†	12.19 d	3.200 b	11.81 c	2.906 c	11.13 d	3.378 c	15.71 b
45	2.654 bc	13.49 c	3.522 ab	12.49 c	3.891 b	11.91 c	3.803 ab	16.10 ab
90	3.130 ab	15.00 b	3.953 a	14.12 b	3.942 b	12.29 c	3.706 bc	15.89 ab
135	3.273 a	14.23 c	3.262 b	14.69 ab	4.287 a	13.18 b	3.864 ab	16.10 ab
180	3.225 a	16.43 a	3.882 a	15.60 a	4.432 a	13.86 ab	3.842 ab	16.36 a
225	3.414 a	15.69 ab	3.531 ab	15.63 a	4.269 a	13.97 a	4.063 a	16.34 a

† Means with the same letter in the same column are not significantly different at the 0.05 significance level based on LSD t-test.

Relating Ground-Based Sensing Data to Spring Wheat Yield

Yield Regression Analysis, 2012

The sensing data from Gardner and Valley City, 2012 were pooled to relate with spring wheat yield. Regression analysis indicated that neither the Crop Circle 2012 first red INSEY nor the Crop Circle 2012 first red edge INSEY can be used as effective predictors to wheat yield. In other words, no significant regression models were found using 2012 Crop Circle INSEYs. As for GreenSeeker, the best prediction model among linear, quadratic polynomial, and exponential models was found to be the exponential model, as illustrated in Figure 29. Existing relevant researches on wheat also found that exponential model was the best choice among several compared common models (Raun et al., 2001; Raun et al., 2005). This model indicates that in this year the GreenSeeker sensing data was highly related to spring wheat yield.

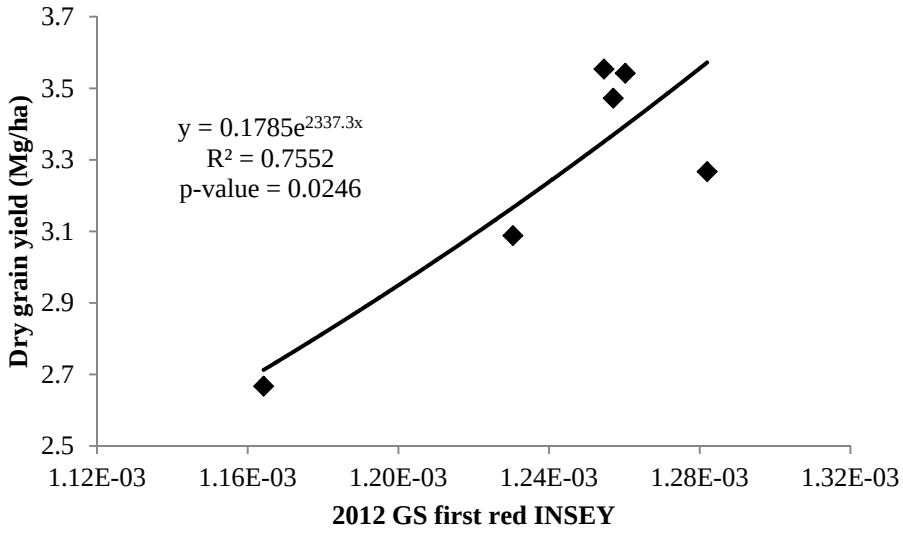

Figure 29. Relationship between 2012 GS first red INSEY and spring wheat yield.

Yield Regression Analysis, 2013

In 2013, for each type of INSEY, both the exponential model and the linear model were highly significant with similar r^2 values. In all cases, the linear models slightly outperformed the corresponding exponential models. In other words, the two models performed similarly. So we still can say that exponential model is one of the best choices for wheat yield prediction using INSEY. Figure 30 through Figure 33 illustrate these linear regression models.

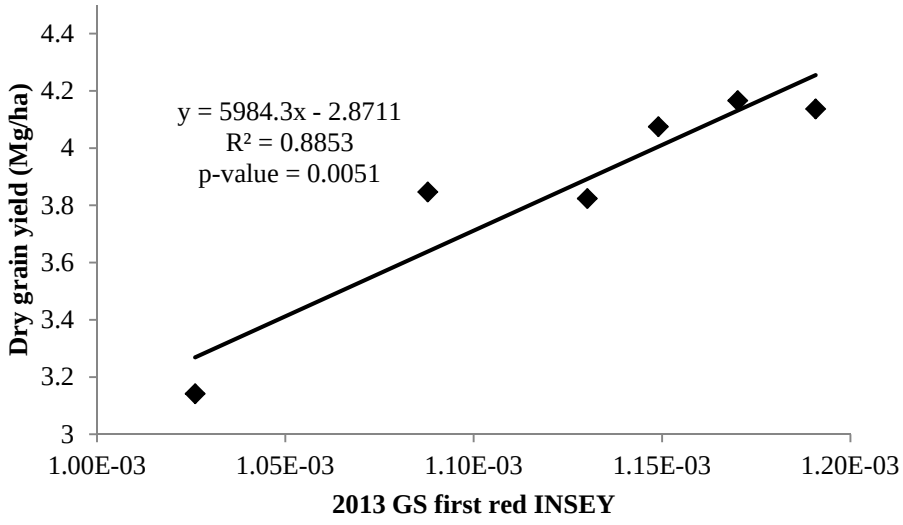

Figure 30. Relationship between 2013 GS first red INSEY and spring wheat yield.

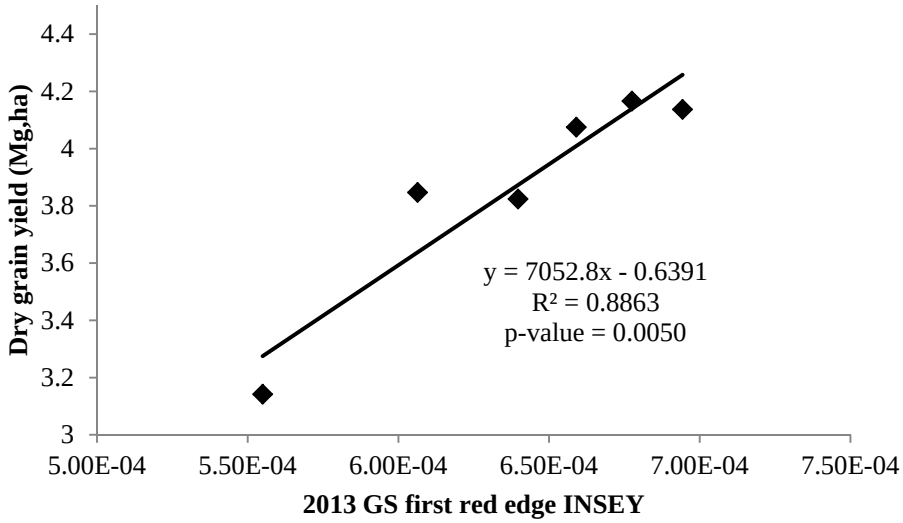

Figure 31. Relationship between 2013 GS first red edge INSEY and spring wheat yield.

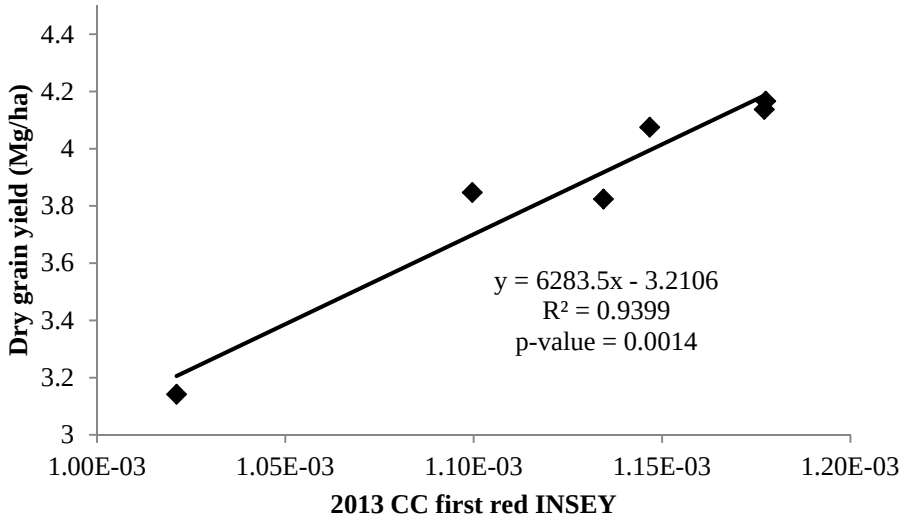

Figure 32. Relationship between 2013 CC first red INSEY and spring wheat yield.

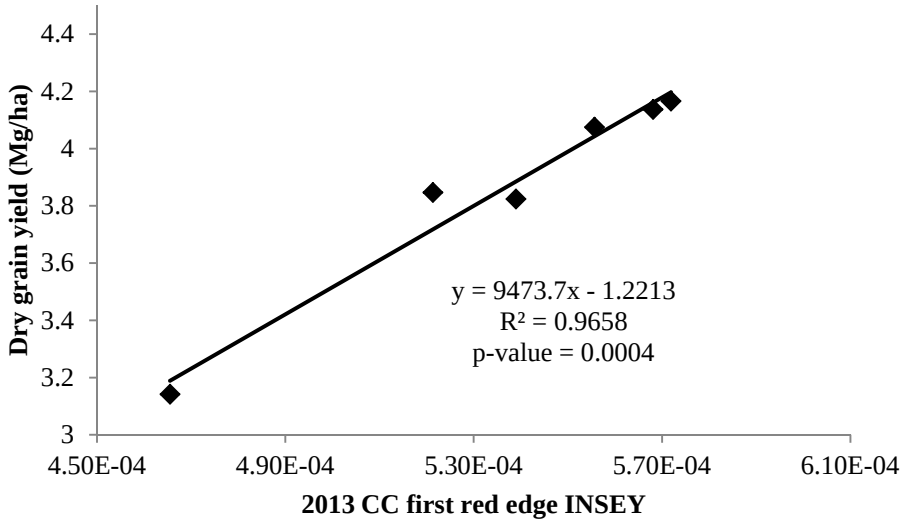

Figure 33. Relationship between 2013 CC first red edge INSEY and spring wheat yield.

Yield Regression Analysis, 2012 and 2013

Four site-years of data were combined to conduct a comprehensive regression analysis. Regression results indicated that the best model using GreenSeeker sensing data was a linear model as illustrated in Figure 34, and the best model for any of the Crop Circle INSEY is an exponential model, as illustrated in Figure 35 and Figure 36. From the results based on two-year pooled data as well as each individual year pooled data, it seems that either linear or exponential models can be very good choices for relating ground-based optical sensor first readings with the spring wheat dry grain yield. These strong relationships between INSEY and wheat yield indicate that early-season spring wheat yield potential and hence early-season wheat N deficiency and requirement can be predicted using optical sensors.

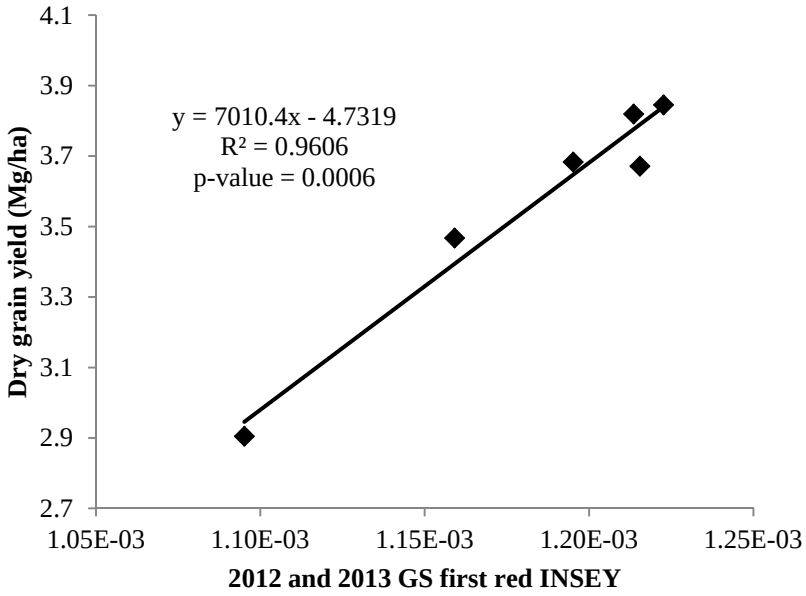

Figure 34. Relationship between 2012 and 2013 GS first red INSEY and spring wheat yield.

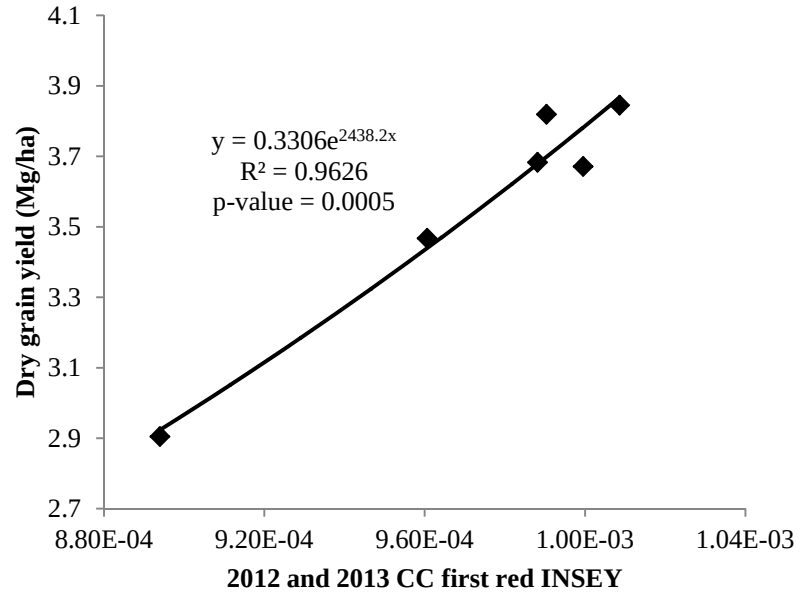

Figure 35. Relationship between 2012 and 2013 CC first red INSEY and spring wheat yield.

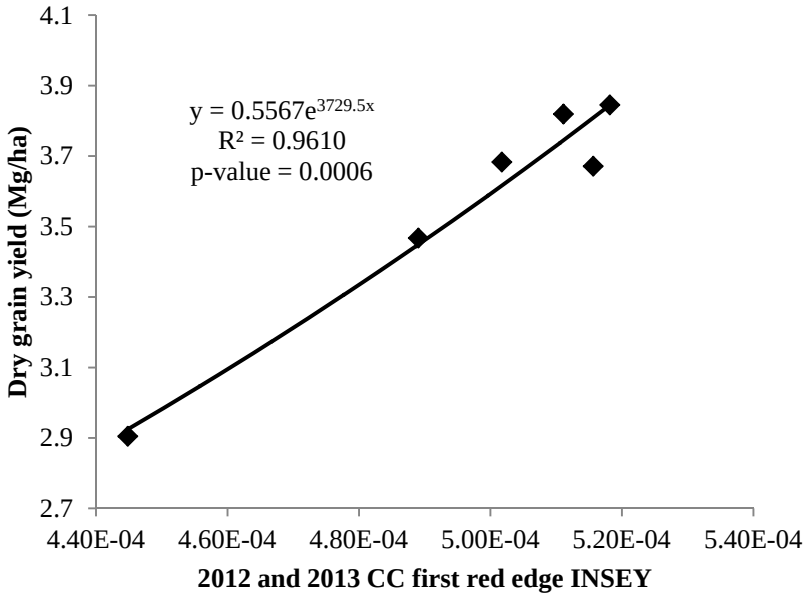

Figure 36. Relationship between 2012 and 2013 CC first red edge INSEY and spring wheat yield.

Relating Ground-Based Sensing Data to Spring Wheat Quality

Protein Content Regression Analysis, 2012

Using the pooled data of 2012, each data set from both sensors at flag leaf INSEY had a highly significant exponential relationship with the adjusted protein content of spring wheat. All of these relationships have very high and similar r^2 values, as illustrated in Figure 37, Figure 38, and Figure 39. Existing researches on wheat focused on the yield prediction using INSEY and rare touched the wheat protein content prediction using optical sensing data. The study based on two-site data of 2012 reveals that exponential model was perhaps the most appropriate model for spring wheat protein content prediction using flag leaf stage INSEY.

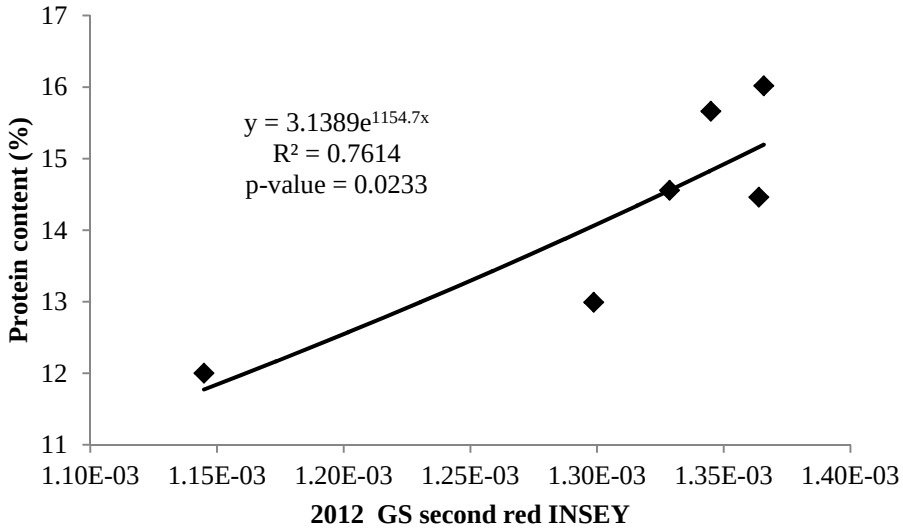

Figure 37. Relationship between 2012 GS second red INSEY and spring wheat protein content.

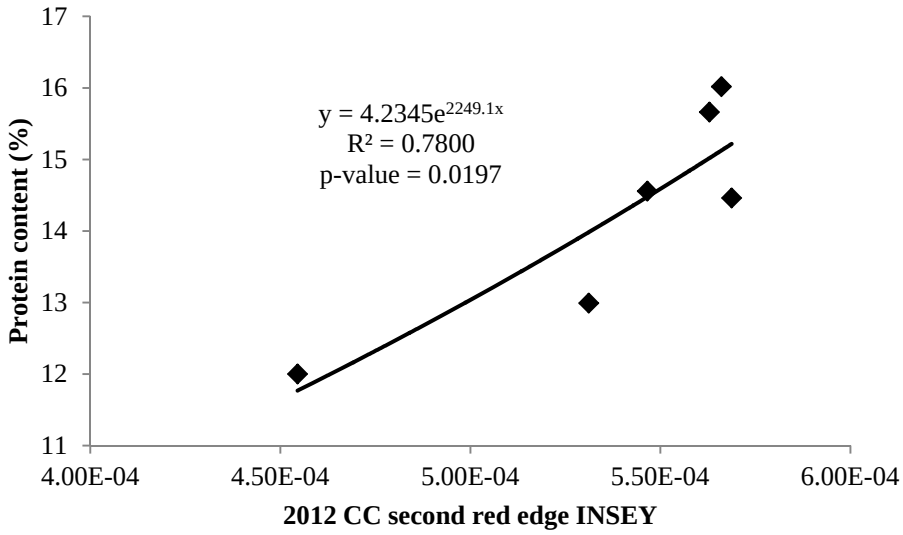

Figure 38. Relationship between 2012 CC second red INSEY and spring wheat protein content.

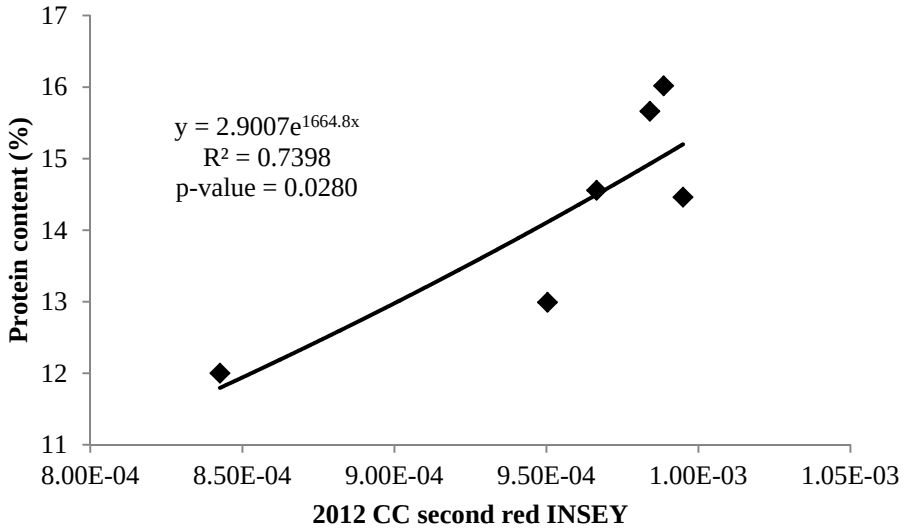

Figure 39. Relationship between 2012 CC second red edge INSEY and spring wheat protein content.

Protein Content Regression Analysis, 2013

Exponential models were still the best choices among the three types of models tested using the pooled data of 2013. Figure 40 through Figure 43 illustrate these models.

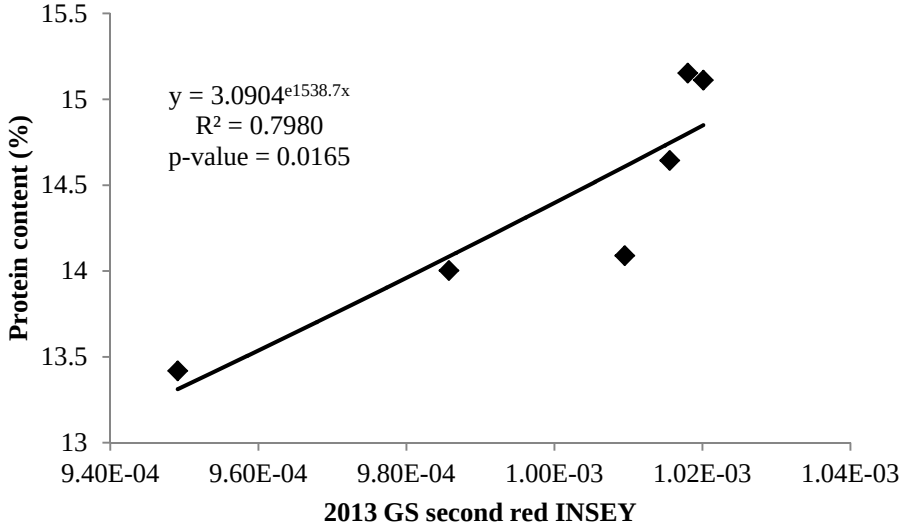

Figure 40. Relationship between 2013 GS second red INSEY and spring wheat protein content.

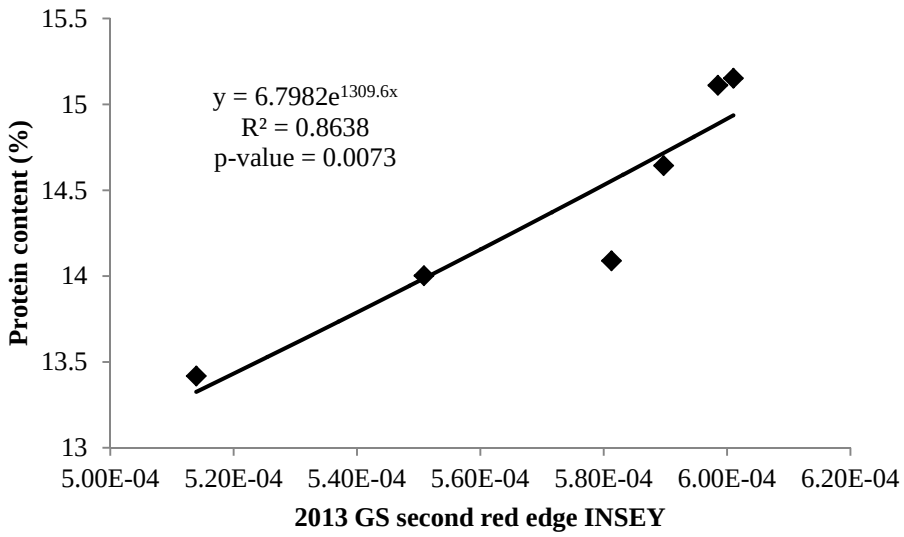

Figure 41. Relationship between 2013 GS second red edge INSEY and spring wheat protein content.

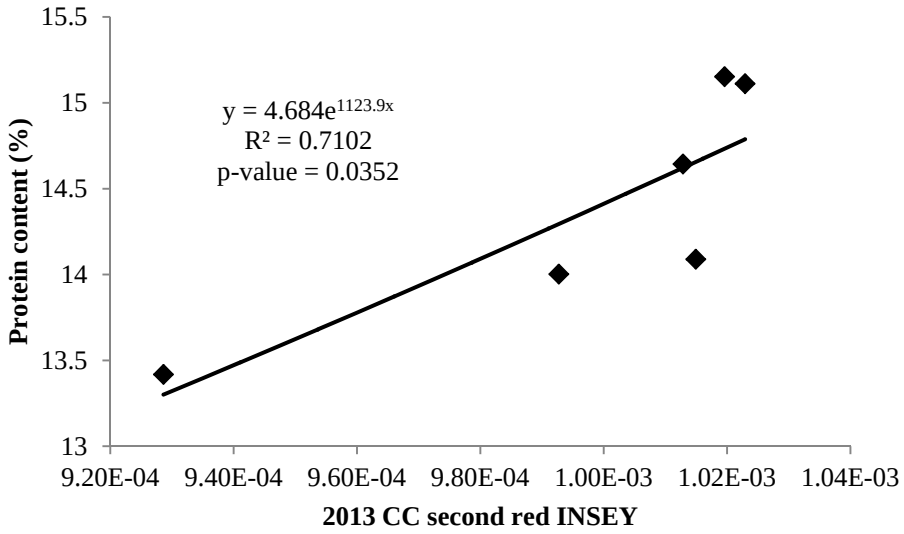

Figure 42. Relationship between 2013 CC second red INSEY and spring wheat protein content.

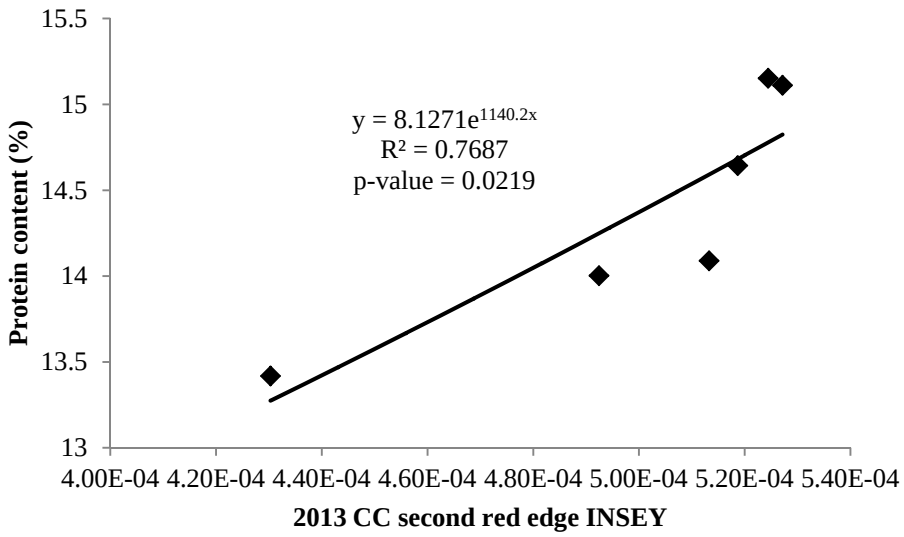

Figure 43. Relationship between 2013 CC second red edge INSEY and spring wheat protein content.

Protein Content Regression Analysis, 2012 and 2013

Figure 44, Figure 45, and Figure 46 illustrate the best regression models, which are all exponential models, using all site-years data. The results based on pooled two year data as well as each individual year pooled data suggested that there consistently exist highly significant and strong exponential relationships between ground-based active optical sensing data and spring wheat protein content. From a closer look at all these figures we can see that the trends in all figures are quite similar. This means reliable in-season protein content prediction can be made using ground-based optical sensing data. Besides, all these ground-based active optical sensing data analysis results show that both sensors perform similarly in most cases.

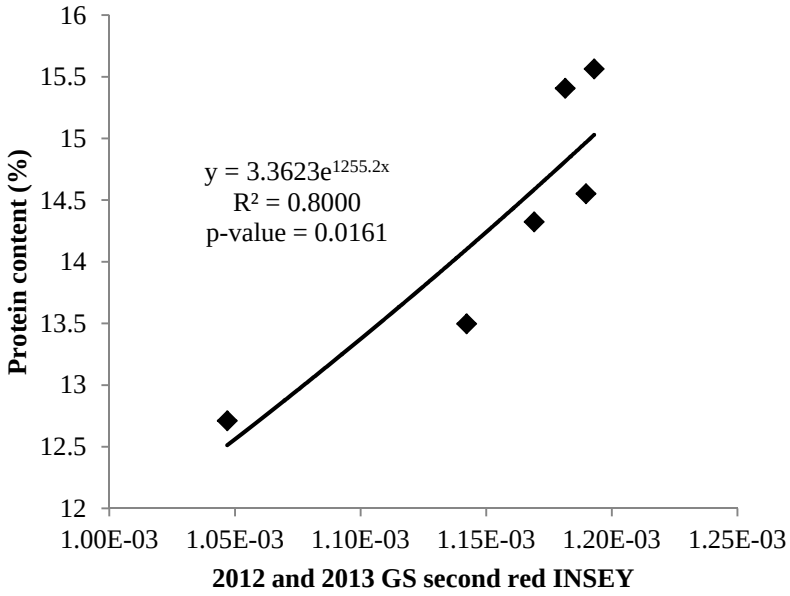

Figure 44. Relationship between 2012 and 2013 GS second red INSEY and spring wheat protein content.

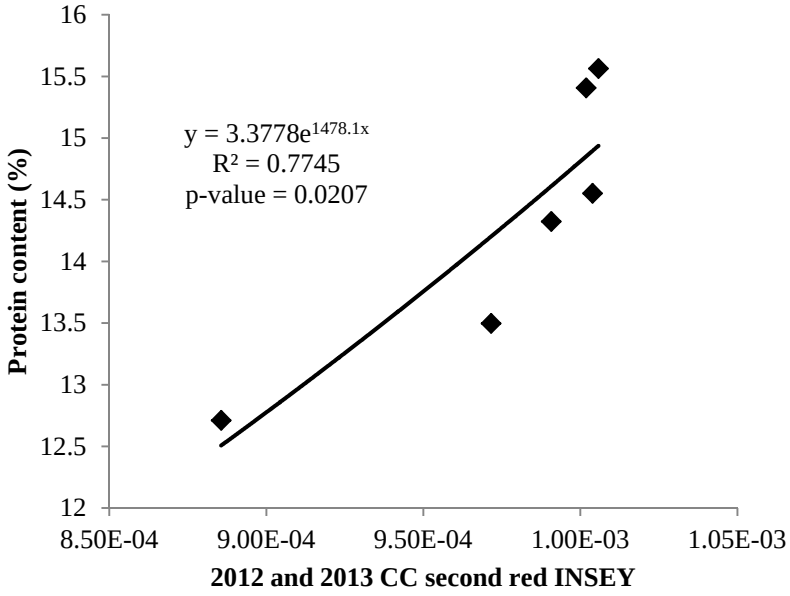

Figure 45. Relationship between 2012 and 2013 CC second red INSEY and spring wheat protein content.

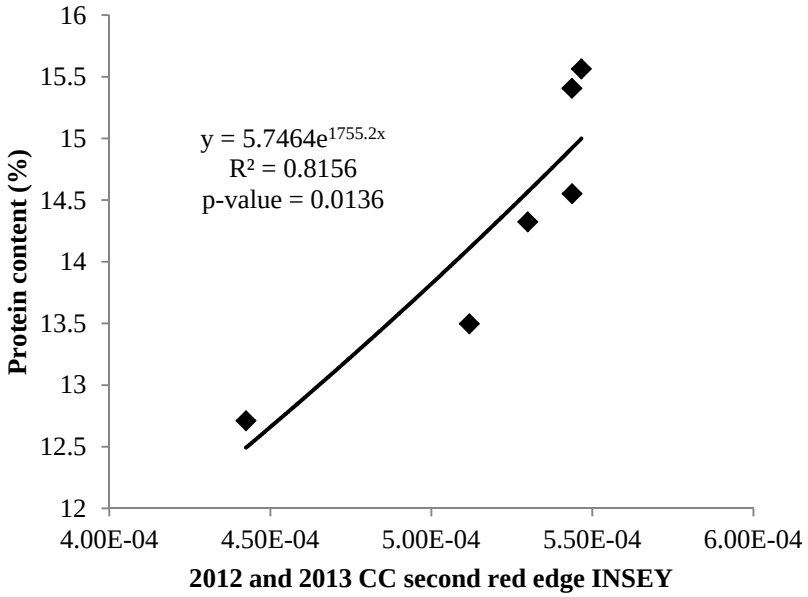

Figure 46. Relationship between 2012 and 2013 CC second red edge INSEY and spring wheat protein content.

Relating Satellite Imagery Data to Spring Wheat Yield or Protein Content

Regression Analysis, 2012

In 2012, only one Gardner site RapidEye satellite imagery of wheat was available for analysis. This imagery was used to relate to both the wheat yield and protein content. The results of relating each of the spectral INSEY to either wheat yield or protein content indicate that using this single site-year data, only the red edge satellite INSEY is valid for prediction purpose. Using 2012 red edge INSEY, a highly significant linear model and a highly significant exponential model for yield prediction and protein content prediction, respectively, were discovered. Figure 47 and Figure 48 illustrate these two models. Some of the red edge INSEY values are negative because of the negative corresponding NDVI values, which were most probably due to the

slightly cloud cover at the sensing moments. The slight cloud interference influenced the NDVI value range but did not affect the overall trend.

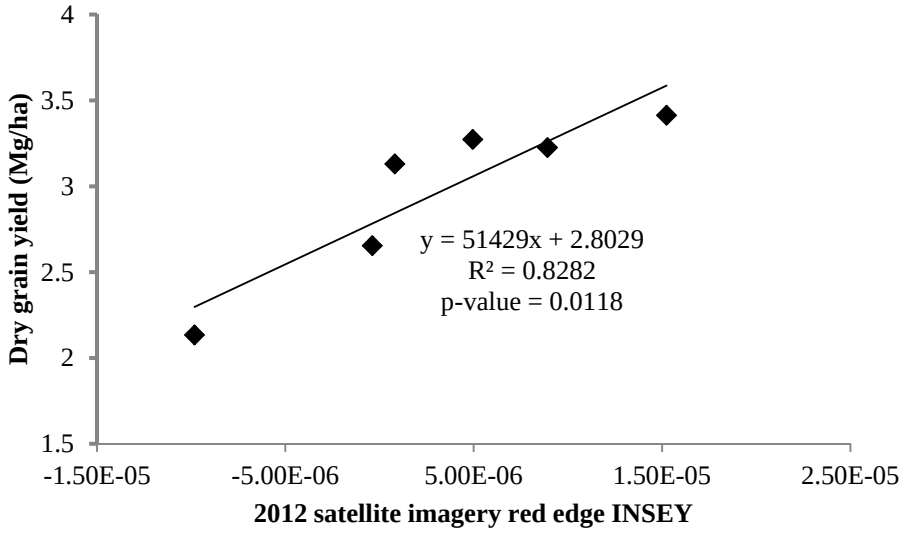

Figure 47. Relationship between 2012 satellite imagery red edge INSEY and spring wheat yield.

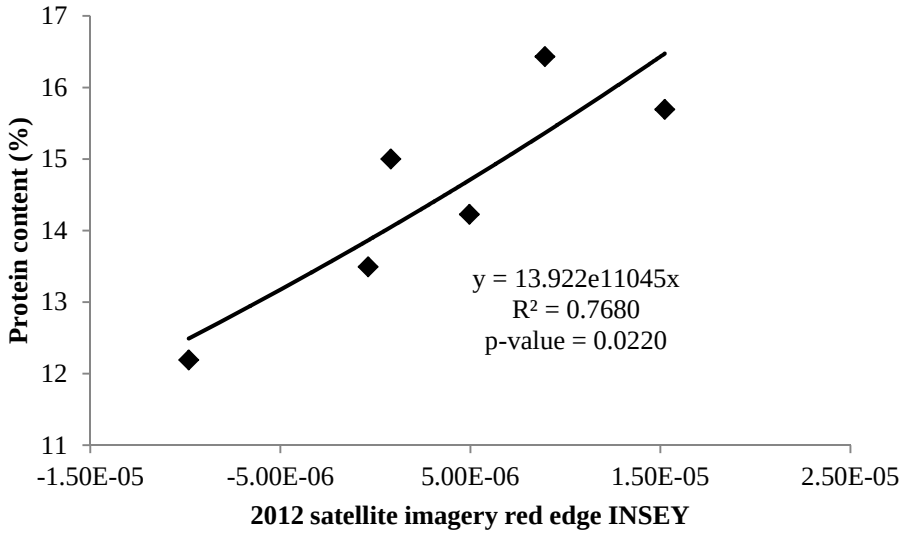

Figure 48. Relationship between 2012 satellite imagery red edge INSEY and spring wheat protein content.

Regression Analysis, 2013

Results of 2013 two site-year pooled data show that 1) no significant relationships between any satellite imagery INSEY and wheat yield were found, and 2) highly significant linear relationships were found between red, or green, or blue INSEY and wheat protein content. Figure 49, Figure 50, and Figure 51 illustrate these prediction models, of which the blue INSEY performed best (r^2 is close to 0.9).

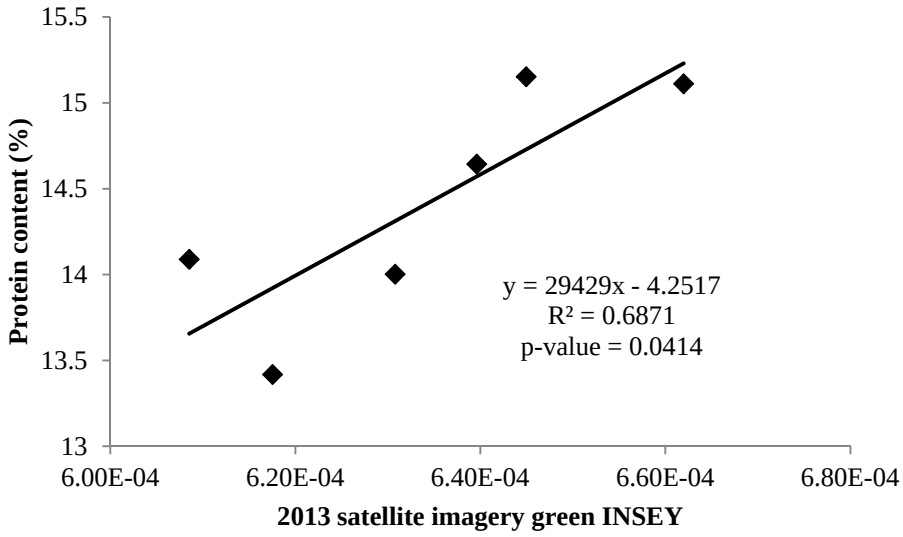

Figure 49. Relationship between 2013 satellite imagery green INSEY and spring wheat protein content.

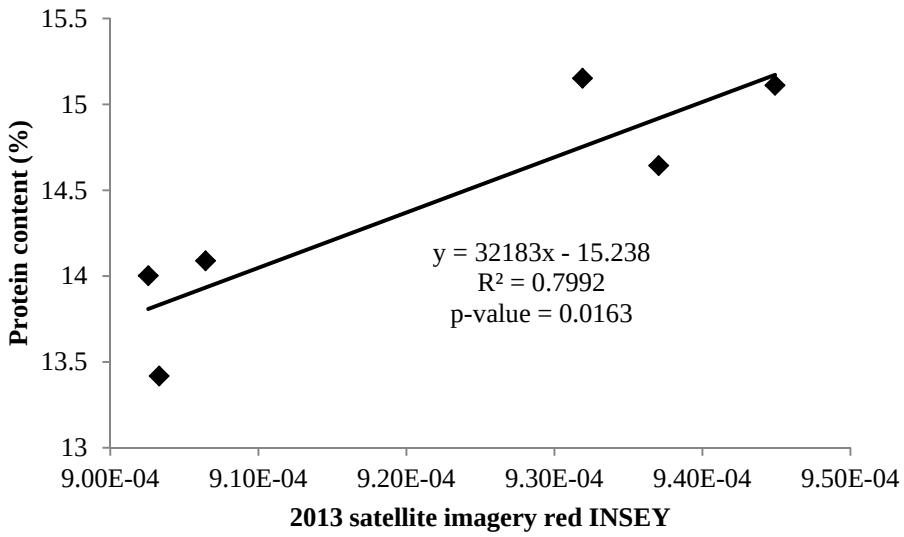

Figure 50. Relationship between 2013 satellite imagery red INSEY and spring wheat protein content.

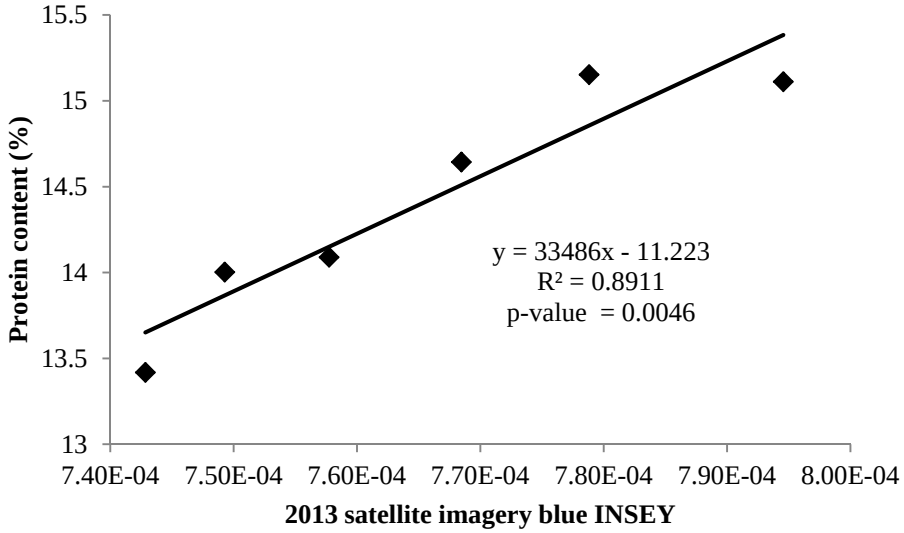

Figure 51. Relationship between 2013 satellite imagery blue INSEY and spring wheat protein content.

Regression Analysis, 2012 and 2013

With all site-year data included, it was found out that only the blue INSEY has very highly significant relation with spring wheat yield. This quadratic relationship (r^2=0.9747) is illustrated in Figure 52. Unlike the positive relationships between wheat yield and INSEY found for each individual year, this quadratic relationship based the two-year satellite imagery data looks different and this was probably because of two reasons. One is that some of the satellite imagery was not in good quality due to cloud cover, and the other is these imagery dates were not close and some of them were captured in the very late season. Thus the quality of the pooled data was substantially and negatively affected. Except green INSEY, all other INSEYs were found to be highly related to wheat protein content, as illustrated in Figure 53 through Figure 55. These protein content prediction models have similar r^2 values. An overview of all regression cases, including each individual year regressions and the combined two year regressions, the blue INSEY seems to be the best spring wheat predictor for both yield and protein content.

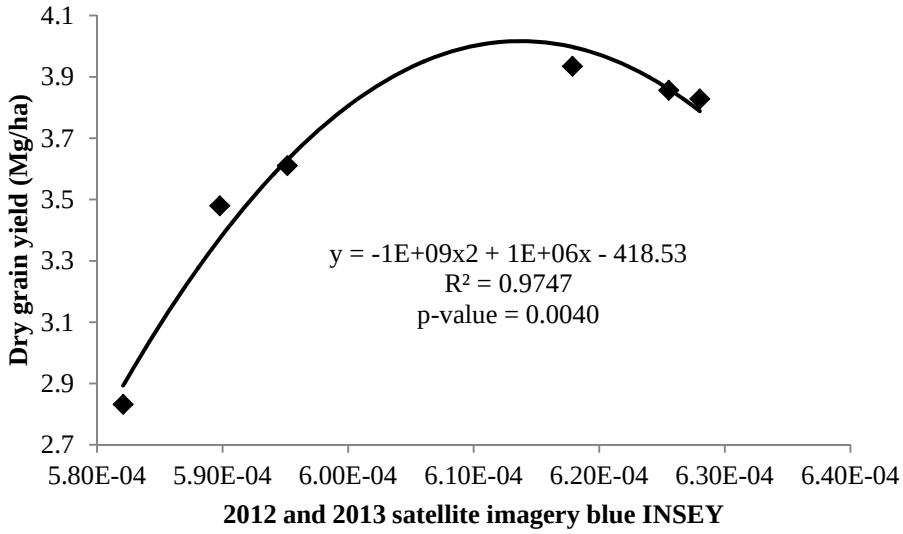

Figure 52. Relationship between 2013 satellite imagery blue INSEY and spring wheat protein content.

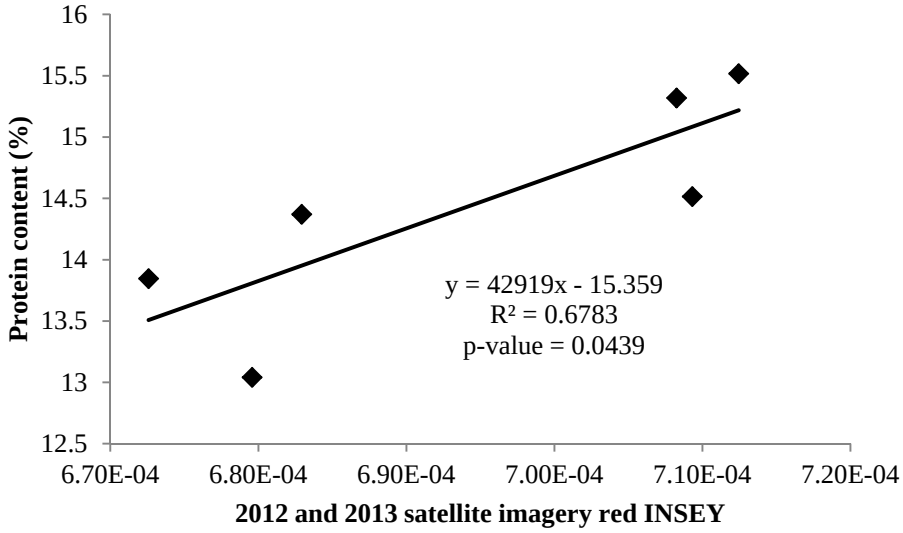

Figure 53. Relationship between 2012 and 2013 satellite imagery red INSEY and spring wheat protein content.

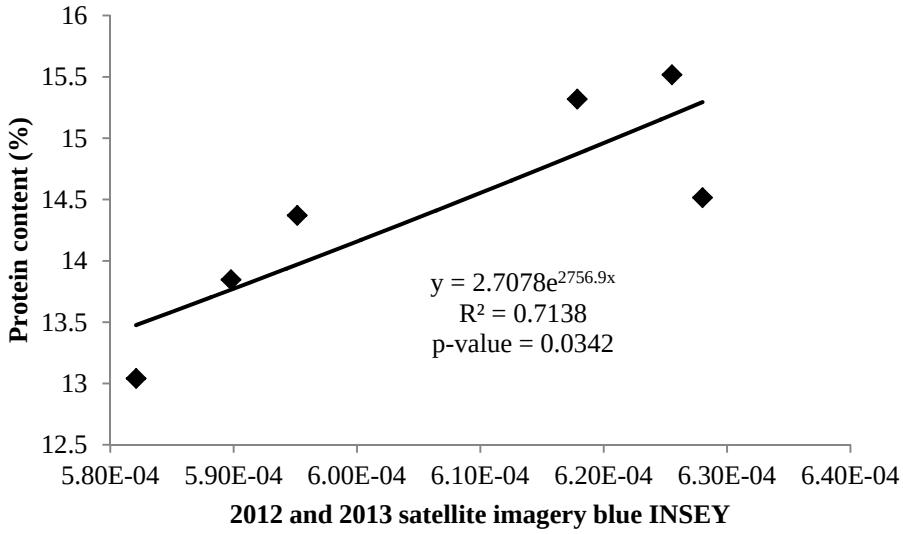

Figure 54. Relationship between 2012 and 2013 satellite imagery blue INSEY and spring wheat protein content.

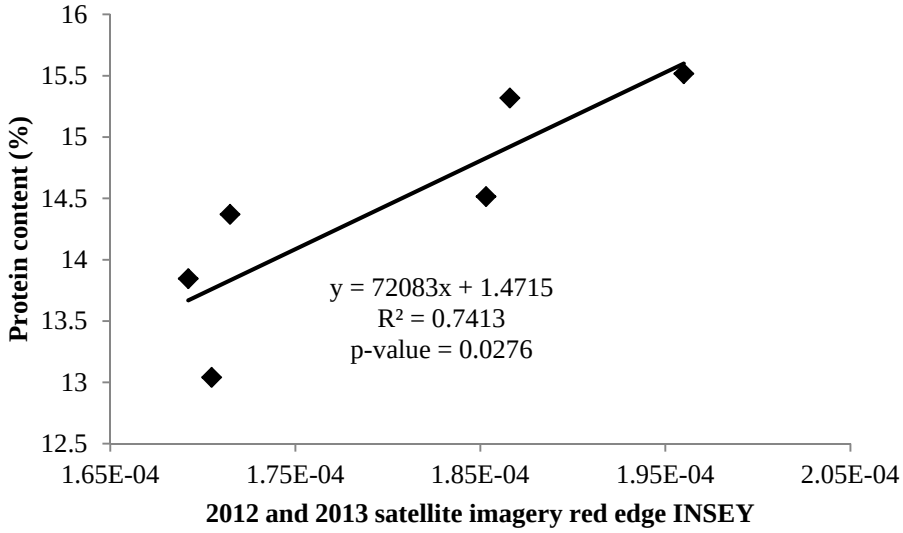

Figure 55. Relationship between 2012 and 2013 satellite red edge INSEY and spring wheat protein content.

Conclusions

GreenSeeker, Crop Circle, and RapidEye satellite imagery are very useful tools for spring wheat yield and protein content early or middle season prediction. With the constructed

regression models, all that farmers need to do in the future is to collect NDVI data using remote sensors, then divide NDVI by GDD to obtain INSEY, and finally input INSEY to the correspondence regression model as independent variable. Spring wheat yield or protein content and hence the site-specific crop N deficiency and requirement can therefore be predicted in early season or mid-season using the algorithm proposed by Raun et al. (2005). Farmers may particularly benefit from the use of the RE INSEY to determine whether to apply a post-anthesis N application for protein enhancement or use of the R INSEY or RE INSEY to direct an in-season variable rate N application at about the 5 leaf growth stage to improve year to year yield consistency and compensate for unanticipated early season N loss. Usually higher protein content results in higher wheat prices for farmers.

RESULTS AND DISCUSSIONS FOR CORN

ANOVA Analysis of Corn Yield Data

ANOVA analyzing results for the four site-year corn yield data are given in Table 50. Except 2012 Durbin site, the N fertilizer rate didn't have shown significant impacts on the adjusted dry grain yield. The nitrate residual in each site of Valley City 2012, Arthur 2013, or Valley City 2013 was much higher than that in Durbin 2012 site, as summarized in the appendix tables A19 through A12. Even in 2012 Durbin, the N rate influence was not that obvious in that only the 0 and 225 Kg ha^{-1} rate yields were significantly different. This was probably due to many unfavorable weather or soil conditions.

Table 50. Corn yield ANOVA analysis.

N rate	2012	2012	2013	2013
	Durbin	Valley City	Arthur	Valley City
---kg ha^{-1}---	----------Mg ha^{-1}----------			
0	3.319 b†	8.347 a	6.744 a	8.385 a
45	4.458 ab	7.526 a	6.464 a	7.895 a
90	4.163 ab	7.357 a	6.647 a	8.477 a
135	4.069 ab	8.471 a	7.497 a	7.597 a
180	4.389 ab	8.320 a	7.952 a	8.283 a
225	5.247 a	8.805 a	7.160 a	7.696 a

† Means with the same letter in the same column are not significantly different at the 0.05 significance level based on LSD t-test.

Relating Yield to Ground-Based Sensing Data

V6 Sensing Regression Analysis, 2012

Significant exponential models were found for all types of V6 sensing INSEY or INSEY*height. These results were in accordance with that of the existing researches (Raun et al., 2002; Raun et al., 2005). The results presented later in this chapter also validated the superiority of exponential models. Table 51 lists the r^2 value for each of these models.

Table 51. r^2 values of exponential models for 2012 corn ground-based V6 sensing

Model†	GS red	GS red×height	CC redEdge	CC redEdge×height	CC red	CC red×height
Exponential	0.189	0.356	0.558	0.565	0.460	0.514

† Model is significant at 0.05 significance level.

From Table 51 it can be seen that Crop Circle performs better than does GreenSeeker in 2012 and that plant height of this year does help improve the model performance. It seems that the impact of plant height was more obvious in GreenSeeker-related models than in Crop Circle-related models. Crop Circle red edge INSEY × plant height became the best yield predictor in this year, and this exponential model is illustrated in Figure 56. Commonly speaking, the higher the INSEY or INSEY × height, the higher the yield.

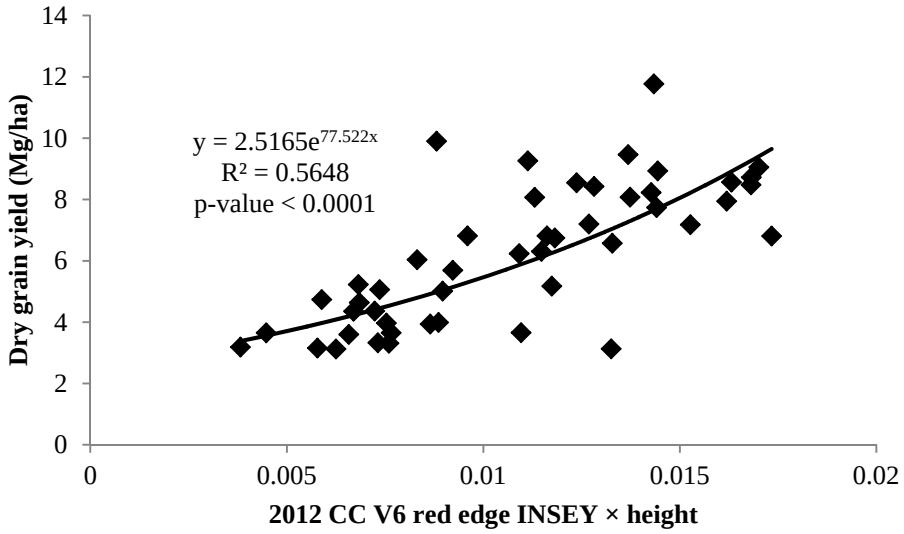

Figure 56. Relationship between 2012 corn CC V6 red edge INSEY × height and dry grain yield.

V12 Sensing Regression Analysis, 2012

Significant exponential models were found for all types of INSEY or INSEY × plant height. Table 52 lists the r^2 value for each of these models. Figure 57 illustrate the exponential relationship between yield and Crop Circle red edge INSEY × height. The data in Table 52 strongly indicate that the original models performed poorly and including the plant height data into a model greatly improved model performance.

Table 52. r^2 values of exponential models for 2012 corn ground-based V12 sensing.

Model†	GS red	GS red×height	CC edEdge	CC redEdge×height	CC red	CC red×height
Exponential	0.125	0.572	0.184	0.689	0.082	0.545

† Model is significant at 0.05 significance level.

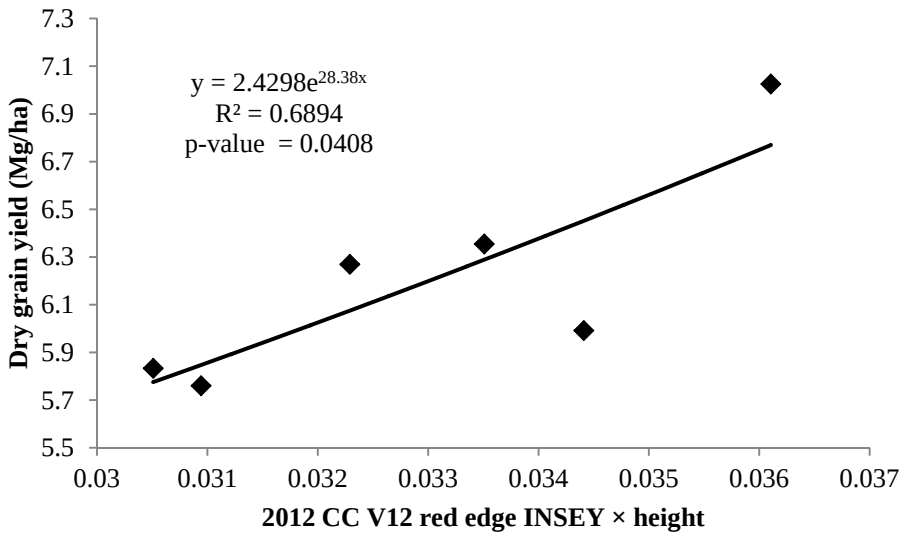

Figure 57. Relationship between 2012 corn CC V12 red edge INSEY × height and dry grain yield.

V6 Sensing Regression Analysis, 2013

A linear model and an exponential model using the Crop Circle red INSEY as predictor were found to be significant, with the linear model slightly outperforming the exponential model. Figure 58 illustrates this linear model. Besides, significant quadratic polynomial models were found for all types of INSEY or INSEY × height. Table 53 and Table 54 list the r^2 value for each of these models. Plant height was not useful for improving model performance. In fact, all models that included plant height using 2013 V6 sensing data had low or very low r^2 values.

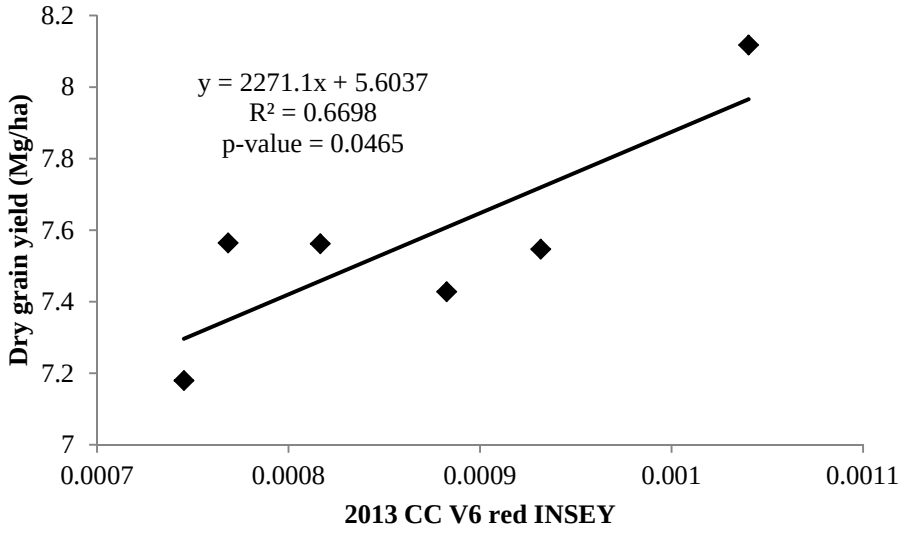

Figure 58. Relationship between 2013 corn CC V6 red INSEY and dry grain yield.

Table 53. r^2 values of quadratic polynomial models for 2013 corn GreenSeeker V6 sensing

Model†	red	red× tapeHeight	red× sensorHeight	RedEdge	redEdge× tapeHeight	redEdge× sensorHeight
Polynomial 2	0.369	0.278	0.177	0.344	0.268	0.168

† Model is significant at 0.05 significance level.

Table 54. r^2 values of quadratic polynomial models for 2013 corn Crop Circle V6 sensing

Model†	RedEdge	redEdge× tapeHeight	redEdge× sensorHeight	red	red× tapeHeight	red× sensorHeight
Polynomial 2	0.391	0.321	0.243	0.399	0.317	0.241

† Model is significant at 0.05 significance level.

V12 Sensing Regression Analysis, 2013

Significant models with very low r^2 values were found for all types of INSEY or INSEY × height except GS red INSEY × sensorHeight, CC red edge INSEY, and CC red INSEY × height. Table 55 and Table 56 list the r^2 value for each of these models. The major reason for the

poor performance of these models is that the ground-based optical second sensing data were not collected using the best distance (approximately 0.5 m to 1 m) specified by the sensors manufacturers due to the higher corn height this year and the fact that we didn't have extensions longer enough at that time.

Table 55. r^2 values of regression models for 2013 corn GreenSeeker V12 sensing.

Model†	Red	red×tapeHeight	redEdge	redEdge×tapeHeight	redEdge×sensorHeight
Linear	0.160	NS	0.110	NS	NS
Polynomial 2	NS	0.178	NS	0.198	0.133

† NS means model is not significant at 0.05 significance level; otherwise model is significant at 0.05 significance level.

Table 56. r^2 values of regression models for 2013 corn Crop Circle V12 sensing.

Model†	redEdge×tapeHeight	redEdge×sensorHeight	red	red×tapeHeight
Linear	NS	NS	0.138	NS
Polynomial 2	0.213	0.129	NS	0.167

† NS means model is not significant at 0.05 significance level; otherwise model is significant at 0.05 significance level.

V6 Sensing Data Regression, 2012 and 2013

Significant linear and exponential models with very high r^2 values were found for all types of INSEY or INSEY × height, with the linear models slightly outperforming the corresponding exponential models. So in this case, either linear model or exponential model was a good choice. Table 57 lists the r^2 values for all linear models. From this table we can see that instead of improving the performance of the regression models, the plant height information decreased all the corresponding models r^2 values. Figure 59, Figure 60, and Figure 61 illustrate the best model for each type of INSEY.

Table 57. r^2 values of linear models for all site-year corn ground-based V6 sensing.

Model†	GS red	GS red×tapeHeight	CC redEdge	CC redEdge×tapeHeight	CC red	CC red×tapeHeight
Linear	0.844	0.693	0.804	0.667	0.822	0.688

† Model is significant at 0.05 significance level.

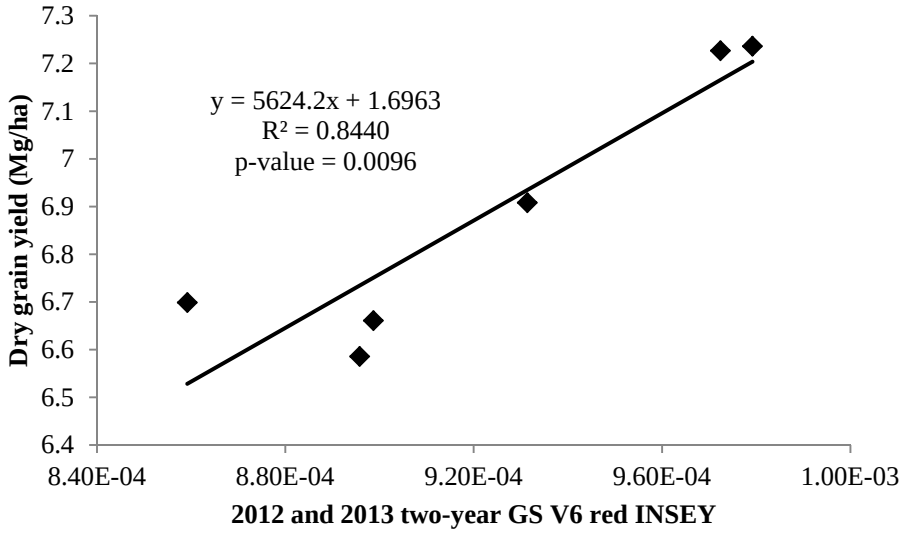

Figure 59. Relationship between 2012 and 2013 two-year corn GS V6 red INSEY and dry grain yield.

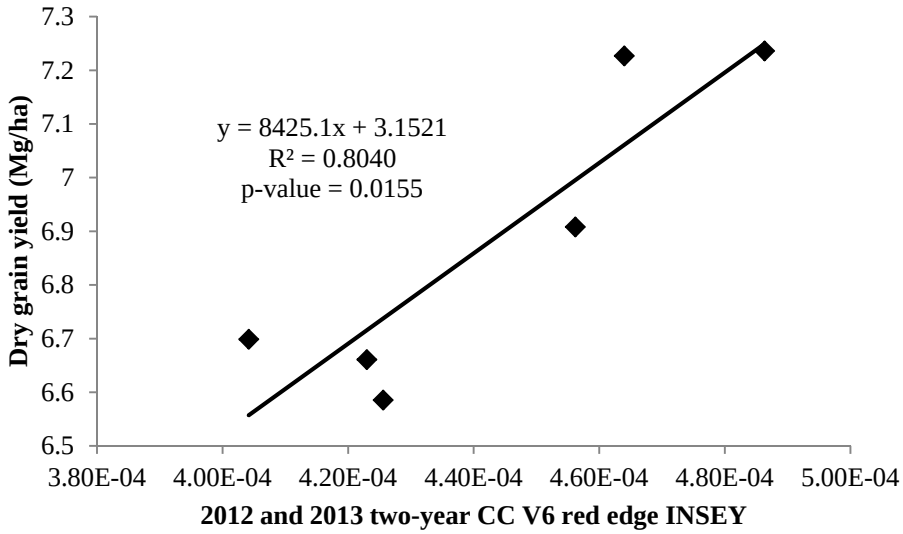

Figure 60. Relationship between 2012 and 2013 two-year corn CC V6 red edge INSEY and dry grain yield.

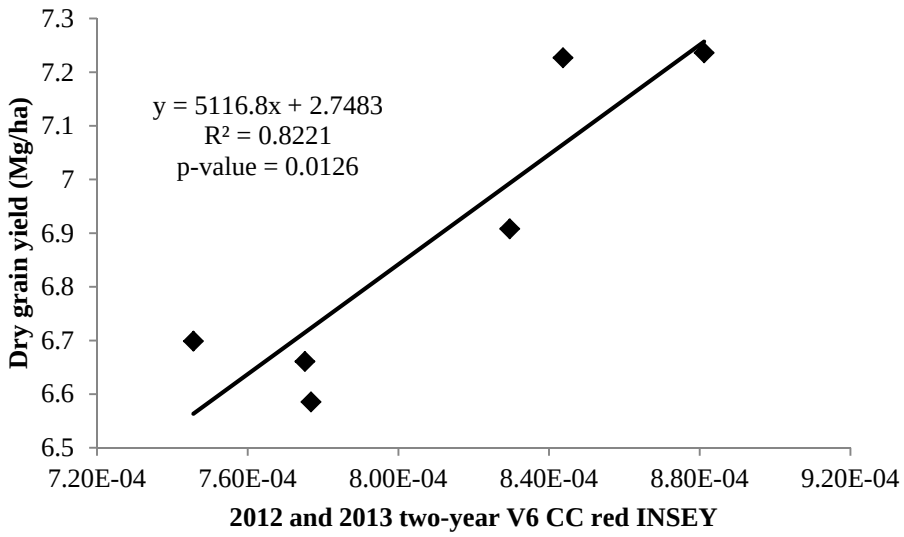

Figure 61. Relationship between 2012 and 2013 two-year corn CC V6 red INSEY and dry grain yield.

V12 Sensing Data Regression, 2012 and 2013

Three significant quadratic polynomial regression models with plant height information included were found, as listed in Table 58. All these models have low r^2 values. This was most probably due to the inconsistency in V12 growth stage sensing data collection, as in that stage the corn height was unfavorable for using the best sensing distance. This adverse factor influenced not only the r^2 values but also the model type.

Table 58. r^2 values of quadratic polynomial models for all site-year corn ground-based V12 sensing.

Model†	GS red×tapeHeight	CC redEdge×tapeHeight	CC red×tapeHeight
Polynomial 2	0.279	0.263	0.270

† Model is significant at 0.05 significance level.

Relating Yield to Satellite Imagery Data

Satellite Imagery Regression Analysis, 2012

Two 2012 RapidEye satellite imagery data sets, one from Durbin August 16 and the other from Valley City August 10, were pooled for regression analysis. Each of the four types spectral INSEY was statistically related to 2012 corn adjusted dry grain yield. Red INSEY and Green INSEY were found to be very effective corn yield predictors when exponential models or linear models were adopted. Exponential models slightly outperformed the corresponding linear models. Figure 62 and Figure 63 illustrate these two highly significant exponential models that have very high r^2 values. An existing research found that cumulative NDVI from satellite imagery had strong linear relationship with the corn grain yield (Mkhabela et al., 2005), but no existing researches were found regarding the relationship between satellite imagery INSEY and corn grain yield.

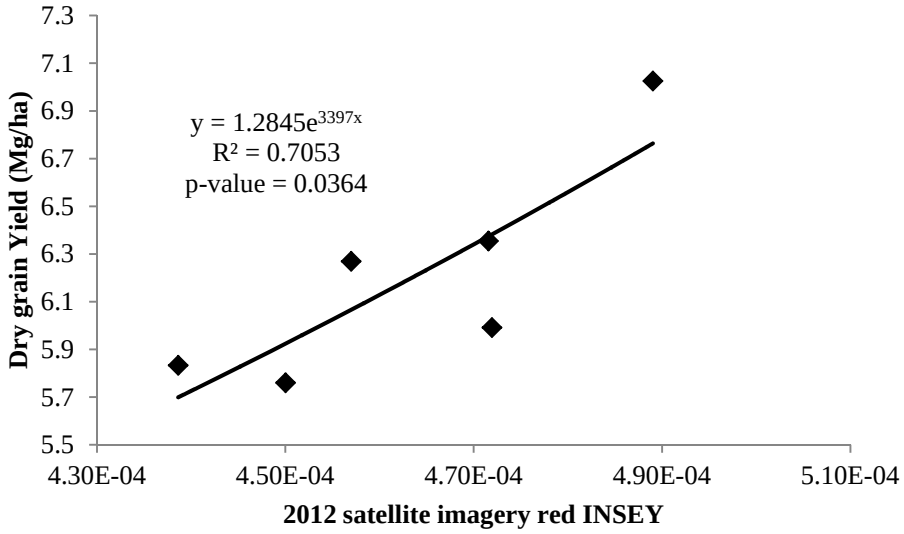

Figure 62. Relationship between 2012 corn satellite imagery red INSEY and dry grain yield.

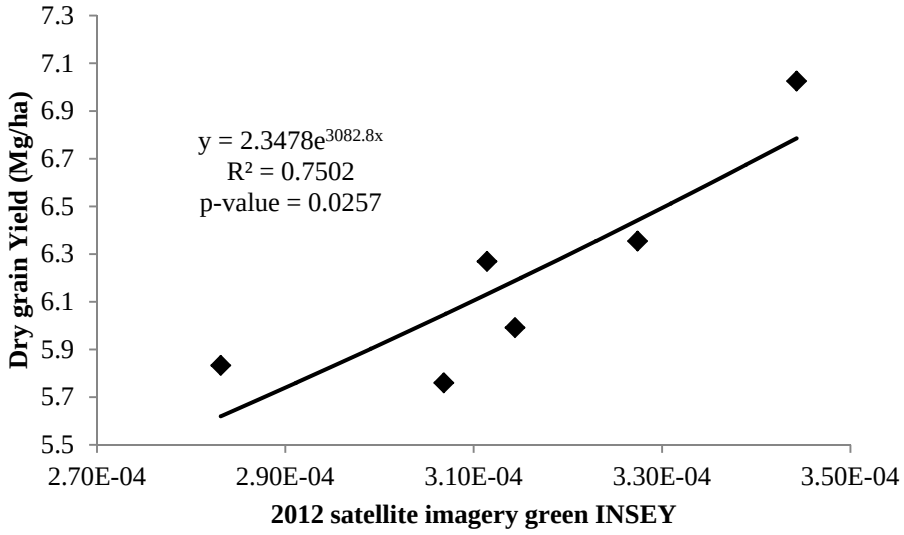

Figure 63. Relationship between 2012 corn satellite imagery green INSEY and the dry grain yield.

Satellite Imagery Regression Analysis, 2013

In 2013 two satellite imagery INSEY data sets and corresponding adjusted dry grain yield data sets were pooled together for regression analysis. One imagery INSEY data is from Arthur June 24, and the other from Valley City July 21. Statistical regression analysis results indicate that no significant relationships were found between this year's satellite imagery INSEY and corn yield. This is partly because of the light cloud haze over Valley City corn site on the space sensing day. However, significant exponential relationships with very high r^2 values between each types of INSEY but the blue INSEY of Arthur June 24 imagery and corn yield were revealed, as illustrated in Figure 64 through Figure 66.

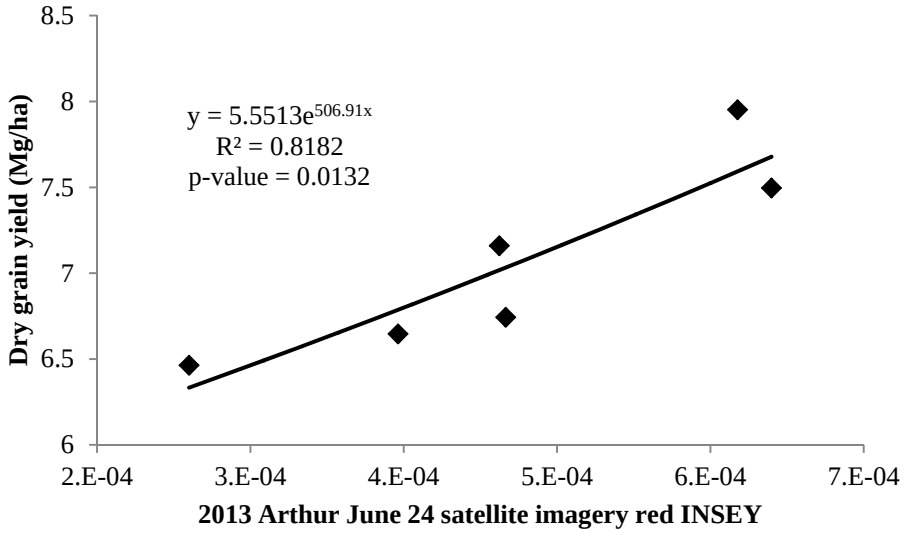

Figure 64. Relationship between 2013 Arthur June 24 corn satellite imagery red INSEY and the dry grain yield.

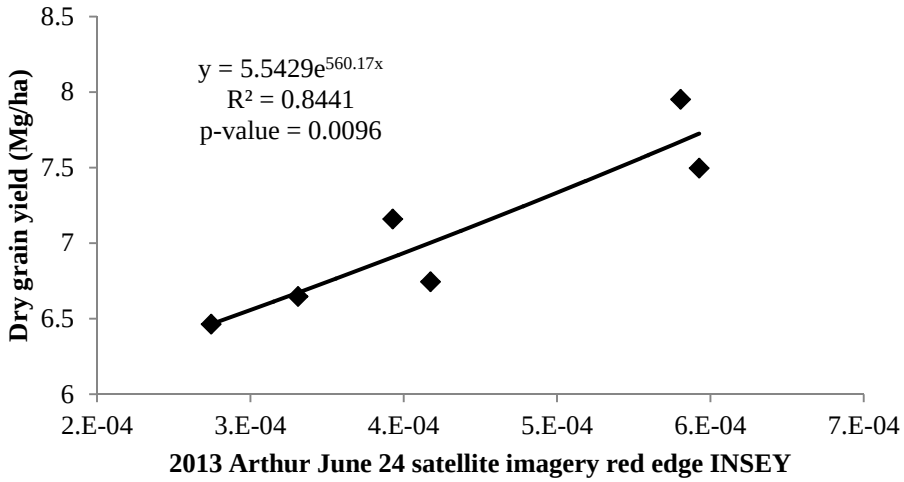

Figure 65. Relationship between 2013 Arthur June 24 corn satellite imagery red edge INSEY and the dry grain yield.

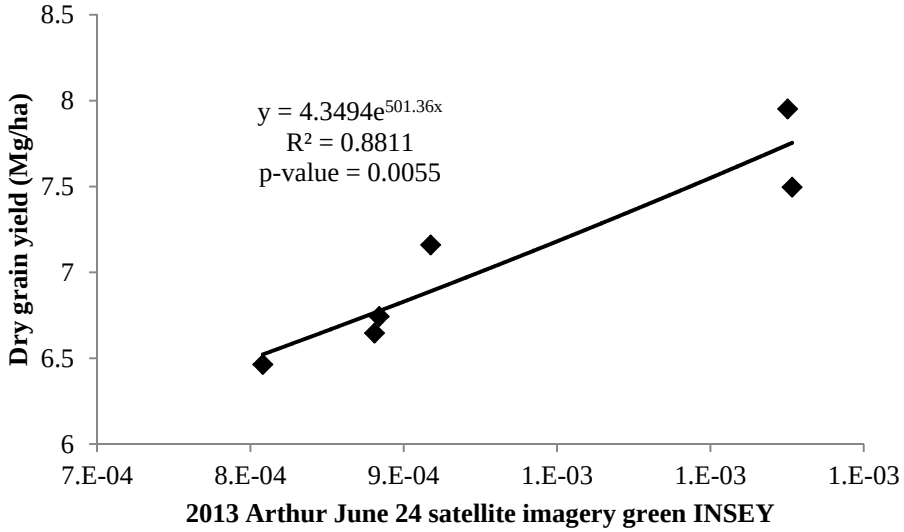

Figure 66. Relationship between 2013 Arthur June 24 corn satellite imagery green INSEY and dry grain yield.

Satellite Imagery Regression Analysis, 2012 and 2013

All site-year pooled data, which are the combination of 2012 data and 2013 data described above, were subject to regression analysis to find out if there are significant

relationships between satellite imagery INSEY and corn yield. Except blue INSEY, all types of INSEY have significant and strong exponential relationships with corn grain yield, as illustrated in Figure 67 through Figure 69.

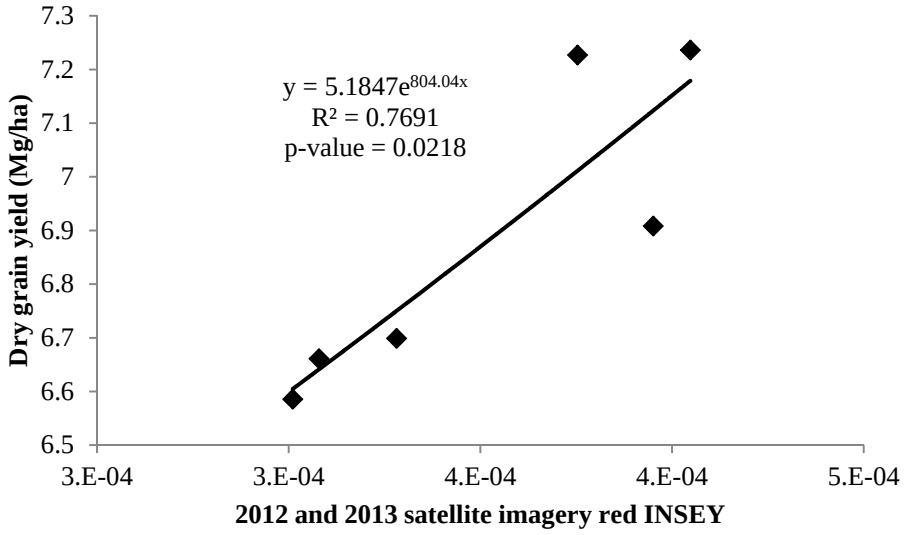

Figure 67. Relationship between 2012 and 2013 corn satellite imagery green INSEY and dry grain yield.

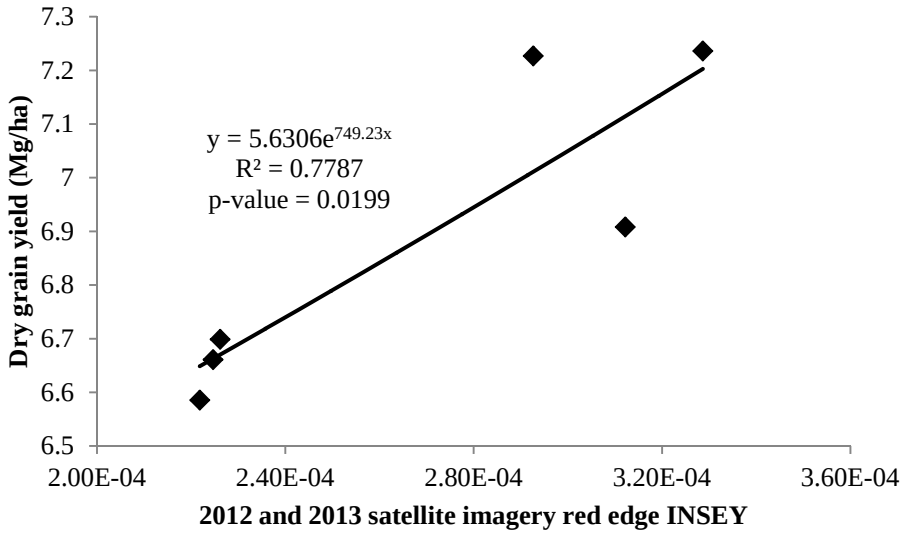

Figure 68. Relationship between 2012 and 2013 corn satellite imagery red edge INSEY and dry grain yield.

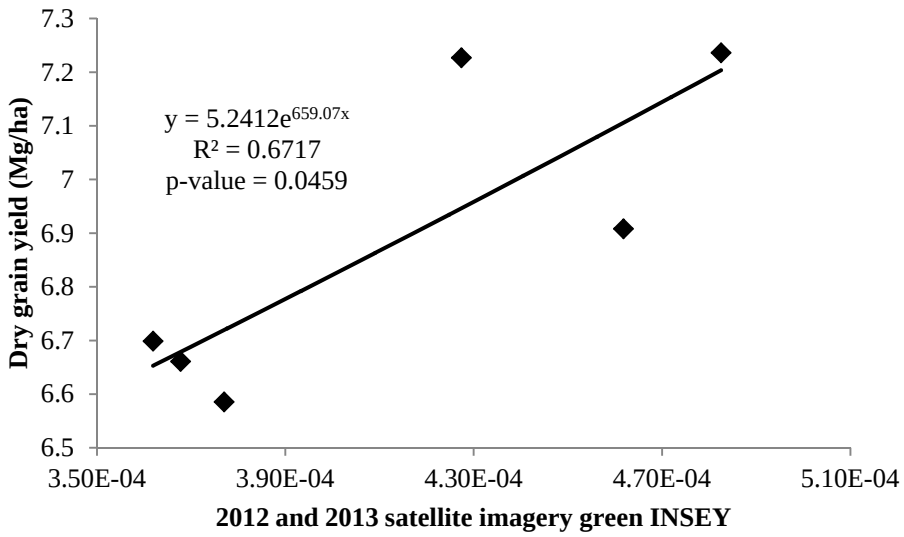

Figure 69. Relationship between 2012 and 2013 corn satellite imagery green INSEY and dry grain yield.

Conclusions

Both the ground-based active optical sensing data and the passive satellite imagery data have strong potential for in-season corn yield prediction and hence site-specific N deficiency and demand determination. These in-season prediction models enable precision N management in-season, potentially increasing N efficiency, saving farmer fertilizer cost as well as improving corn grain yield. The sensors are similar in their prediction ability within this study. The inconsistent performance of the plant height in improving regression model performance is most probably due to the inconsistency of the height sampling method. The red and green RapidEye satellite NDVIs were the most appropriate NDVIs for corn grain yield prediction.

RESULTS AND DISCUSSIONS FOR SUNFLOWER

Valley City Oilseed Sunflower Data Analysis

ANOVA Analysis of the Yield and Quality

ANOVA analysis results for 2012 and 2013 Valley City NuSun oilseed sunflower dry seed yield and oil% per 10% moisture are listed in Table 59. Yield was adjusted using the plant stand information. Except 2012 yield, no significant influence of N application rate was found. The appendix table A16 indicates that there was very high total nitrate residual in 2013 Valley City sunflower site, which explained why in 2013 the yield and oil content was not significantly affected by N rate. In Valley City 2012, the soil test (Appendix Table A14) showed that the percentage of organic matter was very high and was more than twice that of Valley City 2013. Higher organic matter content implies higher N source for plant. This might explain why no significant influence of N rate on oil content of 2012 Valley City. Existing research did find significant influence of N rate on oilseed sunflower oil content (Mollashahi et al., 2013).

Yield Regression Analysis, 2012

Our regression analysis based two-site data of 2012 indicated that no significant relationships were found between dry seed yield and ground-based optical active sensing V6-8 INSEY. This probably because at V6-8 stage, the sunflowers were still very small and the optical sensing were greatly and adversely influenced by soil background. Another possible reason might be that the selected sensing samples were not good enough to be used as representatives.

Highly significant exponential models and linear models with high r^2 values, however, were found between dry seed yield and the INSEYs from satellite imagery of August 10, 2012, as summarized in Table 60. This was reasonable as in August the biomass of sunflower was already very dense. Except the green INSEY, all other types of INSEY were found to be very good predictors of the yield. The exponential models and the linear models have similar performance. Pena-Barragan et al. (2010) also found a significant linear relationship between remote sensing data of aerial photography and sunflower yield, but their study used absolute NDVI instead of normalized INSEY. Figure 70 illustrates the exponential relationship between yield and blue INSEY.

Table 59. ANOVA analysis of Valley City oilseed sunflower yield and quality.

N rate (kg ha^{-1})	2012		2013	
	yield (Mg ha^{-1})	Oil content (%)	yield (Mg ha^{-1})	Oil content (%)
0	1915ab†	46.05a	2476a	41.00a
45	2282bc	46.00a	2881a	40.29a
90	1750a	46.29a	2405a	41.23a
135	2319bc	44.99a	2242a	40.59a
180	2698c	45.61a	3041a	40.61a
225	2664c	45.16a	3007a	41.31a

† Means with the same letter in the same column are not significantly different at the 0.05 significance level based on LSD t-test.

Table 60. r^2 values of the relationships between 2012 Valley City sunflower dry seed yield and satellite imagery INSEY.

Model†	red INSEY	red edge INSEY	blue INSEY
Exponential	0.768	0.721	0.826
Linear	0.788	0.712	0.816

† Model is significant at 0.05 significance level.

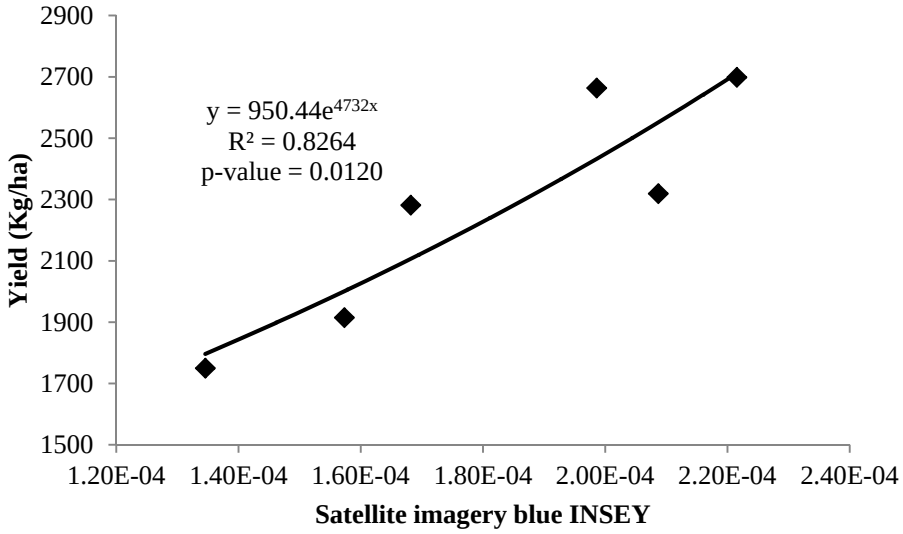

Figure 70. Relationship between 2012 Valley City sunflower seed yield and satellite imagery blue INSEY.

Yield Regression Analysis, 2013

No significant relationships were found between dry seed yield and ground-based optical active sensing V6-8 INSEY. Similar reasons as mentioned above can be said for this result. A highly significant exponential model and a linear model with high r^2 values were found only between dry seed yield and green INSEY from satellite imagery of June 24, 2013. Figure 71 illustrates the exponential relationship between yield and green INSEY.

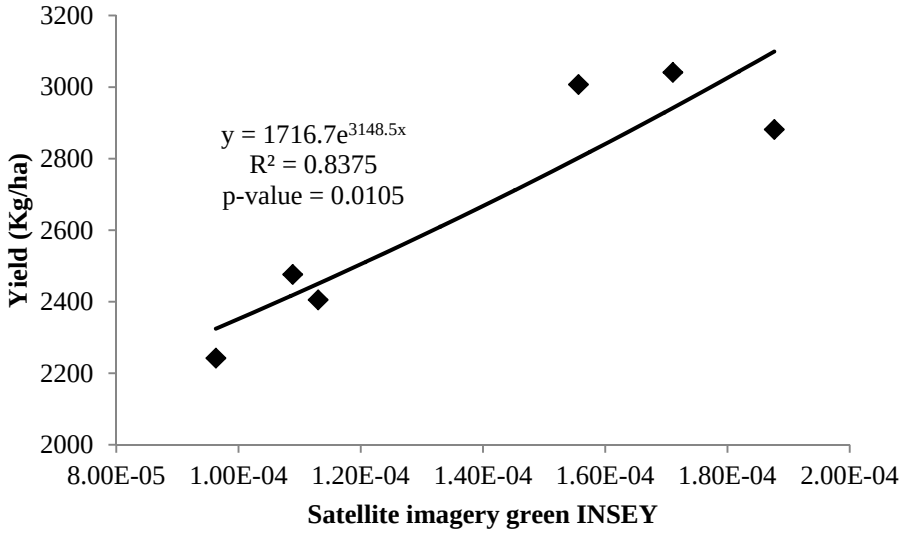

Figure 71. Relationship between 2012 Valley City sunflower seed yield and satellite imagery green INSEY.

Yield Regression Analysis, 2012 and 2013

No significant relationships were found between Valley City sunflower seed yield and pooled two site-years ground-based sensing INSEY. Poor performance in each individual year explained the poor performance for combined two-year data. Highly significant exponential and linear relationships between yield and pooled satellite imagery red INSEY or green INSEY were found, as illustrated in Table 61 and Figure 72.

Table 61. r^2 values of the relationships between 2012 and 2013 Valley City sunflower dry seed yield and satellite imagery INSEY.

Model†	red INSEY	green INSEY
Exponential	0.740	0.824
Linear	0.753	0.811

† Model is significant at 0.05 significance level.

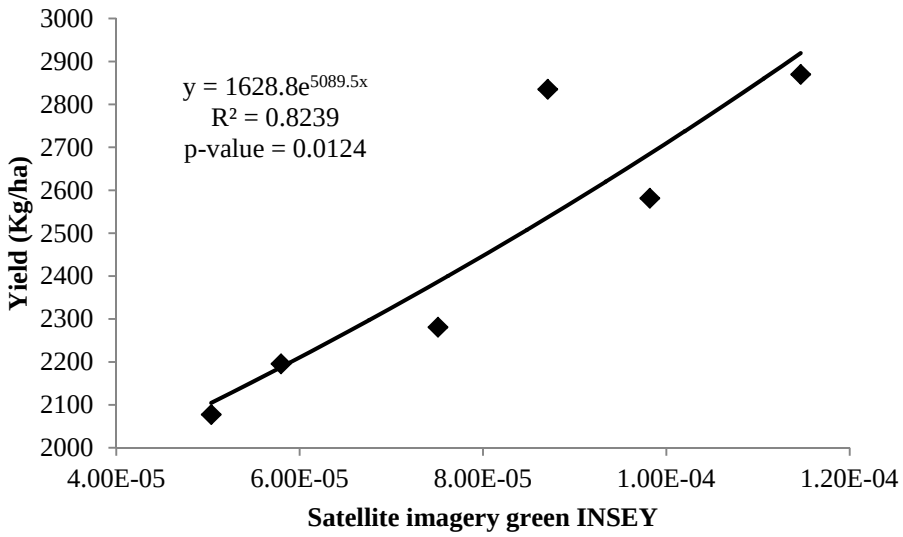

Figure 72. Relationship between 2012 and 2013 Valley City sunflower seed yield and satellite imagery green INSEY.

Oil Content Regression Analysis, 2012

Neither ground-based active sensing V12-16 INSEY nor passive satellite imagery INSEY were found to be valid predictors of oil% per 10% moisture in 2012. One-year data seems to be not enough for revealing the relationship between V12-16 INSEY and oilseed sunflower oil content.

Oil Content Regression Analysis, 2013

No significant relationships were found between ground-based active sensing V12-16 INSEY and sunflower seed oil% per 10% moisture. A highly significant quadratic polynomial regression model was found between satellite imagery green INSEY and oil content, as illustrated in Figure 73. Since no reported work on the relationship between satellite imagery INSEY and sunflower oil content, we cannot make direct comparison with existing work.

Theoretically, oil content was expected to have a positive correlation with remote sensing INSEY. This kind of quadratic polynomial trend might be the result of 1) cloud and haze effects on the satellite imagery, 2) harvest samples were not representative enough, and 3) one-year data was not enough.

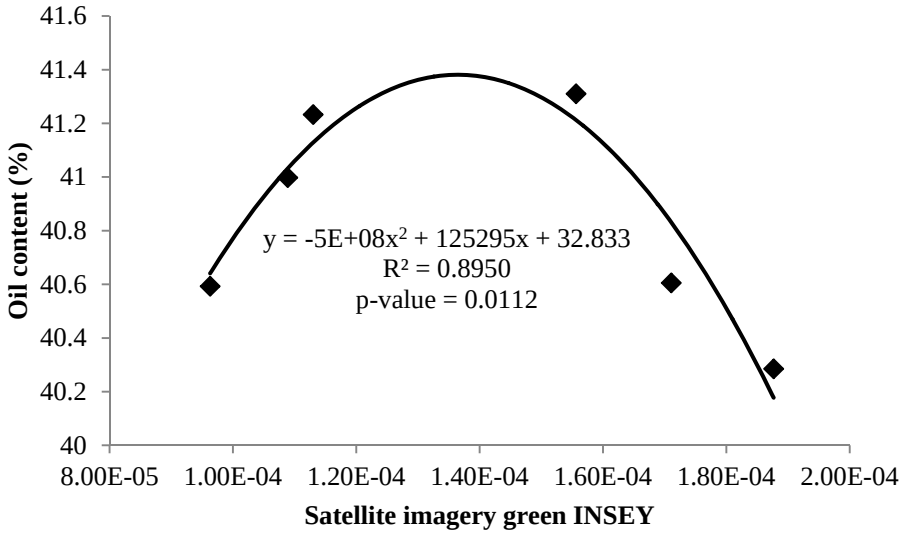

Figure 73. Relationship between 2013 Valley City sunflower seed oil content and satellite imagery green INSEY.

Oil Content Regression Analysis, 2012 and 2013

Analysis of the pooled two site-year INSEY data and oil content data revealed that GreenSeeker red INSEY, Crop Circle red edge INSEY, satellite red INSEY, and satellite red edge INSEY are valid predictors of sunflower seed oil content, as summarized in Table 62. Compared to the results of each individual year, it seems that at least two-year data were necessary for finding reliable regression models. Figure 74 illustrates the linear relationship between oil content and Crop Circle red edge V12-16 INSEY.

Table 62. r^2 values of the relationships between 2012 and 2013 Valley City sunflower dry seed oil content and INSEY.

Model†	GS red INSEY	CC red edge INSEY	Satellite red INSEY	Satellite Red edge INSEY
Exponential	0.320	0.549	0.763	0.751
Linear	0.316	0.550	0.772	0.755

† Model is significant at 0.05 significance level.

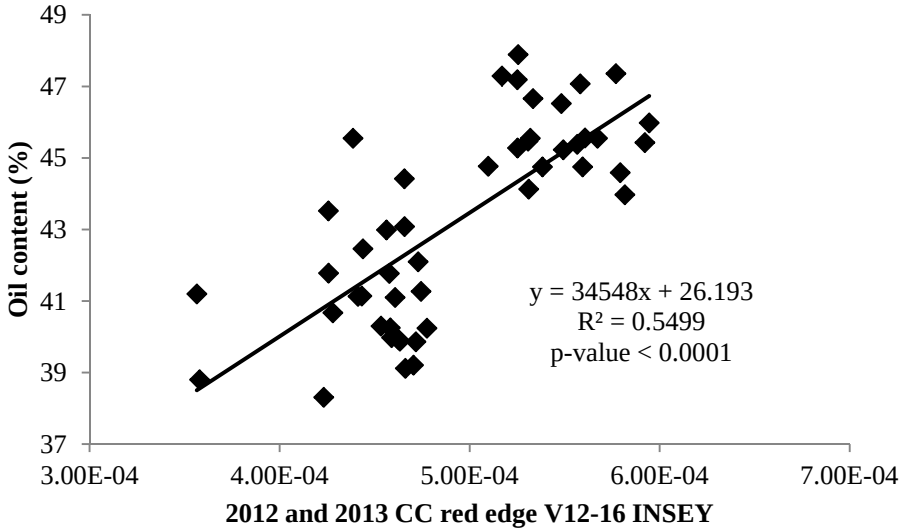

Figure 74. Relationship between 2012 and 2013 sunflower oil content and Crop Circle red edge V12-16 INSEY.

Cummings Confectionery Sunflower Data Analysis

Influence of N Fertilization Rate on Yield and Quality

Table 63 summarizes the ANOVA analysis results for 2012 and 2013 Cummings confectionery sunflower harvest data, respectively. No clear trend of the influence of N rate on the seed yield or qualities of 2012 Cummings confectionery sunflower was observed due to very high nitrate residual level in 2012 Cummings site (see Appendix Table A13). In 2013, the yield and the 0.87 cm content (22/64" content) were significantly and positively affected by N rate.

Residual nitrate in 2013 Cummings site was low, as indicated by the soil test results shown in Appendix Table A15. Best sunflower seed yield and qualities were all found when 135 kg ha^{-1} N rate was applied, even when the treatment was not a significant influential factor. This implies two possible facts: over application of N may result in reduced sunflower seed yield, and one of the other nutrients or conditions may become the most limiting factor for sunflower growth.

Table 63. ANOVA analysis of 2012 and 2013 Cummings confectionery sunflower seed yield and quality.

Year	N rate (kg ha^{-1})	Yield (Mg ha^{-1})	Length (mm)	Width (mm)	Meat/shell	0.87 cm content (%)
2012	0	2288a†	15.95bc	8.74b	1.01a	69.44a
	45	2541a	16.22abc	9.12a	0.92a	81.24a
	90	2094a	16.26abc	8.93ab	0.98a	77.41a
	135	2095a	15.87c	8.81ab	0.94a	74.67a
	180	2252a	16.47ab	8.97ab	1.02a	80.87a
	225	2509a	16.57a	8.91ab	0.95a	81.88a
2013	0	1616a	15.37a	8.53a	0.88a	33..14a
	45	2168ab	15.37a	8.80a	0.90a	48.61ab
	90	2217abc	15.76a	8.78a	0.95a	58.58b
	135	2866c	16.41a	9.04a	1.14b	82.58c
	180	2737bc	16.33a	8.92a	0.99ab	79.92c
	225	2862c	16.38a	8.94a	1.01ab	66.20bc

† Means with the same letter in the same column for the same year are not significantly different at the 0.05 significance level based on LSD t-test.

Yield Regression Analysis, 2012

The r^2 values for the significant exponential relationships between 2012 Cummings sunflower seed yield and INSEY were summarized in Table 64. Only one significant exponential regression model using ground-based sensing INSEY was found. All the rest models were based on satellite imagery INSEY. Although all the listed models were highly significant, their r^2

values were not that satisfying. One site-year data might not be enough for having reliable discoveries. Also harvest was conducted on only one row for each treatment in each replication, implying that data might not always be reliable or representative.

Table 64. r^2 values of the exponential relationships between 2012 Cummings sunflower dry seed yield and INSEY.

†GS red V8 INSEY	Sat July01 Red INSEY	Sat July01 Blue INSEY	Sat July01 Green INSEY	Sat Aug16 Red INSEY	Sat Aug16 Red edge INSEY	Sat Aug16 blue INSEY
0.309	0.242	0.320	0.310	0.353	0.266	0.297

† Model is significant at 0.05 significance level.

Maximum Length Regression Analysis, 2012

Only one significant quadratic polynomial relationship (r^2=0.382) between Cummings 2012 sunflower seed maximum length and green INSEY of July 1 satellite imagery was found. The quality tests were conducted using even smaller number of samples, making the interested relationships weak or trend abnormal when data were not representative.

Maximum Width Regression Analysis, 2012

A significant linear relationship (r^2=0.169) between Cummings 2012 sunflower seed maximum width and blue INSEY of July 1 satellite imagery, and a significant quadratic polynomial relationship (r^2=0.876) between Cummings 2012 sunflower seed maximum width and red edge INSEY of August 16 satellite imagery were found.

Meat to Shell Ratio Regression Analysis, 2012

Only a significant exponential relationship (r^2=0.188) between Cummings 2012 sunflower seed meat to shell ratio and red INSEY of August 16 satellite imagery was found.

0.87 cm Content Regression Analysis, 2012

Two significant quadratic polynomial relationships between Cummings 2012 sunflower 22/64" content and red edge INSEY from Crop Circle (r^2=0.971) and August 16 satellite imagery (r^2=0.924), respectively, were found. Figure 75 illustrates the first regression model. Notice that the 0.87 cm content first increases with INSEY and then declines with the increase of INSEY. We don't believe this trend is normal because as mentioned earlier, quality test sample numbers were very small, and also this was just one site-year data.

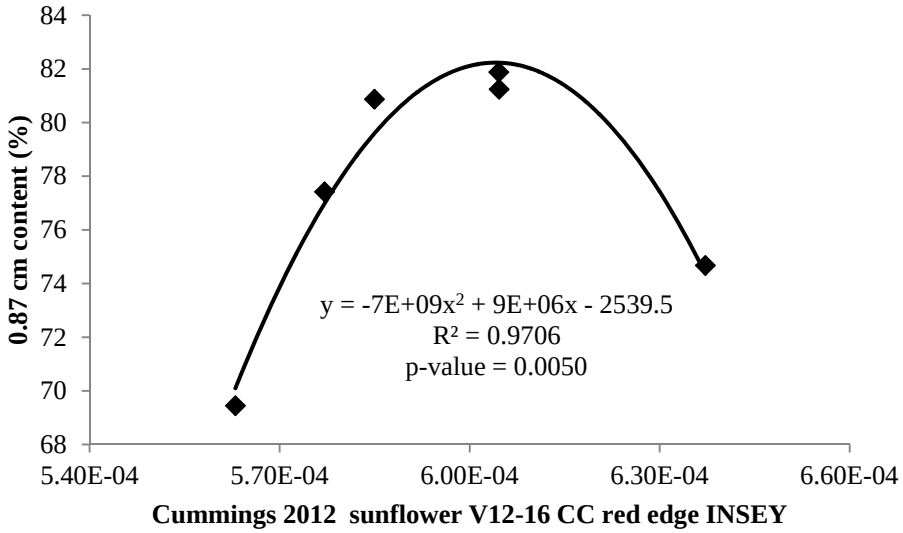

Figure 75. Relationship between Cummings 2012 sunflower 0.87 cm content and V12-16 CC red edge INSEY.

Yield Regression Analysis, 2013

No INSEYs from satellite imagery were found to be valid predictors of Cummings 2013 sunflower seed yield. This was mainly due to the bad influence of cloud and haze on the quality of satellite imagery. This reason applied also to the results in the following sections. However, there existed highly significant exponential and linear relationships with very high r^2 values between yield and ground-based active V6-8 sensing INSEYs, as summarized in Table 65 and Table 66. Results in these two tables show that GreenSeeker and Crop circle performed similarly, and that the exponential models and linear models performed similarly. These results indicate that strong positive correlation exists between V6-8 ground-based optical sensing INSEY and sunflower seed yield. The plant height measured either by tape or by height sensor didn't help improve the original models' performance. The plant height data colleting methods need to be improved in that when using tape only three representative samples were measured and when using height sensor the bumpy soil surface greatly influenced the measured height data at the time when sunflower was still very small. Figure 76 and Figure 77 illustrate two significant linear regression models, one based on GS red INSEY and the other based on CC red edge INSEY.

Table 65. r^2 values of the relationships between 2013 Cummings sunflower seed yield and GS V6-8 INSEY.

Model†	Red INSEY	Red INSEY× tapeHeight	Red INSEY× sensorHeight	Red edge INSEY	Red edge INSEY× tapeHeight	Red edge INSEY× sensorHeight
Exponential	0.938	0.907	0.888	0.910	0.890	0.872
Linear	0.945	0.931	0.900	0.921	0.916	0.886

† Model is significant at 0.05 significance level.

Table 66. r^2 values of the relationships between 2013 Cummings sunflower seed yield and CC V6-8 INSEY.

Model†	Red INSEY	Red INSEY× tapeHeight	Red INSEY× sensorHeight	Red edge INSEY	Red edge INSEY× tapeHeight	Red edge INSEY× sensorHeight
Exponential	0.930	0.908	0.882	0.936	0.909	0.890
Linear	0.927	0.927	0.890	0.940	0.931	0.901

† Model is significant at 0.05 significance level.

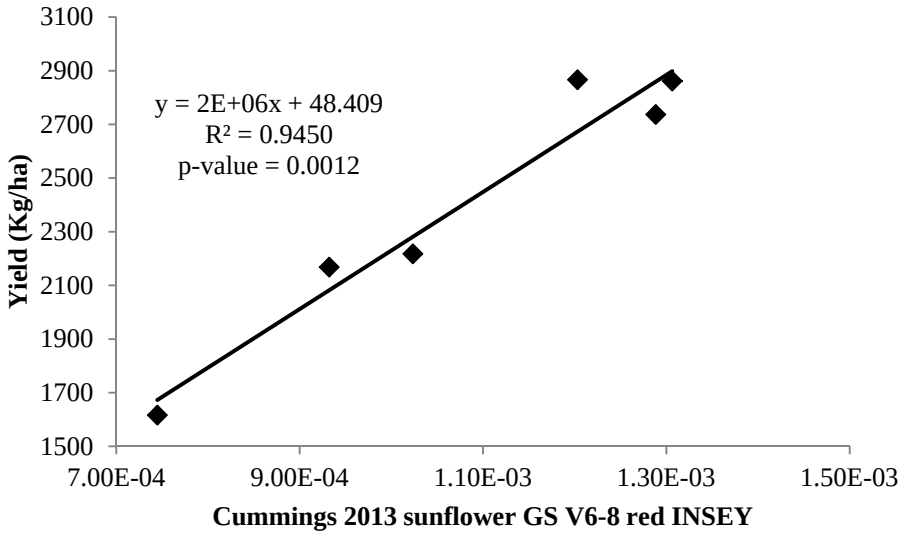

Figure 76. Relationship between Cummings 2013 sunflower seed yield and GS V6-8 red INSEY.

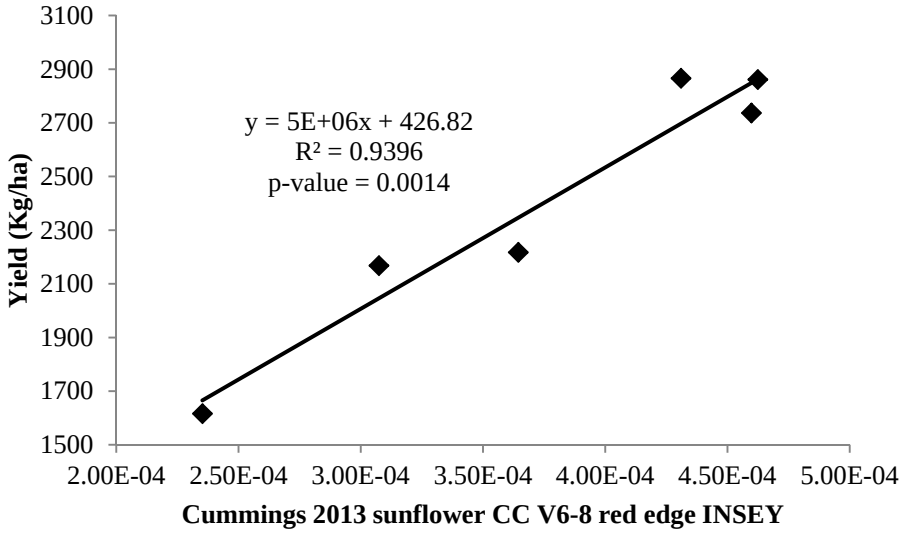

Figure 77. Relationship between Cummings 2013 sunflower seed yield and CC V6-8 red edge INSEY.

Maximum Length Regression Analysis, 2013

No INSEYs from satellite imagery were found to be valid predictors of Cummings 2013 sunflower seed maximum length. Highly significant quadratic polynomial relationships with very high r^2 values between Cummings 2013 sunflower seed maximum length and CC V12-16 INSEY were found, as summarized in Table 67. Tape-measured plant height slightly improved the performance of the regression models. Figure 78 illustrates the quadratic polynomial relationship between seed maximum length and CC red edge INSEY × tapeHeight, indicating the positive correlation between INSEY and sunflower maximum length.

Table 67. r^2 values of the quadratic polynomial relationships between 2013 Cummings sunflower seed maximum length and CC V12-16 INSEY.

†Red INSEY	Red INSEY× tapeHeight	Red edge INSEY×	Red edge INSEY× tapeHeight	Red edge INSEY× sensorHeight
0.956	0.964	0.944	0.982	0.865

† Model is significant at 0.05 significance level.

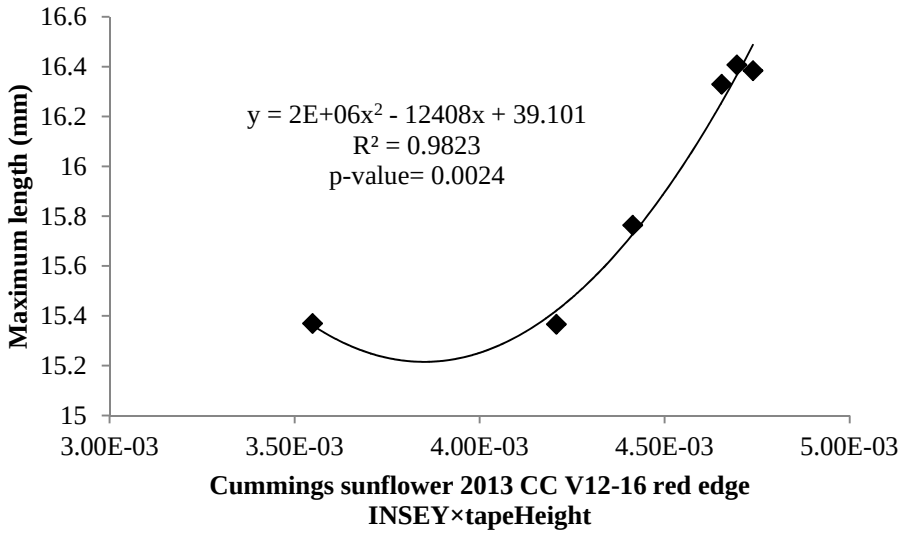

Figure 78. Relationship between Cummings 2013 sunflower seed maximum length and CC V12-16 red edge INSEY × tapeHeight.

Maximum Width Regression Analysis, 2013

No INSEYs from satellite imagery were found to be valid predictors of Cummings 2013 sunflower seed maximum width. Highly significant exponential and linear relationships with very high r^2 values between Cummings 2013 sunflower seed maximum width and ground-based optical sensing V12-16 INSEYs were found, as summarized in Table 68 and Table 69. Plant height information was shown to be very useful in improving the regression models' performance. Plant height measured by sensor performed a little bit better than that measured by

tape. At the sunflower V12-16 stage, the height sensor can take more consistent and representative readings. Figure 79 illustrates the linear relationship between seed maximum width and CC V12-16 red edge INSEY × sensorHeight.

Table 68. r^2 values of the relationships between 2013 Cummings sunflower seed maximum width and GS V12-16 INSEY.

Model†	Red INSEY	Red INSEY× tapeHeight	Red INSEY× sensorHeight
Exponential	0.719	0.886	0.889
Linear	0.712	0.881	0.894

† Model is significant at 0.05 significance level.

Table 69. r^2 values of the relationships between 2013 Cummings sunflower maximum width and CC V12-16 INSEY.

Model†	Red INSEY	Red INSEY× tapeHeight	Red INSEY× sensorHeight	Red edge INSEY	Red edge INSEY× tapeHeight	Red edge INSEY× sensorHeight
Exponential	0.839	0.918	0.933	0.870	0.918	0.935
Linear	0.832	0.913	0.937	0.865	0.914	0.937

† Model is significant at 0.05 significance level.

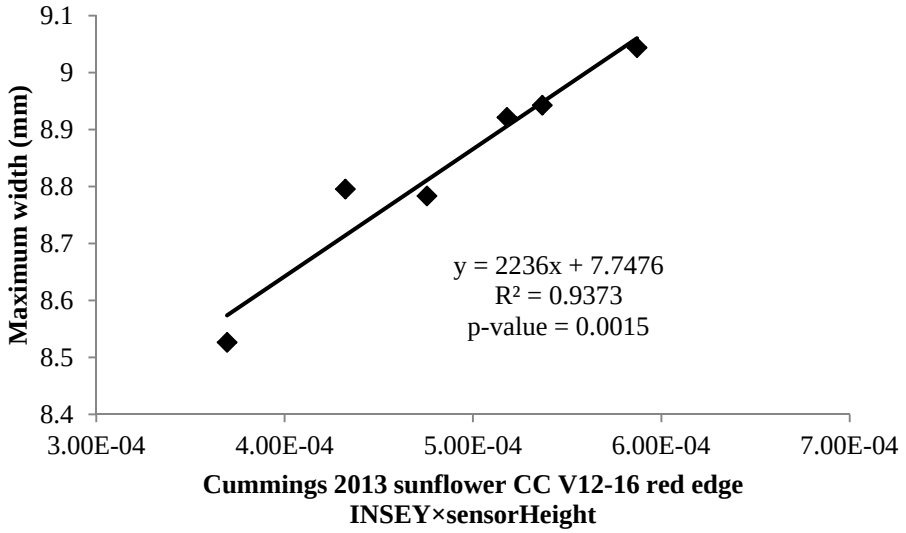

Figure 79. Relationship between Cummings 2013 sunflower seed maximum width and CC V12-16 red edge INSEY × sensorHeight.

Meat to Shell Ratio Regression Analysis, 2013

No INSEYs from satellite imagery were found to be valid predictors of Cummings 2013 sunflower seed meat to shell ratio due to the bad quality of this year's satellite imagery. Several ground-based optical sensing INSEY × sensorHeights demonstrated strong ability in predicting meat to shell ratio, as summarized in Table 70. All these significant models took great advantage of the plant height information measured by height sensor as their corresponding original models without plant height information included were not significant. At later growth stage when sunflower were very big, the height sensor could perform its best in data measurement and collecting and thus contribute positively to the model performance. Figure 80 illustrates the polynomial quadratic relationship between meat to shell ratio and CC V12-16 red INSEY × sensorHeight.

Table 70. r^2 values of the relationships between 2013 Cummings sunflower meat to shell ratio and ground-based sensing V12-16 INSEY.

Model†	GS red INSEY×sensorHeight	CC red INSEY×sensorHeight	CC red edge INSEY×sensorHeight
Exponential	0.960	0.937	0.909
Linear	0.954	0.921	0.887
Polynomial 2	NS	0.997	0.994

† NS means model is not significant at 0.05 significance level; otherwise model is significant at 0.05 significance level.

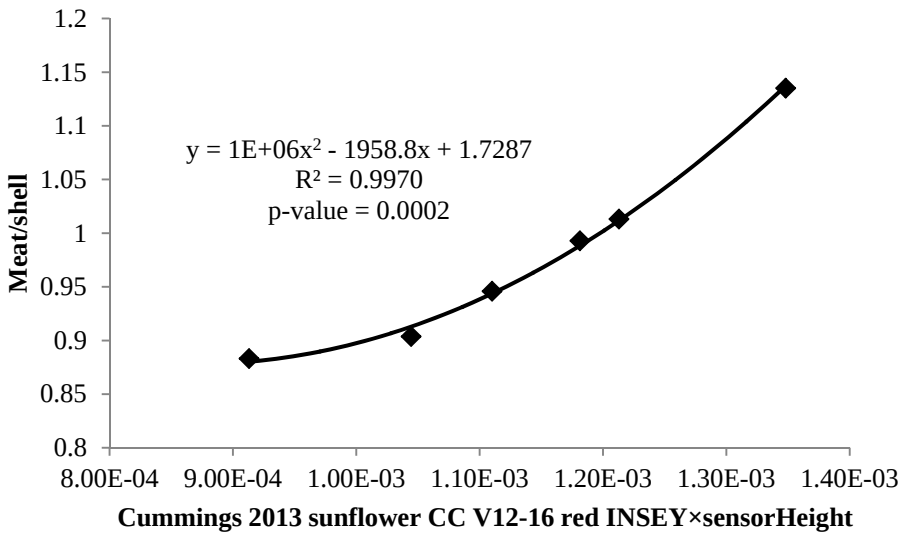

Figure 80. Relationship between Cummings 2013 sunflower seed meat to shell ratio and CC V12-16 red INSEY×sensorHeight.

0.87 cm Content Regression Analysis, 2013

No INSEYs from satellite imagery were found to be valid predictors of Cummings 2013 sunflower seed 0.87 cm content due to bad satellite imagery quality. Highly significant exponential and linear relationships with very high r^2 values between Cummings 2013 sunflower seed 0.87 cm content and ground-based optical sensing V12-16 INSEYs were found, as summarized in Table 71 and Table 72. Plant height at this growth stage proved to be effective in improving r^2 values of the regression models. 0.87 cm content is a comprehensive size index. Its results in this section agree with those for the maximum length and maximum width. Figure 81 illustrates the exponential relationship between 0.87 cm content and CC V12-16 red edge INSEY × tapeHeight.

Pooled Data Regression Analysis, 2012 and 2013

Due to the extremely poor performance of Cummings 2012 ground-based sensing INSEY and poor performance of Cummings 2013 satellite imagery INSEY, only a few significant regression models were found when relating the two site-year pooled INSEY to sunflower seed yield or qualities. Specifically, only a few valid ground-based sensing predictors were found for seed yield, maximum width, and 0.87cm content, as summarized in Table 73. No valid predictors were found for seed maximum length and meat to shell ratio.

Table 71. r^2 values of the relationships between 2013 Cummings sunflower seed 0.87 cm content and GS V12-16 INSEY.

Model†	Red INSEY× tapeHeight	Red INSEY× sensorHeight
Exponential	0.733	0.785
Linear	NS	0.796

† Model is significant at 0.05 significance level.

Table 72. r^2 values of the relationships between 2013 Cummings sunflower 0.87 cm content and CC V12-16 INSEY.

Model†	Red INSEY	Red INSEY× tapeHeight	Red INSEY× sensorHeight	Red edge INSEY	Red edge INSEY× tapeHeight	Red edge INSEY× sensorHeight
Exponential	0.816	0.877	0.879	0.887	0.915	0.905
Linear	0.700	0.779	0.880	0.795	0.835	0.900

† Model is significant at 0.05 significance level.

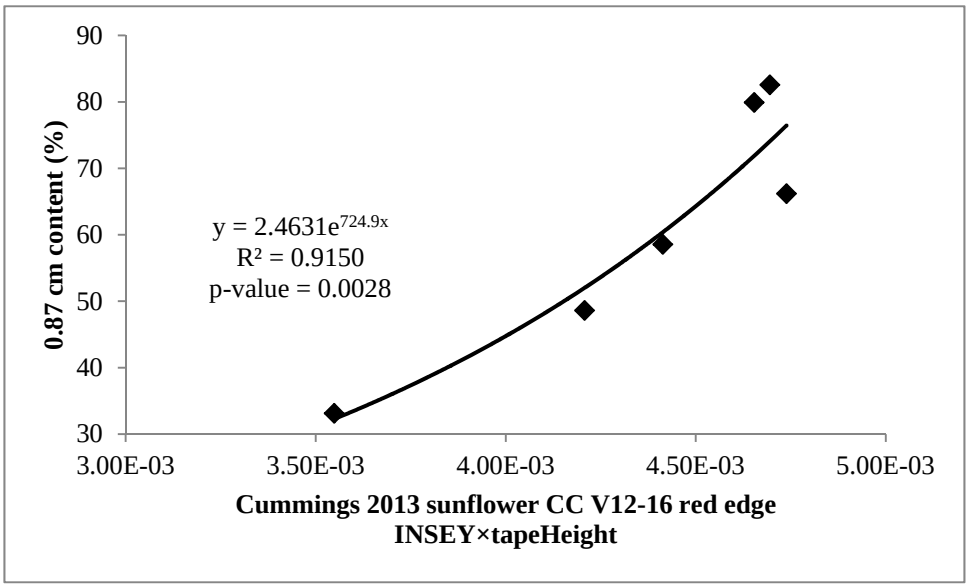

Figure 81. Relationship between Cummings 2013 sunflower seed 0.87 cm content and CC V12-16 red edge INSEY × tapeHeight

Table 73. r^2 values of the relationships between 2012 and 2013 two-year Cummings sunflower yield or quality and INSEY.

Model†	Yield	Maximum width		0.87 cm content	
	GS V6-8 Red INSEY	CC V12-16 red edge INSEY	CC V12-16 red INSEY	CC V12-16 red edge INSEY	CC V12-16 red INSEY
Exponential	0.897	0.762	0.813	0.873	0.734
Linear	0.879	0.761	0.812	0.847	0.695

† Model is significant at 0.05 significance level.

Conclusions

Strong relationships found between remote sensing INSEY and sunflower seed or quality indices implied that using these significant models, farmers can predict their sunflower seed yield early season and predict sunflower quality indices in mid-season. Variable N deficiency and N requirement can be detected and the sensors could be used to direct an in-season N application. Precision N management at a scale of applicator width times length of row to

integrate sensor readings are therefore possible. Including plant height information at the V12-16 stage was shown to be very useful in improving regression model performance. This was not the case for height measured at the early season. Improving plant height measurement at early season might increase the positive effects of plant. More site-year data is necessary for validating the above-mentioned conclusions and finding the best consistent regression models.

GENERAL CONCLUSIONS AND SUGGESTIONS FOR FUTURE WORK

Strong statistical relationships found between remote sensing INSEY and all crops yield or quality indices support the feasibility and great potential of using optical sensing data to predict crop yield and quality in season, and to detect in-season N application needs, rates, and places. These easy-to-use prediction technologies and models can benefit the farmers, the relevant big companies, and the environment as well through improved NUE and optimized logistics activities. Table 74 summarizes the r^2 values of the best models in terms of both r^2 value and model consistence based on the combined two-year data with an exception being sugar beet top total N had only one-year data. Overall the exponential models and linear models were more consistent and reliable, which conforms to the most relevant existing researches (Raun et al., 2002; Raun et al., 2005; Gehl and Boring, 2011; Inman et al., 2007; Li et al., 2009; Lofton et al., 2012b). Additional site-years of data are necessary for better regression model validation, selection, and correction to ensure that the selected models can be used over wide areas and years. Also, with more data available, it may be worthwhile to explore more complicated prediction approaches such as crop growth models, multiple regression, nonlinear regression, artificial neural networks, and support vector machines.

Currently, there are no strong and enough evidences to indicate which NDVI (INSEY) source, GreenSeeker, Crop Circle, or RapidEye satellite imagery, is significantly better than others. This conclusion was supported by Table 74 to a large extent. Each type of remote sensing system has its own advantages and disadvantages. Ground-based active optical sensing can be

conducted almost any time, but its use usually only collects a small number of samples. On the contrary, passive satellite imagery can only be obtained at certain days and is strongly and adversely influenced by the cloud or haze, but it can cover a very large area efficiently with all samples included. Incorporating both sources of information in prediction models may improve prediction accuracy.

Table 74. Summary of r^2 values of the best models for each sensing system, each crop, and each yield or quality index.

crop	sugar beet			spring wheat		corn	oilseed sunflower		confectionery sunflower		
index	root yield	RSY§§	Top Total N	yield	protein content	yield	yield	oil content	yield	Max. width	0.87 cm content
GS	0.917 (E†)	0.907 (Q‡)	0.760 (E)	0.961 (L§)	0.800 (E)	0.844 (L)	/††	0.320 (E)	0.897 (E)	/	/
CC	0.881 (E)	0.963 (Q)	0.820 (E)	0.963 (E)	0.816 (E)	0.822 (L)	/	0.550 (L)	/	0.813 (E)	0.873 (E)
RSI*	0.588 (L)	0.449 (E)	0.957 (L)	0.975 (Q)	0.678 (L)	0.779 (E)	0.824 (E)	0.755 (E)	/	/	/

*RapidEye satellite imagery

†Exponential model

‡Quadratic polynomial model

§Linear model

§§Recoverable sugar yield

††No significant models found.

Plant height information performed inconsistently in improving models efficiency. This is probably due to five reasons: 1) height data collection methods themselves were inconsistent or unreliable, 2) impact of extremely different weather conditions after measurements were obtained, 3) the multiplication method we used when incorporating height information into the prediction model may not be the best or most consistent, 4) NDVI data collection was not reliable, and 5) experimental data was too limited for thorough investigation.

An alternative crop yield or quality predictor to INSEY is the N-rich-strip-based relative NDVI (Dellinger et al., 2008; Inman et al., 2007), which is worthy of trial in the future. Other measures that can be considered for improving prediction models performance in the future include but not limited to: classifying the INSEY data based on soil texture type before constructing the models; keep constant distance of the ground-based sensors from plant top; use other sources of satellite imagery with better quality.

REFERENCES

Abedi T., A. Alemzadeh, and S.A. Kazemeini. 2011. Wheat yield and grain protein response to nitrogen amount and timing. Austr. J. Crop Sci. 5:330-336.

Akkuzu, E., U. Kaya, G. Camoglu, G.P. Mengu, and S. Asik. 2013. Determination of crop water stress index and irrigation timing on olive trees using a handheld infrared thermometer. J. Irrig. Drain. E. 139:728-737.

Amaral, L.R., H.J.A. Rosa, G. Portz, F.B. Finazzi, and J.P. Molin. 2013. Comparison of crop canopy sensors in sugarcane. Precis. Agric. 13:103-110.

Amoros-Lopez, J., L. Gomez-Chova, L. Alonso, L. Guanter, R. Zurita-Milla, J. Moreno, and G. Camps-Valls. 2013, Multitemporal fusion of Landsat/TM and ENVISAT/MERIS for crop monitoring. Int. J. Appl. Earth. Obs. 23:132-141.

Arnall, D., W. Raun, J. Solie, M. Stone, G. Johnson, K. Girma, K. Freeman, R. Teal, and K. Martin. 2006. Relationship between coefficient of variation measured by spectral reflectance and plant density at early growth stages in winter wheat. J. Plant Nutr. 29:1983-1997.

Arnall, D., B. Tubana, S. Holtz, K. Girma, and W. Raun. 2009. Relationship between Nitrogen Use Efficiency and Response Index in Winter Wheat. J. Plant Nutr. 32: 502-515.

Arnall, D.B., and C.B. Godsey. 2013. Use of CVs for Refining Mid-Season Fertilization Nitrogen-Rates in Winter Wheat. J. Plant Nutr. 36:1733-1742.

Awan, U.K., B. Tischbein, and C. Martius. 2013. Combining hydrological modeling and GIS approaches to determine the spatial distribution of groundwater recharge in an arid irrigation scheme. Irrigation Sci. 31:793-806.

Baez-Gonzalez, A.D., J.R. Kiniry, S.J. Maas, M. Tiscareno, J. Macias, J.L. Mendoza, C.W. Richardson, J. Salinas, and J.R. Manjarrez. 2005. Large-area maize yield forecasting using leaf area index based yield model. Agron. J. 97:418-425.

Bakhsh, A., D.B. Jaynes, T.S. Colvin, and R.S. Kanwar. 2000. Spatio-temporal analysis of yield variability for a corn-soybean field in Iowa. Trans. ASAE. 43:31-38.

Bala, S.K., and A.S. Islam. 2009. Correlation between potato yield and MODIS-derived vegetation indices. Int. J. Remote Sens. 30:2491-2507.

Baligar, V., N. Fageria, and Z. He. 2001. Nutrient use efficiency in plants. Commun. Soil Sci. Plant Anal. 32:921-950.

Barker, D.W., and J.E. Sawyer. 2010. Using Active Canopy Sensors to Quantify Corn Nitrogen Stress and Nitrogen Application Rate. Agron. J. 102:964-971.

Barker, D.W., and J.E. Sawyer. 2013. Factors Affecting Active Canopy Sensor Performance and Reflectance Measurements. Soil Sci. Soc. Am. J. 77:1673-1683.

Bausch, W., and R. Khosla. 2010. QuickBird satellite versus ground-based multi-spectral data for estimating nitrogen status of irrigated maize. Precis. Agric. 11:274-290.

Bausch, W.C., and M.K. Brodahl. 2012. Strategies to evaluate goodness of reference strips for in-season, field scale, irrigated corn nitrogen sufficiency. Precis. Agric. 13: 104-122.

Becker-Reshef, I., E. Vermote, M. Lindeman, and C. Justice. 2010. A generalized regression-based model for forecasting winter wheat yields in Kansas and Ukraine using MODIS data. Remote Sens. Environ. 114:1312-1323.

Berntsen, J., A. Thomsen, K. Schelde, O. Hansen, L. Knudsen, N. Broge, H. Hougaard, and R. Horfarter. 2006. Algorithms for sensor-based redistribution of nitrogen fertilizer in winter wheat. Precis. Agric. 7:65-83.

Bhatti, A.U., D.J. Mulla, and B.E. Frazier. 1991. Estimation of soil properties and wheat yields on complex eroded hills using geostatistics and thematic mapper images. Remote Sens. Environ. 37:181-191.

Biermacher, J., F. Epplin, B. Brorsen, J. Solie, and W. Raun. 2009. Economic feasibility of site-specific optical sensing for managing nitrogen fertilizer for growing wheat. Precis. Agric. 10:213-230.

Blackmer, T.M. and J.S. Schepers. 1995. Use of a chlorophyll meter to monitor nitrogen status and schedule fertigation for corn. J. Prod. Agric. 8: 56-60.

Blackmer, T.M., J.S. Schepers and G.E. Varvel. 1994. Light reflectance compared with other nitrogen stress measurements in corn leaves. Agron. J. 86: 934-938.

Blackmer, T.M., J.S. Schepers, G.E. Varvel and E.A. WalterShea. 1996. Nitrogen deficiency detection using reflected shortwave radiation from irrigated corn canopies. Agron. J. 88: 1-5.

Bognar, P., C. Ferencz, S. Pasztor, G. Molnar, G. Timar, D. Hamar, et al. 2011. Yield forecasting for wheat and corn in Hungary by satellite remote sensing. Int. J. Remote Sens. 32: 4759-4767.

Boyer, C., B. Brorsen, J. Solie and W. Raun. 2011. Profitability of variable rate nitrogen application in wheat production. Precis. Agric. 12: 473-487.

Brady, N.C. and R.R. Weil. 1999. The nature and properties of soils (12th edition). Prentice-Hall, New Jersey, USA. p. 491-539.

Brown B., M. Westcott, N. Christensen, B. Pan, and J. Stark. 2005. Nitrogen Management for Hard Wheat Protein Enhancement. PNW578.

Bredemeier, C., C. Variani, D. Almeida and A.T. Rosa. 2013. Wheat yield potential estimation using active optical sensor for site-specific nitrogen fertilization. Cienc. Rural 43: 1147-1154.

Cabrera-Bosquet, L., G. Molero, A.M. Stellacci, J. Bort, S. Nogues and J.L. Araus. 2011. NDVI as a potential tool for predicting biomass, plant nitrogen content and growth in wheat genotypes subjected to different water and nitrogen conditions. Cereal Res. Commun. 39: 147-159.

Cao, Q., Z.L. Cui, X.P. Chen, R. Khosla, T.H. Dao and Y.X. Miao. 2012. Quantifying spatial variability of indigenous nitrogen supply for precision nitrogen management in small scale farming. Precis. Agric. 13:45-61.

Cao, Q., Y. Miao, S. Huang, H. Wang, R. Khosla and R. Jiang. 2013. Estimating rice nitrogen status with the Crop Circle multispectral active canopy sensor. Precis. Agric. 13:95-101.

Christy, C.D. 2008. Real-time measurement of soil attributes using on-the-go near infrared reflectance spectroscopy. Comput. Electron. Agric. 61:10-19.

Chung, B., K. Girma, K.L. Martin, B.S. Tubana, D.B. Arnall, O. Walsh, et al. 2008. Determination of optimum resolution for predicting corn grain yield using sensor measurements. Arch. Agron. Soil Sci. 54:481-491.

Chung, B., K. Girma, W.R. Raun and J.B. Solie. 2010. Changes in response indices as a function of time in winter wheat. J. Plant Nutr. 33:796-808.

Claverie, M., V. Demarez, B. Duchemin, O. Hagolle, D. Ducrot, C. Marais-Sicre, et al. 2012. Maize and sunflower biomass estimation in southwest France using high spatial and temporal resolution remote sensing data. Remote Sens. Environ. 124:844-857.

Clay, D.E., K.I. Kim, J. Chang, S.A. Clay and K. Dalsted. 2006. Characterizing water and nitrogen stress in corn using remote sensing. Agron. J. 98:579-587.

Clevers, J.G.P.W. and A.A. Gitelson. 2013. Remote estimation of crop and grass chlorophyll and nitrogen content using red-edge bands on Sentinel-2 and-3. Int. J. Appl .Earth Obs. 23: 344-351.

Crookston, R.K. 2006. A top 10 list of developments and issues impacting crop management and ecology during the past 50 years. Crop Sci. 46:2253-2262.

Das, S.K. and R. Singh. 2013. A multiple-frame approach to crop yield estimation from satellite-remotely sensed data. Int. J. Remote Sens. 34:3803-3819.

Dellinger, A., J. Schmidt and D. Beegle. 2008. Developing Nitrogen Fertilizer Recommendations for Corn Using an Active Sensor. Agron. J. 100:1546-1552.

Doraiswamy, P.C., J.L. Hatfield, T.J. Jackson, B. Akhmedov, J. Prueger and A. Stern. 2004. Crop condition and yield simulations using Landsat and MODIS. Remote Sens. Environ. 92:548-559.

Doraiswamy, P.C., T.R. Sinclair, S. Hollinger, B. Akhmedov, A. Stern and J. Prueger. 2005. Application of MODIS derived parameters for regional crop yield assessment. Remote Sens. Environ. 97:192-202.

Duveiller, G., F. Baret and P. Defourny. 2012. Remotely sensed green area index for winter wheat crop monitoring: 10-Year assessment at regional scale over a fragmented landscape. Agr. Forest. Meteorol. 166:156-168.

Erdle, K., B. Mistele and U. Schmidhalter. 2011. Comparison of active and passive spectral sensors in discriminating biomass parameters and nitrogen status in wheat cultivars. Field Crop. Res. 124:74-84.

Evans, J.R. 1983. Nitrogen and photosynthesis in the flag leaf of wheat (triticum-aestivum l). Plant Physiol. 72:297-302.

Ferencz, C., P. Bognar, J. Lichtenberger, D. Hamar, G. Tarscai, G. Timar, et al. 2004. Crop yield estimation by satellite remote sensing. Int. J. Remote Sens. 25:4113-4149.

Fernandes, R., C. Butson, S. Leblanc and R. Latifovic. 2003. Landsat-5 TM and Landsat-7 ETM+ based accuracy assessment of leaf area index products for Canada derived from SPOT-4 vegetation data. Can. J. Remote Sens. 29:241-258.

Flynn, E.S., C.T. Dougherty and O. Wendroth. 2008. Assessment of pasture biomass with the normalized difference vegetation index from active ground-based sensors. Agron. J. 100:114-121.

Franzen, D.W. 2003. Fertilizing sugarbeet. SF-714 (rev.). North Dakota State University Extension Services, Raleigh.

Franzen, D.W., M.V. McMullen, and D.S. Mosset. 2008. Spring Wheat and Durum Yield and Disease Responses to Copper Fertilization of Mineral Soils. Agron. J. 100: 371-375.

Freeman, K.W., K. Girma, D.B. Arnall, R.W. Mullen, K.L. Martin, R.K. Teal, et al. 2007. By-plant prediction of corn forage biomass and nitrogen uptake at various growth stages using remote sensing and plant height. Agron. J. 99:530-536.

Gehl, R.J. and T.J. Boring. 2011. In-Season Prediction of Sugarbeet Yield, Quality, and Nitrogen Status Using an Active Sensor. Agron. J. 103:1012-1018.

Genu, A.M., D. Roberts and J.A.M. Dematte. 2013. The use of multiple endmember spectral mixture analysis (MESMA) for the mapping of soil attributes using Aster imagery. Acta Sci. Agron. 35:377-386.

Girma, K., K. Martin, R. Anderson, D. Arnall, K. Brixey, M. Casillas, et al. 2006. Mid-season prediction of wheat-grain yield potential using plant, soil, and sensor measurements. J. Plant Nutr. 29:873-897.

Gitelson, A., Y. Kaufman and M. Merzlyak. 1996. Use of a green channel in remote sensing of global vegetation from EOS-MODIS. Remote Sens.Environ. 58:289-298.

Gitelson, A.A., A. Vina, V. Ciganda, D.C. Rundquist and T.J. Arkebauer. 2005. Remote estimation of canopy chlorophyll content in crops. Geophysical Research Letters 32: L08 403.1–L08 403.4.

Graham, S. 1999. Remote Sensing. Earth observatory. NASA. http://earthobservatory.nasa.gov/Features/RemoteSensing/ (accessed 5 Dec. 2013).

GRASS Development Team, 2012. Geographic Resources Analysis Support System (GRASS) Software. Open Source Geospatial Foundation Project. http://grass.osgeo.org.

Harrell, D.L., B.S. Tubana, T.W. Walker and S.B. Phillips. 2011. Estimating Rice Grain Yield Potential Using Normalized Difference Vegetation Index. Agron. J. 103:1717-1723.

Havlin, J.L., j.D. Beaton, S.L. Tisdale and W.L. Nelson. 2005. Soil fertility and fertilizers : an introduction to nutrient management (7th edition). Pearson Education Inc., New Jersy, U.S.A.

Hirel, B., J. Le Gouis, B. Ney and A. Gallais. 2007. The challenge of improving nitrogen use efficiency in crop plants: towards a more central role for genetic variability and quantitative genetics within integrated approaches. J. Exp. Bot. 58:2369-2387.

Holland Scientific, Inc. 2011. Crop Circle ACS-470 User's Guide. Holland Scientific, Inc.

Holland Scientific, Inc. 2013. Crop Circle mapping / VRT system. Holland Scientific, Inc. http://hollandscientific.com/crop-circle-mappingvrt-system/ (accessed 23 Nov. 2013).

Holzapfel, C.B., G.P. Lafond, S.A. Brandt, P.R. Bullock, R.B. Irvine, M.J. Morrison, et al. 2009. Estimating canola (Brassica napus L.) yield potential using an active optical sensor. Can. J. Plant Sci. 89:1149-1160.

Humburg, D.S., P. Thanapura, C. Ren and D.E. Clay. 2006. Sugarbeet quality correlation to landsat canopy data from a large GIS database. T. ASABE. 49:775-782.

Inman, D., R. Khosla, R.M. Reich and D.G. Westfall. 2007. Active remote sensing and grain yield in irrigated maize. Precis. Agric. 8:241-252.

Jego, G., E. Pattey and J. Liu. 2012. Using Leaf Area Index, retrieved from optical imagery, in the STICS crop model for predicting yield and biomass of field crops. Field Crop. Res. 131:63-74.

Jiang, D., X. Yang, N. Clinton and N. Wang. 2004. An artificial neural network model for estimating crop yields using remotely sensed information. Int. J. Remote Sens. 25:1723-1732.

Johnson, G. and W. Raun. 2003. Nitrogen response index as a guide to fertilizer management. J.Plant Nutr. 26:249-262.

Jordan, C. 1969. Derivation of Leaf-Area Index from Quality Of Light on Forest Floor. Ecology 50:663-666.

Kharrou, M.H., M. Le Page, A. Chehbouni, V. Simonneaux, S. Er-Raki, L. Jarlan, et al. 2013. Assessment of Equity and Adequacy of Water Delivery in Irrigation Systems Using Remote Sensing-Based Indicators in Semi-Arid Region, Morocco. Water Resour. Manag. 27:697-4714.

Kim, Y., D.M. Glenn, J. Park, H.K. Ngugi and B.L. Lehman. 2012. Characteristics of active spectral sensor for plant sensing. T. ASABE 55:293-301.

Kouadio, L., G. Duveiller, B. Djaby, M. El Jarroudi, P. Defourny and B. Tychon. 2012. Estimating regional wheat yield from the shape of decreasing curves of green area index temporal profiles retrieved from MODIS data. Int. J. Appl. Earth Obs. 18:111-118.

Li, F., Y. Miao, F. Zhang, Z. Cui, R. Li, X. Chen, et al. 2009. In-Season Optical Sensing Improves Nitrogen-Use Efficiency for Winter Wheat. Soil Sci. Soc. Am. J. 73:1566-1574.

Li, F., Y.X. Miao, X.P. Chen, H.L. Zhang, L.L. Jia and G. Bareth. 2010. Estimating winter wheat biomass and nitrogen status using an active crop sensor. Intell. Autom. Soft. Co. 16:1221-1230.

Li, F., Y.X. Miao, S.D. Hennig, M.L. Gnyp, X.P. Chen, L.L. Jia, et al. 2010. Evaluating hyperspectral vegetation indices for estimating nitrogen concentration of winter wheat at different growth stages. Precis. Agric. 11:335-357.

Li, H., C.K. Zhang, Y. Zhang, D. Zhang, J. Gao and Z. Gong. 2013. Predicting water content using linear spectral mixture model on soil spectra. J. Appl. Remote Sens. 7: 073539.

Li, Y., S.B. Liu, Z.H. Liao and C.S. He. 2012. Comparison of two methods for estimation of soil water content from measured reflectance. Can. J. .Soil Sci. 92:845-857.

Liang, B. and A. Mackenzie. 1994. Corn yield, nitrogen uptake and nitrogen use efficiency as influenced by nitrogen-fertilization. Can. J. .Soil Sci. 74:235-240.

Liu, S.B., Y. Li and C.S. He. 2013. Spectral Analysis and Estimations of Soil Salt and Organic Matter Contents. Soil Sci. 178:138-146.

Lo, C.P. and A.K.W. Yeung. 2007. Chapter 8: Remote sensing and GIS Integration. In: K.C. Clarke, editor, Concepts and Techniques of Geographic Information Systems. Prentice Hall. N.J., USA. p. 290.

Lofton, J., B.S. Tubana, Y. Kanke, J. Teboh and H. Viator. 2012. Predicting Sugarcane Response to Nitrogen Using a Canopy Reflectance-Based Response Index Value. Agron. J. 104:106-113.

Lofton, J., B.S. Tubana, Y. Kanke, J. Teboh, H. Viator and M. Dalen. 2012. Estimating Sugarcane Yield Potential Using an In-Season Determination of Normalized Difference Vegetative Index. Sensors. 12:7529-7547.

Long, D.S., R.E. Engel and M.C. Siemens. 2008. Measuring grain protein concentration with in-line near infrared reflectance spectroscopy. Agron. J. 100:247-252.

Lukina, E., K. Freeman, K. Wynn, W. Thomason, R. Mullen, M. Stone, et al. 2001. Nitrogen fertilization optimization algorithm based on in-season estimates of yield and plant nitrogen uptake. J. Plant Nutr. 24:885-898.

Maas, S.J. 1993. Parameterized model of gramineous crop growth .1. leaf-area and dry mass simulation. Agron. J. 85:348-353.

Maas, S.J. 1993. Parameterized model of gramineous crop growth: II. within-season simulation calibration. Agron. J. 85:354-358.

Mayfield, A. and S. Trengove. 2009. Grain yield and protein responses in wheat using the N-Sensor for variable rate N application. Crop Pasture Sci. 60:818-823.

Mkhabela, M.S., P. Bullock, S. Raj, S. Wang and Y. Yang. 2011. Crop yield forecasting on the Canadian Prairies using MODIS NDVI data. Agr. Forest Meteorol. 151:385-393.

Mkhabela, M.S. and N.N. Mashinini. 2005. Early maize yield forecasting in the four agro-ecological regions of Swaziland using NDVI data derived from NOAAs-AVHRR. Agr. Forest Meteorol. 129:1-9.

Moll, R., E. Kamprath and W. Jackson. 1982. Analysis and Interpretation of Factors Which Contribute to Efficiency of Nitrogen-Utilization. Agron. J. 74:562-564.

Mollashahi, M., H. Ganjali, and H. Fanaei. 2013. Effect of different levels of nitrogen and potassium on yield, yield components and oil content of sunflower. Intl. J. Farm. & Alli. Sci. 2(S): 1237-1240.

Moller, M., V. Alchanatis, Y. Cohen, M. Meron, J. Tsipris, A. Naor, et al. 2007. Use of thermal and visible imagery for estimating crop water status of irrigated grapevine. J. Exp. Bot. 58:827-838.

Montes, J.M., F. Technow, B.S. Dhillon, F. Mauch and A.E. Melchinger. 2011. High-throughput non-destructive biomass determination during early plant development in maize under field conditions. Field Crop. Res. 121:268-273.

Moriondo, M., F. Maselli and M. Bindi. 2007. A simple model of regional wheat yield based on NDVI data. Eur. J. .Agron. 26:266-274.

Morris, K.B., K.L. Martin, K.W. Freeman, R.K. Teal, K. Girma, D.B. Arnall, et al. 2006. Mid-season recovery from nitrogen stress in winter wheat. J. Plant Nutr. 29:727-745.

Mulla, D.J. 2013. Twenty five years of remote sensing in precision agriculture: Key advances and remaining knowledge gaps. Biosyst. Eng. 114:358-371.

Mullen, R., K. Freeman, W. Raun, G. Johnson, M. Stone and J. Solie. 2003. Identifying an in-season response index and the potential to increase wheat yield with nitrogen. Agron. J. 95:347-351.

NASA. 2013. Landsat Overview. Landsat 8. NASA. http://www.nasa.gov/mission_pages/landsat/overview/#.UuKO-9KCknI (accessed 9 Jan. 2014).

Neale, C.M.U., H.M.E. Geli, W.P. Kustas, J.G. Alfieri, P.H. Gowda, S.R. Evett, et al. 2012. Soil water content estimation using a remote sensing based hybrid evapotranspiration modeling approach. Adv. Water Resour. 50:152-161.

Obade, V.D., R. Lal and J.Q. Chen. 2013. Remote Sensing of Soil and Water Quality in Agroecosystems. Water Air Soil Pollut. 224:1658.

Olfs, H.W., K. Blankenau, F. Brentrup, J. Jasper, A. Link and J. Lammel. 2005. Soil- and plant-based nitrogen-fertilizer recommendations in arable farming. J. Plant Nutr. Soil Sci. 168:414-431.

Oliveira, L.F., P.C. Scharf, E.D. Vories, S.T. Drummond, D. Dunn, W.G. Stevens, et al. 2013. Calibrating Canopy Reflectance Sensors to Predict Optimal Mid-Season Nitrogen Rate for Cotton. Soil Sci. Soc. Am. J. 77:173-183.

Olivier, M., J.P. Goffart and J.F. Ledent. 2006. Threshold value for chlorophyll meter as decision tool for nitrogen management of potato. Agron. J. 98:496-506.

Ortiz-Monasterio, J.I. and W. Raun. 2007. Reduced nitrogen and improved farm income for irrigated spring wheat in the Yaqui Valley, Mexico, using sensor based nitrogen management. J. Agr. Sci. 145:215-222.

Padilla, F.L.M., S.J. Maas, M.P. Gonzalez-Dugo, F. Mansilla, N. Rajan, P. Gavilan, et al. 2012. Monitoring regional wheat yield in Southern Spain using the GRAMI model and satellite imagery. Field Crop. Res. 130:145-154.

Pena-Barragan, J.M., F. Lopez-Granados, M. Jurado-Exposito, and L. Garcıa-Torres. 2010. Sunflower yield related to multi-temporal aerial photography, land elevation and weed infestation. Precision. Agric. 11: 568-585.

Portz, G., J. Molin and J. Jasper. 2012. Active crop sensor to detect variability of nitrogen supply and biomass on sugarcane fields. Precis. Agric. 13:33-44.

Prasad, A.K., L. Chai, R.P. Singh and M. Kafatos. 2006. Crop yield estimation model for Iowa using remote sensing and surface parameters. Int. J. Appl. Earth Obs. 8:26-33.

Raper, T.B., J.J. Varco and K.J. Hubbard. 2013. Canopy-Based Normalized Difference Vegetation Index Sensors for Monitoring Cotton Nitrogen Status. Agron. J. 105:1345-1354.

Raun, W. and G. Johnson. 1999. Improving nitrogen use efficiency for cereal production. Agron. J. 91:357-363.

Raun, W., J. Solie, G. Johnson, M. Stone, E. Lukina, W. Thomason, et al. 2001. In-season prediction of potential grain yield in winter wheat using canopy reflectance. Agron. J. 93:131-138.

Raun, W., J. Solie, G. Johnson, M. Stone, R. Mullen, K. Freeman, et al. 2002. Improving nitrogen use efficiency in cereal grain production with optical sensing and variable rate application. Agron. J. 94:815-820.

Raun, W.R., J.B. Solie, G.V. Johnson, M.L. Stone, R.W. Whitney, H.L. Lees, et al. 1998. Microvariability in soil test, plant nutrient, and yield parameters in Bermudagrass. Soil Sci. Soc. Am. J. 62:683-690.

Raun, W.R., J.B. Solie and M.L. Stone. 2011. Independence of yield potential and crop nitrogen response. Precis. Agric. 12:508-518.

Raun, W.R., J.B. Solie, M.L. Stone, K.L. Martin, K.W. Freeman, R.W. Mullen, et al. 2005. Optical sensor-based algorithm for crop nitrogen fertilization. Commun. Soil Sci. Plant Anal. 36:2759-2781.

Raun, W.R., J.B. Solie, R.K. Taylor, D.B. Arnall, C.J. Mack and D.E. Edmonds. 2008. Ramp calibration strip technology for determining midseason nitrogen rates in corn and wheat. Agron. J. 100:1088-1093.

Ren, J., Z. Chen, Q. Zhou and H. Tang. 2008. Regional yield estimation for winter wheat with MODIS-NDVI data in Shandong, China. Int. J. Appl. Earth Obs. 10:403-413.

Roberts, D., B. Brorsen, R. Taylor, J. Solie and W. Raun. 2011. Replicability of nitrogen recommendations from ramped calibration strips in winter wheat. Precis. Agric. 12:653-665.

Rouse, J.W., R.H.Haas, J.A. Schell, and D.W. Deering. 1973. Monitoring vegetation systems in the Great Plains with ERTS. 3rd ERTS symposium, NASA SP-351.

Sakamoto, T., A.A. Gitelson and T.J. Arkebauer. 2013. MODIS-based corn grain yield estimation model incorporating crop phenology information. Remote Sens. Environ. 131:215-231.

Salazar, L., F. Kogan and L. Roytman. 2007. Use of remote sensing data for estimation of winter wheat yield in the United States. Int. J. Remote Sens. 28:3795-3811.

Samborski, S.M., N. Tremblay and E. Fallon. 2009. Strategies to Make Use of Plant Sensors-Based Diagnostic Information for Nitrogen Recommendations. Agron. J. 101:800-816.

SAS Institute, Inc., 2013. SAS 9.3. Cary, NC, USA.

Scharf, P.C. and J.A. Lory. 2009. Calibrating Reflectance Measurements to Predict Optimal Sidedress Nitrogen Rate for Corn. Agron. J. 101:615-625.

Schepers, J.S., T.M. Blackmer, W.W. Wilhelm and M. Resende. 1996. Transmittance and reflectance measurements of corn leaves from plants with different nitrogen and water supply. J. Plant Physiol. 148:523-529.

Schlemmer, M., A. Gitelson, J. Schepers, R. Ferguson, Y. Peng, J. Shanahan, et al. 2013. Remote estimation of nitrogen and chlorophyll contents in maize at leaf and canopy levels. Int. J. Appl. Earth Obs. 25:47-54.

Schut, A.G.T., D.J. Stephens, R.G.H. Stovold, M. Adams and R.L. Craig. 2009. Improved wheat yield and production forecasting with a moisture stress index, AVHRR and MODIS data. Crop Pasture Sci. 60:60-70.

Semenov, M., P. Jamieson and P. Martre. 2007. Deconvoluting nitrogen use efficiency in wheat: A simulation study. Eur. J. Agron. 26:283-294.

Shamseddin, A.M. and A.M. Adeeb. 2012. Using remotely sensed and ancillary data to predict spatial variability of rainfed crop yield. Int. J. Remote Sens. 33:3798-3815.

Shanahan, J.F., J.S. Schepers, D.D. Francis, G.E. Varvel, W.W. Wilhelm, J.M. Tringe, et al. 2001. Use of remote-sensing imagery to estimate corn grain yield. Agron. J. 93:583-589.

Shaver, T.M., R. Khosla and D.G. Westfall. 2011. Evaluation of Two Ground-Based Active Crop Canopy Sensors in Maize: Growth Stage, Row Spacing, and Sensor Movement Speed. Soil Sci. Soc. Am. J. 74: 2101-2108.

Shou, L., L. Jia, Z. Cui, X. Chen and F. Zhang. 2007. Using high-resolution satellite imaging to evaluate nitrogen status of winter wheat. J. Plant Nutr. 30:1669-1680.

Singh, B., R. Sharma, K. Jaspreet, M.L. Jat, K.L. Martin, S. Yadvinder, et al. 2011. Assessment of the nitrogen management strategy using an optical sensor for irrigated wheat. Agron. Sustain. Dev. 31:589-603.

Soderstrom, M., T. Borjesson, C. Pettersson, K. Nissen and O. Hagner. 2010. Prediction of protein content in malting barley using proximal and remote sensing. Precis. Agric. 11:587-599.

Solari, F., J. Shanahan, R. Ferguson, J. Schepers and A. Gitelson. 2008. Active sensor reflectance measurements of corn nitrogen status and yield potential. Agron. J. 100:571-579.

Solari, F., J.F. Shanahan, R.B. Ferguson and V.I. Adamchuk. 2010. An Active Sensor Algorithm for Corn Nitrogen Recommendations Based on a Chlorophyll Meter Algorithm. Agron. J. 102:1090-1098.

Solie, J.B., W.R. Raun and M.L. Stone. 1999. Submeter spatial variability of selected soil and bermudagrass production variables. Soil Sci. Soc. Am. J. 63:1724-1733.

Sowers, K.E., W.L. Pan, B.C. Miller and J.L. Smith. 1994. Nitrogen use efficiency of split nitrogen applications in soft white winter-wheat. Agron. J. 86:942-948.

Spargo, J., M. Alley, R. Follett and J. Wallace. 2008. Soil nitrogen conservation with continuous no-till management. Nutr. Cycl. Agroecosys. 82:283-297.

Sripada, R., J. Schmidt, A. Dellinger and D. Beegle. 2008. Evaluating Multiple Indices from a Canopy Reflectance Sensor to Estimate Corn N Requirements. Agron. J. 100:1553-1561.

Stamatiadis, S., L. Evangelou, A. Blanta, C. Tsadilas, A. Tsitouras, C. Chroni, et al. 2013. Satellite Visible-Near Infrared Reflectance Correlates to Soil Nitrogen and Carbon Content in Three Fields of the Thessaly Plain (Greece). Commun. Soil Sci. Plant Anal. 44:28-37.

Tang, Q., S. Li, K. Wang, R. Xie, B. Chen, F. Wang, et al. 2010. Monitoring Canopy Nitrogen Status in Winter Wheat of Growth Anaphase with Hyperspectral Remote Sensing. Spectrosc. Spect. Anal. 30:3061-3066.

Teal, R.K., B. Tubana, K. Girma, K.W. Freeman, D.B. Arnall, O. Walsh, et al. 2006. In-season prediction of corn grain yield potential using normalized difference vegetation index. Agron. J. 98:1488-1494.

The Mathworks, Inc., 2012. Matlab 8.0. Natick, MA, USA.

Thenkabail, P.S., R.B. Smith and E. De Pauw. 2000. Hyperspectral vegetation indices and their relationships with agricultural crop characteristics. Remote Sens. Environ. 71:158-182.

Thenkabail, P.S., R.B. Smith and E. De Pauw. 2002. Evaluation of narrowband and broadband vegetation indices for determining optimal hyperspectral wavebands for agricultural crop characterization. Photogramm. Eng. Remote Sens. 68:607-621.

Thomason, W.E., S.B. Phillips, P.H. Davis, J.G. Warren, M.M. Alley and M.S. Reiter. 2011. Variable nitrogen rate determination from plant spectral reflectance in soft red winter wheat. Precis. Agric. 12: 666-681.

Tremblay, N., Z.J. Wang, B.L. Ma, C. Belec and P. Vigneault. 2009. A comparison of crop data measured by two commercial sensors for variable-rate nitrogen application. Precis. Agric. 10:145-161.

Tubana, B., D. Arnall, S. Holtz, J. Solie, K. Girma and W. Raun. 2008. Effect of Treating Field Spatial Variability in Winter Wheat at Different Resolutions. J. Plant Nutr. 31:1975-1998.

Tubana, B., D. Arnall, O. Walsh, B. Chung, J. Solie, K. Girma, et al. 2008. Adjusting midseason nitrogen rate using a sensor-based optimization algorithm to increase use efficiency in corn. J. Plant Nutr. 31:1393-1419.

Tubana, B., S. Viator, J. Teboh, J. Lofton and Y. Kanke. 2011. Feasibility of using remote sensing technology in nitrogen management in sugarcane production. Int. Sugar J. 113:747-747.

Tucker, C. 1979. Red and Photographic Infrared Linear Combinations for Monitoring Vegetation. Remote Sens. Environ. 8:127-150.

Varvel, G.E., W.W. Wilhelm, J.F. Shanahan and J.S. Schepers. 2007. An algorithm for corn nitrogen recommendations using a chlorophyll meter based sufficiency index. Agron. J. 99: 701-706.

Wagner, P. and K. Hank. 2013. Suitability of aerial and satellite data for calculation of site-specific nitrogen fertilisation compared to ground based sensor data. Precis. Agric. 14:135-150.

Walsh, O.S., A.R. Klatt, J.B. Solie, C.B. Godsey and W.R. Raun. 2013. Use of soil moisture data for refined GreenSeeker sensor based nitrogen recommendations in winter wheat (Triticum aestivum L.). Precis. Agric. 14:343-356.

Wheat Marketing Center. 2008. Wheat and Flour Testing Methods: A Guide to Understanding Wheat and Flour Quality (Version 2). Kansas State University, USA.

Elachi, C. and Zyl J.J.V. 2006. Introduction to the physics and techniques of remote sensing (2nd edition). Wiley-Interscience. N.J. USA.

Yang, c. and J.H. Everitt. 2012. Using spectral distance, spectral angle and plant abundance derived from hyperspectral imagery to characterize crop yield variation. Precis. Agric. 13:62-75.

Yang, C., J.H. Everitt and J.M. Bradford. 2009. Evaluating high resolution SPOT 5 satellite imagery to estimate crop yield. Precis. Agric. 10:292-303.

Yara-International. 2013. Yara N-sensor™. Crop Nutrition. Yara. http://www.yara.co.uk/crop-nutrition/Tools-and-Services/n-sensor/ (accessed 12 Nov. 2013).

Zillmann, E., S. Graeff, J. Link, W.D. Batchelor and W. Claupein. 2006. Assessment of cereal nitrogen requirements derived by optical on-the-go sensors on heterogeneous soils. Agron. J. 98:682-690.

APPENDIX

Table A1. Soil test results for Amenia sugar beet site in 2012

Depth (inches)	NO_3-N (kg ha^{-1})	P (ppm)	K (ppm)	pH	OM (%)	Zn (ppm)
0-6	58	9	380	7.6	4.9	0.65
6-24	94	/†	/	/	/	/

† No data.

Table A2. Soil test results for Crookston sugar beet site in 2012

Depth (inches)	NO_3-N (kg ha^{-1})	P (ppm)	K (ppm)	pH	OM (%)
0-6	15	9	300	7.4	4.9
6-24	20	/†	/	/	/

† No data.

Table A3. Soil test results for Casselton sugar beet site in 2013

Depth (inches)	NO_3-N (kg ha^{-1})	P (ppm)	K (ppm)	pH	OM (%)	Zn (ppm)
0-6	43	7	370	7.6	5.4	0.37
6-24	111	/†	/	/	/	/

No data.

Table A4. Soil test results for Thompson sugar beet site in 2013

Depth (inches)	NO_3-N (kg ha^{-1})	P (ppm)	K (ppm)	pH	OM (%)	Zn (ppm)
0-6	15	10	225	7.8	5.7	1.10
6-24	74	/†	/	/	/	/

† No data.

Table A5. Soil test results for Gardner spring wheat site in 2012

Depth (inches)	NO_3-N (kg ha^{-1})	P (ppm)	K (ppm)	pH	OM (%)	Zn (ppm)
0-6	30	24	185	7.5	5.3	1.15
6-24	50	/†	/	/	/	/

† No data.

Table A6. Soil test results for Valley City spring wheat site in 2012

Depth (inches)	NO_3-N (kg ha^{-1})	P (ppm)	K (ppm)	pH	OM (%)	Zn (ppm)
0-6	31	32	128	5.4	3.8	1.10
6-24	37	/†	/	/	/	/

† No data.

Table A7. Soil test results for Gardner spring wheat site in 2013

Depth (inches)	NO_3-N (kg ha^{-1})	P (ppm)	K (ppm)	pH	OM (%)
0-6	28	16	245	5.6	4.8
6-24	104	/†	/	/	/

† No data.

Table A8. Soil test results for Valley City spring wheat site in 2013

Depth (inches)	NO_3-N (kg ha^{-1})	P (ppm)	K (ppm)	pH	OM (%)
0-6	34	16	245	5.6	4.8
0-24*	143	/†	/	/	/

* No soil residual nitrate for 6-24 inches soil was tested.

† No data.

Table A9. Soil test results for Durbin corn site in 2012

Depth (inches)	NO_3-N (kg ha^{-1})	P (ppm)	K (ppm)	pH	OM (%)	Zn (ppm)
0-6	24	40	650	7.4	5.4	0.77
6-24	20	/†	/	/	/	/

† No data.

Table A10. Soil test results for Valley City corn site in 2012

Depth (inches)	NO_3-N (kg ha^{-1})	P (ppm)	K (ppm)	pH	OM (%)	Zn (ppm)
0-6	40	8	275	6.3	3.9	0.39
6-24	47	/†	/	/	/	/

† No data.

Table A11. Soil test results for Arthur corn site in 2013

Depth (inches)	NO_3-N (kg ha^{-1})	P (ppm)	K (ppm)	pH	OM (%)	Zn (ppm)
0-6	12	11	270	7.9	4.7	1.44
6-24	54	/†	/	/	/	/

† No data.

Table A12. Soil test results for Valley City corn site in 2013

Depth (inches)	NO_3-N (kg ha^{-1})	P (ppm)	K (ppm)	pH	OM (%)	Zn (ppm)
0-6	31	18	150	6.1	4.5	0.78
6-24	57	/†	/	/	/	/

† No data.

Table A13. Soil test results for Cummings sunflower site in 2012

Depth (inches)	NO_3-N (kg ha^{-1})	P (ppm)	K (ppm)	pH	OM (%)
0-6	58	9	380	4.9	0.65
6-24	94	/†	/	/	/

† No data.

Table A14. Soil test results for Valley City sunflower site in 2012

Depth (inches)	NO_3-N (kg ha^{-1})	P (ppm)	K (ppm)	pH	OM (%)
0-6	35	8	275	3.9	6.3
6-24	47	/†	/	/	/

† No data

Table A15. Soil test results for Cummings sunflower site in 2013

Depth (inches)	NO_3-N (kg ha^{-1})	P (ppm)	K (ppm)	pH	OM (%)
0-6	13	24	160	8.2	4.9
6-24	30	/†	/	/	/

† No data.

Table A16. Soil test results for Valley City sunflower site in 2013

Depth (inches)	NO_3-N (kg ha^{-1})	P (ppm)	K (ppm)	pH	OM (%)
0-6	22	21	270	6.0	3.1
6-24	155	/†	/	/	/

† No data.